THERMODYNAMIC DEVELOPMENT OF A NOVEL INTEGRATED AIR-CONDITIONING SYSTEM WITH DOAS USING LIQUID DESICCANT

MINGXIAN CUI

Ph.D
The Hong Kong
Polytechnic University
2013

The Hong Kong Polytechnic University

Department of Building Services Engineering

Thermodynamic Development of a Novel Integrated Air-Conditioning System with DOAS Using Liquid Desiccant

Mingxian CUI

A thesis submitted in partial fulfillment of the requirements for the Degree of Doctor of Philosophy

October, 2011

CERTIFICATE OF ORIGINALITY

I hereby declare that this thesis is my own work and that, to the best of my knowledge and belief, it reproduces no material previously published or written, nor material that has been accepted for the award of any other degree or diploma, except where due acknowledgement has been made in the text.

Signature: __________________________

Name: Mingxian Cui

Department of Building Services Engineering

The Hong Kong Polytechnic University

Hong Kong SAR

October, 2011

ABSTRACT

A dedicated outdoor air system (DOAS) used for air-conditioning has recently attracted many attentions because it can significantly improve both energy efficiency and indoor air quality. Cooling-based dehumidification has inherent weaknesses because the process air has to be cooled down below its dew-point temperature for dehumidification and reheated thereafter. Currently available DOASs with solid or liquid desiccants have their own thermodynamic weaknesses. These obstruct the wide applications of DOAS with desiccant dehumidification in practice. Therefore, thermodynamic development and study of a novel integrated air-conditioning system with DOAS using liquid desiccant is conducted in this thesis.

Mathematical models of primary components of the proposed system are developed. Simplified numerical model for internally cooled/heated dehumidifier/regenerator and a robust numerical solution are developed, which is characterized by linearization of the non-linear term in the model and multi-gridding approach to guarantee convergence in a wide range of component size and operation conditions. A semi-empirical model for chiller with a recovery exchanger installed between the compressor and the condenser is developed. All the models are validated by either experimental or manufacturers' data, providing a basis for this study.

New exergy analysis method is adopted to develop air-conditioning system with high thermodynamic perfection by introducing concepts of dry-, wet-, cold- and heat-exergies, beneficial and unbeneficial exergies to quantify real exergy gains and destructions/losses and to identify each factor causing exergy loss. Application of the newly proposed concepts and method to analysis of the standard liquid desiccant

system with DOAS results in the proposed system. It mainly consists of a DOAS subsystem for dehumidification, heat recovery chiller for cooling, and heat pump utilizing waste condensing heat from chiller for desiccant regeneration. The DOAS subsystem is characterized by effectively harvest the sensible and latent load of the exhaust air by an enthalpy exchanger and two sensible heat recovers. The rational exergy efficiency of the proposed system is 8.0% as compared to 3.1% of the standard system.

The proper design methods of the proposed system are then developed. They consist of 1) a new RTS-based design cooling load calculation method for sizing of chiller; and 2) a ε-NTU method for design of liquid desiccant dehumidifier. The new design cooling load calculation method overcomes the weakness of RTS method for intermittent cooling by accounting for additional cooling load due to intermittent operation. The ε-NTU method for dehumidifier is characterized by two performance indices of enthalpy effectiveness and mass transfer effectiveness. The iterative design procedure of the system is presented and a design tool is provided for engineer.

The thermodynamic study of the proposed system indicates that energy efficiency is enhanced by more than 60% for air-conditioning in a typical office building of Hong Kong, with the average COP reaching 4.21. The thermal analysis also reveals the indispensable role of total heat exchanger to minimize and balance the dehumidification load on dehumidifier. The effects of weather conditions on the performance of the system are analyzed in detail.

The sensitivity analysis of key independent operation parameters of the proposed system are carried out to identify their optimal ranges to provide guidelines for the optimal design of the proposed system. The operation parameters studied are condensing temperature of chiller, cooling and hot water flow rates and solution flow rate. The results indicate that: 1) condensing temperature of chiller affects the energy consumption of the system the most and should be as low as possible; 2) the effects of cooling and hot water flow rates are consistent and their optimal value should be about 0.5~1.0 times of fresh air flow rate; 3) the effect of solution flow rate is small and it optimal value is limited by the largest flow rate without desiccant carry-over.

PUBLICATIONS ARISING FROM THIS STUDY

Journal Papers Published

Tingyao Chen, Mingxian Cui, 2010, A RTS-based method for direct and consistent calculating intermittent peak cooling loads, Energy Conversion and Management 51(6):1170-1178

Conference Papers Published

Mingxian Cui, Tingyao Chen, 2009, A Revised radiant time series method for intermittent cooling load calculation, The 11th International IBPSA Conference, 27-30 July, 2009, Glasgow, Scotland

Tingyao Chen, Mingxian Cui, 2010, A Novel Integrated Energy-efficient Dedicated Outdoor Air System (DOAS) with Liquid Desiccant, First International Conference on Sustainable Urbanization, 15-17 Dec 2010,Hong Kong

Tingyao Chen, Mingxian Cui, 2010,Thermodynamic analysis of innovative liquid desiccant dehumidification system, Third International Conference on Applied Energy, 16-18 May, 2011, Perugia, Italy

ACKNOWLEDGEMENT

I would like to express my earnest appreciation to my chief supervisor, Dr. Chen Tingyao for his readily available supervision, valuable recommendations and continuous support during the entire course of my research work.

I am grateful to Mr Leung Tat-wah and Mr Lee Chun-kit, Philip for their kind support for experimental related work.

I would also express my deepest appreciation to my wife, Hongbo Liu, for her support, encouragement, understanding and patience, and for her taking care of our daughter alone in the past years. I would also like to dedicate this thesis to my beloved parents for their unconditional love and support in my life.

Finally I would like to thank everyone who offered direct or indirect help and support to this thesis.

TABLE OF CONTENTS

LIST OF FIGURES

LIST OF TABLES

NOMENCLATURE

A	Area, m^2
$\mathbf{A}$	Matrix of coefficients
a	Coefficient
$\mathbf{B}$	Matrix of unknown parameters
c	Wall conduction time series, or coefficient
c_p	Specific heat, kJ/(kg·K)
c_{sat}	Saturation specific heat, kJ/(kg·K)
C_{min}	Minimum heat capacity
C_r	Ratio of the heat capacity
C_r*	Equivalent heat capacity ratio
d_{ch}	Channel depth, m
d_{eq}	Equivalent channel diameter, m
e	Exergy, kJ/kg
e_t	Slope of change of equilibrium humidity ratio with temperature
e_X	Slope of change of equilibrium humidity ratio with solution concentration
E	Exergy rate, kW
E^g	Desired exergy rate, kW
E^b	Unbeneficial exergy rate, kW
F	View factor
g	Periodic heat transfer coefficient, W/K
h	Enthalpy, kJ/kg

hc	heat transfer coefficient, kW/(m^2·K)
h_D	Mass transfer coefficient, kg//(m^2·s)
h_d	Integral heat of dilution, kJ/kg
$h_{fg,0}$	Evaporation heat of water at 0°C
H	Height, m
i_x	Index of flow direction of the x fluid
Le	Lewis Number
m	Mass flow rate, kg/s
n	Number
Nu	Nusselt number
p	Pressure, Pa
Pr	Prandtl number
q	Heat transfer rate or cooling/heating load, kW
R	Thermal resistance
R_a	Specific ideal gas constant of air, 0.287 kJ/(kg·K)
Re	Reynolds number
r_{ns}	Non-solar radiant time series
$r_{rw,cv}$	Convective ratio of sensible heat gain
$r_{rw,,r}$	Radiant ratio of sensible heat gain
s	Entropy, kJ/(kg·K)
t	Temperature, ℃
T	Temperature, K

U	Overall heat transfer coefficient, kW/(m^2·K)
v	Specific volume, m^3/kg
V_s	Refrigerant volume flow rate, m^3/s
V_{pump}	Diverted refrigerant volume flow rate, m^3/s
W	Electricity power, kW
x	Relative area
X	Solution mass concentration, kg/kg
$\mathbf{X}$	Matrix of unknown parameters
Y	Thermal admittance
s	Entropy, kJ/K
z	Coordinate axis
$\bar{z}$	Relative position

Greek

α	Compressor power loss factor proportional to internal power or ratio of chemical exergy to heating value of the fuel
β	NTU ratio of moisture to sensible heat
ω	Humidity ratio, kg/kg
γ	Isentropic coefficient of the refrigerant or activity coefficient for exergy analysis
λ	Thermal conductivity, kW/K
ϕ	Osmotic coefficient
φ	Relative humidity ratio
Φ	Rational exergy efficiency

ν	Dissociation number, equals to 2 for LiCl
ε	Effectiveness for heat or mass transfer
η_{el}	Efficiency of electricity generation and transmission

Subscripts

a	Air
ae	Exhaust air
as	Supply air
c	Cooling
cd	Condenser
ch	Chemical
chw	Chilled water
clw	Cooling water
d	Destruction
des	Desired
deh	Dehumidification
e	Exhaust air or equilibrium condition
ev	Evaporator
evw	Evaporated water
fld	Fluid
g	Gas
gen	Generated
h	Heating
hw	Hot water
i	Inlet
k	Node number

l	Latent
m	mass
o	Outlet
oa	Outdoor air
w	Water
R	Refrigerant
s	Desiccant solution or supply air
sol	Desiccant solution
sc	Sub-cooling
sh	Superheated
st	Heat storage
t	Total
th	Thermal
tf	Transfer
tp	Two-phase
v	Water vapor
0	Reference state

Abbreviations

APCL	Additional peak cooling load
ASMR	Mass flow ratio of air to solution
AWMR	Mass flow ratio of air to water
COP	Coefficient of performance
CTS	Conduction time series
DEC	Direct evaporative cooler

DOAS	Dedicated outdoor air system
LiCl	Lithium chloride
NTU	Number of transfer unit
PLR	Part load ratio
RAPCL	Relative additional peak cooling load
RTS	Radiant time series
SHGC	Solar heat gain coefficient
SHR	Sensible heat ratio
SWMR	Mass flow ratio of solution to water
THE	Total heat exchanger
WWR	Window-to-wall ratio

CHAPTER 1 INTRODUCTION

1.1 Background and Motivations

In hot and humid climate, such as in Hong Kong and South China, dehumidification plays a key role in the air-conditioning systems. Dehumidification may account for 20-40% energy consumption in air-conditioning (Harriman et al., 1998; Zhang et al., 2005). Due to raised requirement of ventilation specified by ASHRAE Standard 62.1 (ASHRAE, 2007), ventilation of fresh air becomes the major source of moisture load in air-conditioning, which may constitute more than 60% of total peak moisture load in most building types (Harriman, 2008) and 68% for a retail store (Harriman and Judge, 2002). And the relative importance of latent load on the air-conditioning system increases with the ventilation rates and with the humidity ratio of the outdoor air. As a consequence, dehumidification of the ventilation air turns out to be a difficult and imminent task for building services engineers. An energy-efficient dehumidification system that can effectively reduce the energy cost of the air-conditioning system is still in burning need.

Another important issue with dehumidification is the poor indoor air humidity control in many existing air-conditioning systems because they are designed especially for temperature control rather than for humidity control.

Because the sensible and latent loads are treated in a coupled way through the ventilation air, the humidity control is only a byproduct of temperature control in these systems. Therefore, the indoor air humidity ratio will lose control in transition seasons or in cold and humid climate. In the new ASHRAE Standard 55-2010 for thermal comfort, the upper limit for relative humidity ratio is set to be between 67% and 56% for summer comfort zone based on the lightweight clothing (Turner, 2011). Because when the indoor relative humidity ratio is over 70%, the excessive moisture will lead to bugs, mold and rot, and also cause health related effect (Harriman, 2008). Furthermore, when the indoor relative humidity ratio is high, people may feel uncomfortable and tends to turn down the set-point of indoor air temperature, which results in excessive energy consumption (Chao & Kwong, 2007). As it was said "*It's not the heat…it's the humidity.*" (Harriman, 2008) For conventional cooling-based air-conditioning system, the process air may have to be overcooled to provide adequate dehumidification. The reheat of the overcooled air to supply temperature will also consume large amount of energy. Unless waste heat is used, the system may not meet the requirement of ASHRAE Standard 90.1 for energy. These are the motivations for the development of an energy-efficient air-conditioning system.

1.2 Why DOAS + Liquid Desiccant?

A dedicated outdoor air system (DOAS) is not a new idea but has been overlooked for many years in favour of variable air volume (VAV) system (Meckler, 1986). It becomes a favoured alternative in recent years due to increasing concern on thermal comfort, indoor air quality (IAQ) and energy saving since 1990s (Mumma, 2001; Harriman and Judge, 2002; Niu et al., 2002; Jae-Weon and Mumma, 2007; Liu et al., 2007).

The thermal comfort level can be effectively improved by DOAS. In dedicated outdoor air system, the temperature and humidity controls are decoupled. "*This approach allows each component of the HVAC system to do what it does best*." (Morris, 2003) The dew-point temperature of the supply air is dropped low enough by the dehumidifier to remove entire space latent load. The space sensible loads are handled by the sensible-only cooling terminals such as radiant ceiling and fan coil installed in the space (Mumma, 2001). The precise control of indoor air temperature and humidity as demand is therefore no longer a challenge. Furthermore, occupants will no longer feel cool caused by the low-temperature supply air because the cooling terminals can operate with chilled water higher than 16°C.

The DOAS can also effectively improve the indoor air quality. Variable air volume (VAV) or demand control air-conditioning systems (Alalawi, 1999; Chao and Hu, 2004) can hardly satisfy the multi-zones' fresh air flow rates required by ASHRAE Standard 62 (ASHRAE, 2007) without excessive energy use (Kettler, 1998; Mumma and Lee, 1998; Stanke, 1998). Another problem of these systems is the mixture of outdoor and return room air may lead to the high risks of cross respiratory infection, such as SARS (severe acute respiratory syndrome) (Chen and Lee, 2006). The DOAS can deliver required amount of outdoor air to each zone , reducing the possibility of cross infection.

The DOAS can also be energy efficient. It allows a higher evaporating temperature for chiller that is responsible for sensible cooling loads, which results in considerable energy savings.

The problem with current DOAS is its dehumidification unit of cooling coil. Because the latent load in the space is to be removed by small amount of fresh air, the supply air dew-point temperature is much lower than that of VAV systems. Therefore, deep cooling technique is required for chiller and the low evaporating temperature results in low COP. Furthermore, the over-cooled process air should be reheated before supplying into the space, which consumes energy for heating and is a waste of the useful cooling energy at low temperature.

Liquid desiccant dehumidification is a promising alternative of cooling-based technology, although it is still far from mature. It has the advantage of decoupled handling of sensible and latent load and of extremely low dew-point temperature of process air. As compared to solid desiccant, it has additional advantages of low pressure loss in the dehumidifier, air-born pollutants and bacteria removal, and most importantly, the energy storage capacity. Two problems that hinder the application of liquid desiccant units in commercial buildings are (1) the carry-over of the desiccant solution and the resulting corrosion and health problems; (2) the low COP due to the energy required for regeneration of desiccant solution.

The first problem has recently been solved by the development of zero carry-over dehumidifier by Lowenstein et al. (2006). The entrainment of the desiccant droplets by the air stream is prevented by three important modifications over traditional packed-bed dehumidifiers: (1) very low solution flow rate used, which is 10-30 times less than that in traditional ones; (2) internal cooling adopted to remove the absorption heat released, which makes the low-flow of desiccant solution viable; (3) rather than sprayed, the solution flowing down along the plates to form a falling film confined within a wick layer that covers the plates in novel plate-type dehumidifier. It is therefore hard for the air stream to break the film and to bring droplets of solution with it.

The low COP of the liquid desiccant conditioner results from the extensive regeneration heat required. The using of fuel-fired regenerator is definitely energy consuming, even when the double- or multiple-effect regenerator is adopted (Lowenstein et al., 1998). The appropriate way is to use waste heat or other “free” energy like solar energy. The solar energy is preferred due to readily availability and thus has attracted increasing interest for its application in desiccant regeneration (Alizadeh and Saman, 2002; Krause et al., 2005; Gommed and Grossman, 2007; Alizadeh, 2008; Katejanekarn et al., 2009). However, the availability of the solar energy is not steady, especially in cloudy or rainy days and in evening when dehumidification is still necessary. Unless the storage of concentrated solution is available, using solar-regeneration as part of the air-conditioning system would be problematic. Another appropriate alternative of free heat source is the condensing heat of the chiller. The major problem with the condensing heat is the limited hot water temperature provided. A viable solution is to reduce the regeneration temperature required by special design and operation control strategies to try to satisfy the requirement. If the hot water temperature is still below requirement, a water-source heat pump can be adopted to elevate the water temperature. Because the source temperature is high and the temperature lift of the heat pump is low, the COP of the heat pump is appreciably high as 10.0.

Therefore, the integration of the DOAS with liquid desiccant dehumidification and condenser heat recovery would comprise an air-conditioning system that not only is energy-efficient but also guarantees high level of indoor air quality and thermal comfort.

1.2 Objectives of the Study

The DOAS with liquid desiccant can provide improved indoor air quality and precise temperature and humidity control. However, hampered by the regeneration energy consumption, its energy performance is still far more from satisfaction in current studies. Therefore the development of a novel hybrid liquid desiccant air-conditioning system with dedicated outdoor air system that can effectively reduce the regeneration energy consumption is urgent and valuable.

The overall objective of this research project is to thermodynamically develop and properly design a novel energy-efficient air-conditioning system with DOAS using liquid desiccant. The detailed objectives are:

1. To develop an energy-efficient liquid desiccant air conditioning system with dedicated outdoor air system, which can provide precise temperature and humidity control while maintains high coefficient of performance. The proposed system will maximally and effectively harvest the available waste heat from exhaust air and condensing heat of chiller;

2. To develop mathematical models and their numerical solution of various components used in the proposed system, especially for liquid desiccant dehumidifier/regenerator and chiller with partial heat recovery. A simulation platform for the proposed and conventional liquid desiccant systems with specified control strategies is also to be built;

3. To propose a new exergy analysis method to rationally quantify the real exergy gain for the desired function of equipment or system, and each exergy destruction or loss caused by each factor to guide the development of air-conditioning system with high thermodynamic perfection;

4. To develop a simple method for the design of the proposed air-conditioning system. This method will include (1) a new RTS-based method for peak intermittent cooling load calculation, and (2) simplified ε-NTU equations for effective estimating the performance of liquid desiccant dehumidifiers and regenerators. A design tool using this method for the design of the proposed system is to be developed as well;

5. To numerically study the energy and thermal performance of the proposed system for an example building in Hong Kong to provide inside information about the operation of system at different weather conditions;

6. To find the optimized values of the component sizes and independent operation parameters to guide the optimal system design at initial stage.

1.3 Organization of the Thesis

This chapter outlines the background and motivations for the study of a novel integrated liquid desiccant air-conditioning system with DOAS which can provide improved indoor air quality, precise temperature and humidity control, as well as high energy efficiency. The objectives of the study are also presented. The following chapters are organized as following.

Chapter 2 presents a comprehensive literature review of the study and development of the dehumidification technologies and their application, the models for heat and mass transfer in internally-cooled dehumidifier, and design methods of equipment in the proposed system. Gaps are found and suggestions for improvement are provided. The methodology and main tasks for this project are then introduced in Chapter 3.

Chapter 4 presents the models of key components used in the proposed system. The numerical model and solution for internally-cooled liquid desiccant dehumidifier with four flow configurations are developed. A semi-theoretical model of chiller with partial heat recovery is introduced as well.

Chapter 5 presents a new exergy analysis method and exemplifies how it is used to guide the development of an air-conditioning system with high thermodynamic perfection by system.

Chapter 6 & 7 introduce the methods for accurate and simple design of the proposed system. A new peak cooling load calculation method for intermittent cooling based on RTS method is introduced in Chapter 6. Simplified ε-NTU equations for effective estimating the performance of liquid desiccant dehumidifiers and regenerators are presented in Chapter 7. The procedure and tool for design of the proposed system is also presented in Chapter 7.

Chapter 8 & 9 presents the energy performance investigation and proper design of the proposed system. In Chapter 8, the energy performance of the system for an example building in Hong Kong is presented and compared with standard liquid desiccant system. The effects of weather conditions on the performance of the proposed system and its components are investigated. The sensitivity analysis of independent operation parameters is presented in Chapter 9, with proper values of these parameters at different weather conditions to guide optimal system design.

Finally, chapter 10 summarizes the work reported in this thesis and provides recommendations for future research.

CHAPTER 2 LITERATURE REVIEW

2.1 Overview of Dehumidification Technologies

Dehumidification is a critical aspect of air-conditioning for commercial buildings to provide comfortable indoor environment, especially for hot and humid climates.

Dehumidification can be accomplished in various ways. Yet the current dehumidification techniques can be classified into two categories: mechanical cooling-based and chemical desiccant-based. The characteristics, advantages and disadvantages of these dehumidification techniques are presented below. The studies on electrostatic dehumidification technique are also introduced here.

2.1.1 Cooling-based Dehumidification and its Potential Problems

As stated by Lowenstein, the vapor-compression technology is the foundation of the air-conditioning engineering and will last for years (Lowenstein, 2008). The same is for cooling-based dehumidification which is achieved most commonly by cooling coils. The humid air flows in the cooling coil and is cooled to a temperature below its dew-point temperature by the coolant, either chilled water in traditional cooling coil, or refrigerants in direct expansion coil. The water vapor in the air will be condensed into liquid water and then be removed or collected. It gains popularity because of its low initial cost, easy control and maintenance, and coupled cooling of the process air without additional equipment.

Despite of its dominant position in commercial application, cooling-based dehumidification has several disadvantages that should be considered and overcome. The first problem with this technique is that in transit or humid season, indoor air humidity will lose control because the conventional air-conditioning systems are controlled by thermostat installed rather than humidistat (Zhang et al., 2005). When an air-conditioned space experiences only part of its design load, its humidity ratio tends to rise because the thermostatically controlled air-conditioning system tries to maintain the indoor temperature by reducing its cooling capacity (Chua et al., 2007). The fact that cooling coils operate at part-load conditions may thus result in poor dehumidification performance for a system crossing the cooling season. This causes space humidity levels to drift upwards, especially on days when cooling loads are modest. Therefore, dedicated dehumidifier is a favored alternative to provide accurate humidity control in recent year (Harriman, 2008).

Another more severe problem with cooling-based dehumidification is that reheat of the supply air may be possibly required because the supply air has to be deeply cooled to below its dew-point temperature to remove the latent load. This usually occurs for commercial applications that the supply air temperature may have a constraint for comfort reasons or for other applications that only dehumidification rather than cooling is needed (Novoselac and Srebric, 2002). This process of overcooling and subsequent reheating has double energy effects, which presents a serious energy-cost penalty depending on the conditions required. Unless waste heats from either exhaust air or condenser are available for reheating, the energy standard of ASHRAE 90.1 cannot be satisfied (ASHRAE, 2007b).

Furthermore, when the supply air dew-point temperature is lower than normal, low temperature techniques are required to prevent freezing (Mumma, 2007). This happens in dedicated outdoor air system with supply air dew-point temperature to be 6-9°C or even less because a relatively small amount of outdoor air is used to remove the entire latent loads (Mumma, 2001). Meanwhile, because of the low evaporating temperature of chillers, the COP of the chiller would be reduced. The obtainable dew-point temperature of the supply air is limited to above 0°C to prevent freezing of the condensed water. This limits its application where very low dew-point temperature is required, such as supermarkets and pharmaceutical manufactories.

Lastly, the condensed water on the surfaces of the cooling coil provides a favorable condition for the growth of mold and bacteria which deteriorates indoor air quality and causes the sick building syndrome (Yu et al., 2009).

Although measures do exist to overcome the above mentioned problems, these solutions tend to increase the cost for air-conditioning.

2.1.2 Desiccant Dehumidification, a Promising Alternative

Desiccant dehumidification is an appropriate alternative to cooling-based technique, which can address the problems encountered by cooling-based dehumidification. Although it is conventionally used for industry applications such as product drying, humidity control in text mills, its application for commercial buildings has drawn growing interest in recent years (Daou et al., 2006; Lowenstein, 2008). Desiccants, materials with high attraction for water vapor, are basically of two types, depending on their state and principle of water vapor removal: adsorption by solid desiccants and absorption by liquid desiccants. Both solid and liquid desiccants can produce dry air with dew-point temperature lower than -40℃ (ASHRAE, 2008). Because no overcooling of the process air is required, desiccant dehumidification is particularly suitable for applications where the latent load dominates (Waugaman et al., 1993), and where dry air with very low dew-point temperature is needed, for instance, textile mill or archives (TIAX, 2004). Desiccant dehumidification is beneficial for improved humidity control, effective water vapor removal and reduced electric demands (Pesaran et al., 1992). Because most desiccant dehumidification systems are thermal driven, they are most suitable for locations where the peak electricity demand cannot be satisfied or the electricity bill is higher than gas.

Desiccant dehumidification systems also have disadvantages. The COPs of many desiccant systems are low because of high energy consumption for desiccant regeneration. Commercial desiccant wheels are usually reactivated between 82-107℃ (Harriman III et al., 1999). And liquid desiccant can be regenerated at 40-70℃ (Alizadeh and Saman, 2002). Unless free or low cost heat resources are available, the large amount of energy consumed by regeneration results in low COP of the desiccant cooling system (Lowenstein et al., 1998).

Although the solid desiccant is more widely applied for air-conditioning applications of commercial buildings, accounting for two thirds of desiccant systems sold (TIAX, 2004), the liquid desiccant dehumidifier demonstrates many design and performance advantages over the solid desiccant wheel (Oberg and Goswami, 1998). The comparison of the typical features of the solid and liquid desiccant systems is summarized in Table 2.1.The regeneration temperature required for liquid desiccant is lower than that of solid desiccant. For solid desiccant, only the scavenging air with low heat capacity can be heated for regeneration of solid desiccant, while for liquid desiccant, the regeneration temperature can be lowered because desiccant solution can be either heated directly outside the regenerator or internally-heated by hot water in the regenerator. The energy efficiency of the liquid desiccant system is thus higher than that of solid ones (Harriman, 1994). Also, the pressure drop through a liquid-desiccant contactor is smaller than that through a solid desiccant wheel and can be further reduced by the plate-type contactor (Lowenstein et al., 2006). Furthermore, concentrated liquid desiccant provides another way of energy storage besides ice storage for peak load shifting and for times when no suitable source for regeneration is available (Kessling et al., 1998). Liquid desiccant offers more design and installation flexibility. Unlike the solid desiccant wheel where the regeneration happens simultaneously at the same place with dehumidification, the offsite and asynchronous regeneration is possible for liquid desiccant contactors. Finally, the liquid desiccant dehumidifier can remove dirt and bacteria in air, providing improved air quality (Daou et al., 2006).

Table 2.1 Features of liquid and solid desiccant

No.	Item	Liquid desiccant	Solid desiccant
1	Energy efficiency	High	Low
2	Operational flexibility	More flexible	Less flexible
3	Regeneration temperature	Low	High
4	Airside pressure drop	Low	High
5	Removing dirt and bacteria	Higher ability	Lower ability
6	Energy storage	Easy	Difficult
7	Heat recovery	Easy	Difficult
8	Corruption to metals and alloys	Yes	No
9	Desiccant loss due to carryover	Yes	No

Even with such advantages, the primary barrier to the practical application of liquid desiccant in air-conditioning system may be the carry-over problem. The entrainment of desiccant can cause corrosion to duct and other equipment and reduce the lifespan of the system. The carry-over of liquid desiccant in the dehumidifier and regenerator consumes a great amount of solution, which causes a high operation and maintenance cost (Xu, 2011). Furthermore, people are doubted about the hazard of the desiccant diffused into the indoor air on health.

However, the weakness has been tackled and overcome recently by Lowenstein et al (2006) and Conde-petit (2007). They claimed that the low-flow dehumidifier can reach zero carry-over of the liquid desiccant, which will be discussed in detail below. Because the major stumbling block is away, the liquid desiccant may become the most promising alternative to cooling-based dehumidification.

2.1.3 Electrostatic Dehumidification, on the Horizon?

In recent years, the feasibility of dehumidification by electrostatics, also called electrostatic dehumidification technology (EDT), has been studied (Hoenig, 1987; Arif-uz-Zaman and Khan, 1993; Hoenig, 2001a). Electrostatic dehumidification technology utilizes the principle of electrostatics to remove water droplets, clusters and even water vapor molecules in the air. The configurations of typical electrostatic dehumidifiers researched are normally wire-plate type. Thin-wire discharge-electrodes located in the center of grounded collecting electrodes are applied with high voltage with direct current (DC) or alternating current (AC). When the voltage applied exceeds a distinct value which is named corona onset voltage, corona discharge will happen, and the water molecules and droplets will therefore be charged.

In an electrostatic dehumidifier, water molecules or clusters in the air steam will experience body forces in the presence of strong electric field gradient and migrates toward the collecting electrodes for removal (Uchiyama and Jyumonji, 1995). For uncharged water molecules and clusters, dielectrophoretic force resulting in intrinsic dipole movement of water molecules is the dominant body force; while for charged ones due to corona discharge, the Coulomb force which is several times order higher than dielectrophoretic force becomes the dominant body force, and the mechanism of water droplets removing is quite analogous to that of electrostatic precipitation, with contamination particles replaced by water mists or droplets.

Uchiyama and Jyumonji (1989; 1995) of the Hachinohe Institute of Technology firstly performed preliminary study on the feasibility and performance fog-liquefier through a series indoor and field experiments. Dengta (2004) also studied the possibility of fog-removal by wire-mesh electrode. Wang and Wang (1995) analyzed the performance of electrostatic water recovery technology based on his own laboratory experiment. Lu (2005) analyzed the mechanism of electrostatic water recovery technology, especially about the field charge of water droplets.

The first who investigated the feasibility of electrostatic dehumidifier for air-conditioning is Hoenig (1987; 2001a; 2001b; 2002) who published three patents regarding to the application of electrostatics to remove water vapor. His first electrostatic dehumidifier was composed of an array of grounded tube elements with a spark-like square stainless electrode centered in each element and applied with high voltage; the experiment result of this equipment illustrated that the outlet-to-inlet humidity decreased rapidly with the applied voltage when the applied voltage exceeded about 15kV for both negative and positive voltage (Hoenig, 1987). Later in year 2001 (Hoenig, 2001a), he proposed another type of electrostatic dehumidifier composed of an array of hollow needles applied with high voltage and a grounded metal mesh facing the needle array. The water condensate was expected to be sucked into small holes in needles or /and the mesh and to be disposed away. The performance of the apparatus which typically reduced the relative humidity of the air stream from about 90% to 35% indicates that it is quite effective for air dehumidification. However, Hoenig's results may not be so reliable because the results were limited and from the experiment described, it was the fog removed, not the water vapor.

The dehumidification using corona discharge is somewhat energy-consuming. A better solution is to use electrostatics but without corona discharge and phase change of water vapor from vapor to liquid. Arif-us-Zaman's research was in this type (Arif-uz-Zaman and Khan, 1993). The apparatuses connected with two containers were composed by a series of parallel pored thin metal foils and windowed metal plate. They were carried out in static conditions, using the electric field gradient existing near the holes on the foil which were applied with high voltage to "pump" water vapor from one container to another. Nevertheless, the efficiency was not so good, only reducing the humidity by 3.2%. This humidity reduction may also be caused by the error of measuring equipment. This can be interpreted by the fact that no effective vapor removal method was employed and the drawback of the dehumidifier configurations which cannot accelerate the movement of the water molecules between the perforated foils and windowed plates.

Such as it is, Arif-us-Zaman's work indicates that there is still a long way to go for the development of the feasible electrostatic dehumidifier.

2.2 Application of Liquid Desiccant Dehumidification

Because of the advantages of liquid desiccant dehumidification, its application in commercial buildings has drawn much interest. These studies are mainly focused on three fields: the development of dehumidifier/regenerator for HVAC services; the study of energy-efficient air-conditioning systems integrated with liquid desiccant dehumidification and solar-regeneration; the theoretical study on the coupled heat and mass transfer process by air with falling film of solution. This review will cover recent researches on these three fields to find the gaps for this study.

2.2.1 Advances in Liquid-desiccant Dehumidifiers

Dehumidifier, regenerator and solution heat exchanger constitute the main part of liquid desiccant systems. Since the configurations of the regenerators are generally the same with those of the dehumidifier, only the advances in dehumidifier will be introduced.

The conventional liquid-desiccant dehumidifiers are typically adiabatic packed-bed tower, either in structured or random packing, flooded with liquid desiccant from the top to bottom. This type of dehumidifier is the focus of most researches. Comprehensive reviews on the packed-bed type dehumidifier are reported by Ober and Goswami (1998) and Lowenstein (2008).

The common characteristic of the adiabatic dehumidifier is the large flow rate of desiccant solution which can be several times of the flow rate of processing air. Such high solution flow rate is necessary to provide adequate thermal capacity to remove the heat released due to the water absorption; otherwise the dehumidification ability will decrease (Lowenstein, 2008). The biggest problem of packed-bed type dehumidifier is the entrainment of desiccant droplet due to the spraying of the solution at the top or due to the breakdown of the cascading solution film at high flow rate. A droplet filter or demister is consequently necessarily to be installed to prevent the entrainment of the solution out of the dehumidifier. Although the desiccant carryover can be effectively eliminated by the filter or demister in well-maintained system, the carryover of solution still is the paramount problem in many systems due to improper installation or operation (Liu, 2011). Also, the cooling of desiccant solution in dehumidifier and subsequent heating in the regenerator impose two-way penalty on the system performance: the pre-heating of the cooled solution for regeneration and the cooling of heated solution for dehumidification. It was said that the energy consumed to preheat of the weak solution to the regeneration temperature might equal to the energy used for water desorption (Lowenstein et al., 1998). Furthermore, the pumping of such large amount of solution consumes considerable pump power.

An appropriate way to solve these problems is reducing the solution flow rate and increasing the solution concentration change in the dehumidifier and regenerator (Lowenstein et al., 1998). Because of the low solution flow, the energy required for cooling, preheating, and pumping of the solution can be considerably reduced. Due to the lowered solution flow, internally-cooling is thus necessary to remove the adsorption heat. Furthermore, rather than being sprayed to the packing, the desiccant solution can be falling along plates by gravity force to form very thin falling film, which is hard to be breakdown and to result in entrainment.

Khan studied the performance of one type of internally cooled dehumidifier cooled by water- or refrigerant-cooled tube bundles (Khan, 1998; Khan and Sulsona, 1998). However, the desiccant solution was still sprayed, resulting in entrainment; this type of dehumidifier may be quite expensive for implement (Lowenstein, 2008).

Internally-cooled plate-type dehumidifier is a better choice with reduced pressure drop and vanished entrainment and has drawn the focus since 1990s. There are two approaches of cooling used in the literature: evaporative cooling by air and water flowing in internal passages and water cooling by circulated cooling water from cooling tower or chilled water from chiller.

Saman and Alizadeh (2002) developed a cross-flow liquid desiccant dehumidifier that was evaporatively cooled. It takes advantages of direct evaporative cooling in one channel to cool the solution film in its adjacent channels. Water was sprayed into the secondary-air channels with air-to-water counter flow. The primary air and the secondary air were in cross flow with 45° inclination from the horizontal. The ratio of solution-to-air mass flow rates was 0.1, and the maximum enthalpy effectiveness of 0.75 was achieved at an optimal value of air flow rate. This type of dehumidifier is innovative, avoiding the use of cooling tower to produce cooled water and thus requiring less maintenance and pumping power. Compared to water-cooled unit, the evaporative-cooled dehumidifier will have a moderately higher cooling capacity at a lower capital cost (Lowenstein et al., 1998). However, because the solution was sprayed, the entrainment problem may still exist. Also, because there are four fluids in the dehumidifier, how to prevent leakage and mixing is a big installation problem.

Lowenstein et al (2006) in AIL Research Inc. developed a water-cooled low-flow liquid-desiccant dehumidifier which was claimed with zero carryover. The distribution and collection of the desiccant solution were incorporated into the contactor design without sprayers or drip pans. The dehumidifier was composed of a series of thin polypropylene plate. The plates were made from extrusion with inside passages running the cooling water. An important characteristic of the dehumidifier was the thin wick layer (about 0.5mm formed by polypropylene fleece) covering the plate surfaces not only to ensure the even wetting by the solution but also to confine the solution flow in the wick layer to prevent carryover. Lowenstein tested their prototype with a laser particle counter, and found that the process air would almost not carry any desiccant particles under low solution flows.

Conde-petit and Weber (2006) developed a laboratory prototype of an internally-cooled/heated dehumidifier/regenerator with semi-permeable membrane. The membranes are hydrophobic, micro-porous and polymeric. The dehumidifier was assembled by structured plates with membrane constituting the interface between the air channels and solution channels. Because the air and solution are not in direct contact but through a layer of membrane, entrainment of desiccant can be avoided, preventing the corrosion and potential health problems. This idea seems attractive. However, its dehumidification effectiveness may be reduced because of additional resistance introduced by the membrane layer for mass transfer. Since no experimental results were provided in their published papers, its performance is still left for doubt.

2.2.2 Application of Liquid Desiccant Units in Air-conditioning System

A typical conventional liquid desiccant system is composed of five components: dehumidifier, regenerator, solution heat exchanger, cooler and heater (ASHRAE, 2008; Lowenstein, 2008). The dehumidifier and regenerator used are externally cooled/heated packed-bed type. For internally-cooled/heated liquid desiccant conditioner, the liquid desiccant system is composed by only three components of dehumidifier, regenerator and solution heat exchanger (Lowenstein, 2008). Many applications of air-conditioning system that incorporates liquid desiccant units have been investigated and will be reviewed.

Oliveira el al. (2000) proposed an air-conditioning system using adiabatic liquid desiccant conditioner. The outdoor air was firstly dehumidified by the liquid desiccant absorber and then cooled by heat pipe that recovers the sensible cooling energy of the exhaust air increased by direct evaporative cooler. The process air was further cooled by direct evaporative cooling. The two direct evaporative coolers for the process air and return air are the characteristics of many conventional design of the air-conditioning system with liquid desiccant.

Kinsara et al (1996; 1998) also proposed an energy efficient air conditioning system using liquid desiccant. The direct evaporative cooler and air-to-air heat exchanger was used to recover the cooling energy of the exhaust air to cool the dehumidified outdoor air leaving the adiabatic absorber. The process air was further cooled by cooling coil and direct evaporative cooler. The cooling of process air by direct evaporative cooling may not be economical because the deeply dried air may consume more energy for regeneration when no free heat source is available in their system. This system is also superior in its regeneration loop, which will be discussed in next section. The performance of the system was also investigated by parametric study and was compared to conventional air-conditioning system. The performance of the system was highly affected by the ambient temperature and effectiveness of the heat exchangers.

A single component of indirect evaporative cooler using exhaust air as the secondary air has the same function as the two components of direct evaporative cooler and the connected air-to-air heat exchanger (Kinsara et al., 1996) or heat pipe (Oliveira et al., 2000). A liquid desiccant air-conditioning system with indirect evaporative cooler was proposed by Tu et al. (2009). In this system, the outdoor air is dried by an adiabatic dehumidifier and then cooled by an indirect evaporative cooler and a direct evaporative cooler. The exhaust air serves as the secondary air of the indirect evaporative cooler (IEC) to convert its latent cooling energy to sensible cooling energy of the process air. A heat exchanger recovering the heat of scavenging air was also adopted in the system. The effect of key operation parameters on the performance of the system was numerically studied. The results indicated that the COP of the system (defined as ratio of the cooling capacity produced to the regeneration heat energy required) was lower than 1 for most conditions.

While the direct and indirect evaporative cooler can only reduce sensible cooling load of the process air, total heat exchanger that can recover the enthalpy of the exhaust air is more energy-efficient to reduce the sensible and latent loads of process air. This unit has already been applied in the cooling-based dedicated outdoor air system (Zhang and Niu, 2003; Zhang et al., 2005) and in solid desiccant air-conditioning systems (Harriman and Judge, 2002). However, the application of total heat exchanger in liquid desiccant system is few.

Li et al. (2005) adopted the liquid desiccant total heat exchanger in the liquid desiccant cooling system to recover the enthalpy of the exhaust air, similar to that of Thompson (2004). The liquid desiccant total heat exchanger was composed by a dehumidifier and a regenerator, either in one or two stages. The enthalpy transfer efficiency of single stage total heat exchanger was about 54% while for two-stage ones, the enthalpy transfer efficiency reached 70%. The air leaving the total heat exchanger was dehumidified and cooled by another liquid desiccant dehumidifier cooled by vapor compression cooling. The EER of the system reached 6.3-7.3 in summer experimental condition and 4.7-5.0 in winter experimental condition.

Liu et al. (2006) further investigated the performance of the system with liquid desiccant total heat exchanger more systematically. A modification to the system by Li's (Li et al., 2005) was that an air-to-air heat exchanger that recovers the heat of scavenging air was installed to reduce the waste of heating energy.

The performance of the system was compared with conventional system by two factors of reduced primary energy ratio and operation cost ratio. For summer condition of Beijing with SHR from 0.5 to 0.9, the primary energy consumption of the new system was 76-80% of that the conventional HVAC system and the operation cost of the new system was about 75% of that of conventional one.

Liquid desiccant also provides an alternative solution of thermal storage for both cooling and heating. The heat is stored by means of concentration shift of desiccant solution, resulting in lossless chemical heat storage.

Kessling (1998) studied the cooling energy storage performance of an open-cycle liquid desiccant system. The dehumidifier was internally-cooled plate type with very low solution flow and large water flow to produce an almost isothermal absorption process. The arrangement of the system was similar to that of Tu's (2009). The dehumidified outdoor air was cooled by indirect evaporative cooling utilizing the exhaust air as secondary air. The experimental results indicated that a high energy storage capacity of 700 MJ/m^3 was achieved under ARI standard conditions with 1000 m^3/h air flow. They also found that the very-low solution flow rate could result in poor wetting of the plates and deteriorated performance of the dehumidifier.

Jaradat and Heinzen (2008) proposed a liquid-desiccant system that could provide heating energy storage in winter as well as cooling energy storage in summer. The absorber was installed in the exhaust air stream in series with an air-to-air heat exchanger. In heating mode, the water vapor in the exhaust air is absorbed in the adiabatic absorber and releases condensation heat, causing temperature increase of the exhaust air. The supply air stream can then be heated by the exhaust air through the air-to-air heat exchanger. The weakness of this system is that the heat provided is limited unless large desiccant flow rate is used, where the carry-over problem may appear.

2.2.3 Heat Sources for Desiccant Regeneration

The weak desiccant solution leaving the dehumidifier should be concentrated before reusing, and therefore heat is required for desiccant regeneration. That is why liquid desiccant system is usually called thermal driven. Hot water boiler is conventionally used as the heat source for regeneration. However, due to the low energy efficiency of boiler, the COP of the regeneration system seldom exceeds 1.0 and was close to 0.5 (Lowenstein, 2005). Lowenstein (2005) developed a 1½ effect regenerator with a COP of 1.05. Even though, the COP of the regeneration system is still low. Therefore, free low-grade energy, for instance, solar energy, waste heat, or waste hot water, is a desirable alternative.

Many studies have been conducted to investigate the solar energy as the heat source for regeneration. The desiccant solution can be either regenerated directly in the solar collector (Ameel et al., 1995; Alizadeh and Saman, 2002; Katejanekarn et al., 2009), or be regenerated in separate regenerator by hot water produced by solar collector (Factor and Grossman, 1980; Krause et al., 2005; Gommed and Grossman, 2007; Alizadeh, 2008; Hepbasli, 2008). For the first type with direct solar regeneration, forced flow of scavenging air is appreciated to enhance the regeneration performance (Alizadeh and Saman, 2002), otherwise the regeneration rate will be quite limited as indicated by the experimental results by Katejanekarn et al. (2009). The primary advantage of using solar energy for regeneration is that no additional electricity or fuel energy is required, except for the pump energy consumption. The overall efficiency of the air-conditioning system can be appreciably high. The disadvantages of the solar energy are that space at rooftop is required and that the solar energy is not stable or available for cloudy, rainy days and evening hours. These disadvantages may limit its application in certain commercial buildings.

The condensing heat of chiller is another alternative of heat source for regeneration. This kind of energy is readily available whenever chiller is used in the air-conditioning system.

Zhu et al. (2010) used the condensing heat of the chiller directly to heat the weak liquid desiccant for the regeneration, while the liquid desiccant is cooled in evaporator of the chiller for dehumidification. Such operating mode of chiller was called heat pump. The averaged COP of their system was tested to be 5.28. In this system, the chiller or called “heat pump” has to work hard not only to satisfy the cooling load, but also to satisfy the regeneration heating load at elevated condensing temperature. Because of the elevated condensing temperature, the COP of the chiller would be lowered. The COP of the chiller was high because of the raised chilled water supply temperature at about 17°C. Another unavoidable problem with this system is the matching between the cooling load and regeneration heating load, which is not mentioned in their paper. If the heat requirement is smaller than the cooling requirement, it is energy-ineffective to raise the condensing temperature to fulfill the smaller heating requirement. A solution to this problem is to install a heat pump after the chiller to recover the condensing heat as the heat source of the heat pump (McQuay, 2009). The heat required for regeneration can be easily satisfied by heat pump while the performance of chiller is unaffected. Because the performance of heat pump can be separated controlled, the load-matching problem no longer exists.

The system proposed by Kinsara et al. (1996) also utilized heat pump to heat the solution and scavenging air for regeneration. The condensing heat of chiller was also utilized. However, the way of condensing heat utilization seems to be improper because the chiller condensing heat is not served as heat source of the heat pump but is used to preheat the air entering the condenser of heat pump. Although the COP of heat pump can be increased, the increment is relatively small as compared to the measure of using condensing heat of chiller as heat source of heat pump. Furthermore, using air as the heat transfer medium is not so effective as compared to water due to the low heat capacity and heat transfer coefficient of air.

There are applications that only part of the condensing heat is sufficient to serve as the heat source for regeneration. This can be realized by three ways, as shown in Figure 2.1. The first measure is by a recovery condenser connected in series with the primary condenser, as shown in Figure 2.1 (a), where the condensing heat in the superheated region can be recovered. The McQuay's ALS series chiller is in this type (McQuay, 2008). The second measure is by a recovery condenser connected in parallel with the primary condenser, as shown in Figure 2.1 (b) (McQuay, 2009). Part of the condensing heat in the two-phase and superheated regions is then recovered. The third measure is by a recovery heat exchanger installed before the cooling tower, as shown in Figure 2.1 (c) (McQuay, 2002). The last measure is only suitable for water-cooled chillers. The application and controls of the second and third ways was discussed by McQuay (2002). Although the same amount of heat is recovered, the levels of energy (exergy) are different. The first way is better than the other two because the maximum hot water supply temperature of the first way can be a few degrees higher than that of the others. The difference increases at smaller heat recovery ratio.

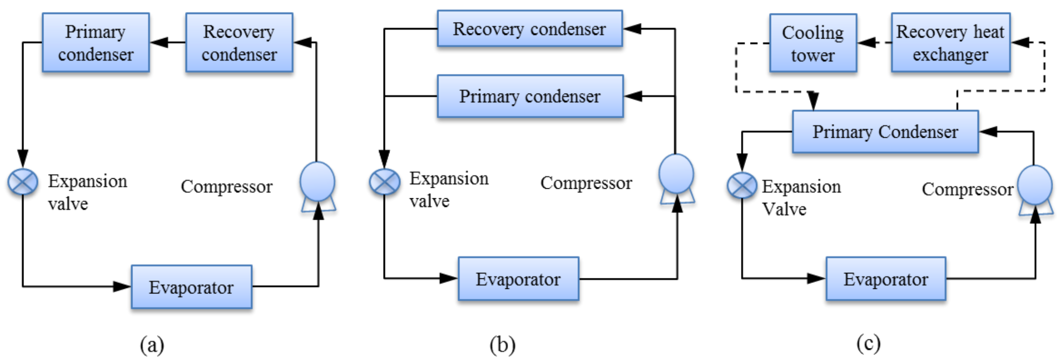

Figure 2.1 Three ways of partial condensing heat recovery

2.3 Models of Heat and Mass Transfer in Liquid-desiccant Dehumidifier

In order to investigate the coupled heat and mass transfer in the liquid desiccant dehumidifier or to predict its performance for energy simulation, many models have been developed. These models can be classified into three categories based on their complexity and solvation time used: detailed numerical model, simplified numerical model and analytical model.

2.3.1 Detailed Nuremical Model

Detailed numerical models investigate the heat and mass transfer process by basic conservation equations of mass, momentum, energy and mass diffusion. Because it is based on theoretical model with less simplification and assumption, detailed model can accurately reflect the heat and mass transfer process between the air and falling film of solution. For cases where experimental data are unavailable, it can provide numerical results that are accurate enough for the investigation of the performance. Unlike simplified models in which heat and mass transfer coefficients are required, the correlations of heat and mass transfer coefficients can be derived from the results by detailed numerical model (Rahamah et al., 1998).

Zografos and Petroff developed numerical model for indirect-evaporative cooled liquid desiccant dehumidifier (Zografos and Petroff, 1991). The turbulent effect was considered in their model. They especially analyzed the effect of the ratio of plate length over spacing and the Reynolds number of the air and provided guidelines for the optimization of design.

Rahamah et al. (1998) developed the detailed numerical model for internally-cooled dehumidifier with solution and air in parallel flow and solved it by finite volume method. New correlations for Nusselt number and Sherwood number was developed in terms of Prandtl number, Reynolds number, channel height and spacing. Although this model was developed for solution-to-air parallel flow, it can be easily extended to other flow configurations with small modification. However, in their model, the wall temperature was assumed to be constant which cannot reflect the real performance of the internally-cooled dehumidifier because the cooling water temperature will increases along its flow direction and thus the wall temperature changes.

Ali et al. (2004) analyzed the heat of mass transfer between air and falling film of solution in cross-flow configuration with constant wall temperature. Their model was similar with that of Rahamah's but considered the effect of addition of Cu-ultrafine particles to enhance the heat and mass transfer process. The effects of air and solution Reynolds number, channel height, length and width, Cu-ultrafine volume fraction on the Nusselt number and Sherwood number were analyzed. The solution Reynolds number was about one order less than air Reynolds number and its effect on the dehumidification was minimal. It is a pity that no correlations of the Nusselt number and Sherwood number were given. The detailed models of other flow types were also provided in his thesis (Ali, 2003). The effect of inclination of the flow channel was examined (Ali and Vafai, 2004). They found that the small inclination angle plays a significant role in improving the dehumidification and regeneration performance.

In Rahamah's and Ali's models, the thickness of the solution film was assumed to be constant. However, in internally-cooled dehumidifier, the solution flow rate can be two orders less than that of the air and thus the thickness of the falling film will increase and the increase may be considerable for very low solution flow. Mesquita et al. (2006) investigated the effect of film thickness variation by using variable thickness model. Generally, the leaving air humidity ratio predicted by the variable thickness model was smaller than that of the constant thickness model and simplified model and agreed better with experimental data. Yet the model is still based on isothermal wall conditions without considering the effect of cooling water temperature change.

2.3.2 Simplified Numerical Model

The simplified numerical model has been widely used for the analysis of coupled heat and mass transfer performance for adiabatic (Fumo and Goswami, 2002; Longo and Gasparella, 2005; Yin and Zhang, 2008) and internally-cooled units (Yin and Zhang, 2010). The theoretical model is simplified by several assumptions including: steady state fully developed laminar flow; constant heat and mass transfer coefficient; no temperature gradient in the transverse direction of the flow. The detailed model can therefore be simplified to a set of differential governing equations of mass and heat transfer and conservation. These governing equations are usually solved by finite difference method. In these studies, unlike the models for adiabatic packed-bed power where the equilibrium humidity ratio of the solution at the air-solution interface is considered (Fumo and Goswami, 2002; Longo and Gasparella, 2005; Babakhani and Soleymani, 2010), it is assumed to be equal to that of the bulk solution. This assumption is reasonable due to the thin solution-film thickness in internally-cooled dehumidifiers as compared to that in adiabatic ones. The previous work done in the literature is summarized in Table 2.2. The performance of internally-cooled dehumidifier for different flow configurations were analyzed using the simplified model.

Table 2.2 Review of Simplified Numerical Model of Internally-cooled Dehumidifier

Source	Configuration	Characteristics and Validation
(Yin and Zhang, 2010)	Plate type; Solution-air parallel flow, Solution-water parallel flow	The performance was compared with the adiabatic ones.
(Yin et al., 2009)	The same as above	The model using the empirical correlation of mass transfer derived from experimental results was validated by experimental results within ±5%.
(Ren et al., 2007)	Plate type; Four configurations without cross flow	The predicted results were compared with their analytical solution with relative error within ±3%.
(Khan, 1998)	Sprayed tubes with fins; Solution-to-air cross-flow, Water-to-air counter-flow	Using piece-wise linear approximation for all the variables in the control volume and under-relaxation technique to guarantee convergence; the predictions agreed well with catalogue data and were within ±10% of their analytical solution.
(Khan and Sulsona, 1998)	Sprayed tubes with fins; Solution-to-air cross-flow, Coolant-to-air counter-flow	Using refrigerant as coolant.
(Liu et al., 2009)	Plate-type; Solution-to-air counter-flow, water-to-air cross-flow	The predictions were within ±13% of the experimental results by Kessling and within ±10% of the results by Lowenstein. Also compared with internally-cooled with other flow types and adiabatic ones.
(Jain and Bansal, 2007)	Tubular type; Solution-to-air parallel flow, Solution-to-water counter-flow	The predictions were within ±30% of their experimental data.

Two problems exist in these simplified models. The first one is that the correlations for heat and mass transfer coefficients were not provided (Ren et al., 2007). Without proper heat and mass transfer coefficients, the model is incomplete and can be only used for theoretical analysis but not for performance prediction of real equipment. The second problem is that in many of these studies, only the models were introduced but how to solve these models and how to prevent divergence were not mentioned. Only Khan explained the two measure of linear approximation for all the variables in the control volume and under-relaxation technique to guarantee convergence (Khan, 1998). These techniques were supposed to be effective to prevent divergence.

Although not important for parallel-flow and cross-flow configurations, how to prevent divergence in the solution is a severe issue for such problem of counter-flow units with coupled heat and mass transfer. The initial values of the variables in the field play an important role on convergence of the solution. Shrivastava and Ameel (2004) discussed the convergence issue of the multi-stream heat exchanger. They claimed that the solution might be diverged for arbitrary partition with poor initial guess of the temperature profile. A multi-stream heat exchanger example divided into 20 or more segments was introduced to exemplify the convergence problem. For coupled heat and mass transfer, the problem will be aggravated due to the release of absorption heat which will cause sharp temperature variation. Furthermore, from our experience, the number of segments divided also influences the solution of the model by finite difference method. When the number of segments is large enough, the effect of initial value will be reduced to certain extent because the fluctuation of the variables in iteration can be limited. For instance, for the counter-flow adiabatic dehumidifier, when the number of segments is less than 20, the solution will tends to divergence especially the ratio of solution to air flow rate is small.

Multi-grid method will be an excellent alternative to provide good initial values of the field and thus to prevent divergence (Tao, 2001). Shrivastava and Ameel (2004) successfully used this method to solve the model of multi-stream heat exchanger.

2.3.3 Analytical Model

For component model used for the applications of energy analysis and online control, two factors are important: robust and less computation time and hardware requirement. Therefore, analytical model is preferred because it requires the least computation time as compared to both detailed and simplified models.

An effectiveness model for counter-flow adiabatic dehumidifier was firstly developed by Stevens et al. (1988; 1989). This model was derived from the effectiveness model of a cooling tower. The heat and mass transfer were decoupled by two critical assumptions differing from the simplified model: unity Lewis number and linear relationship for saturation enthalpy with temperature. Thus the saturation specific heat (analogous to that used in cooling tower) was therefore a constant:

$$C_{sat} = \frac{dh_{t_s,sat}}{dt_s} = \frac{d\left(c_{p,m}t_s + \omega_e h_{fg}\right)}{dt_s} = c_{p,m} + h_{fg}c_2 \qquad (2.1)$$

where $\omega_e = c_1 + c_2 t_s$ is the equilibrium humidity ratio of the solution at temperature t_s. $c_{p,m}$ is the specific heat of the moist air, h_{fg} the heat of evaporation. c_1 and c_2 are constants. This model provides an easy way to predict its performance. However, this model is only applicable for adiabatic dehumidifier with counter-flow configuration.

Liu et al. (2008) presented an analytical model for the cross-flow packed-bed liquid desiccant dehumidifier based on the available solution for cross-flow heat exchanger. The enthalpy effectiveness ε_h and moisture effectiveness ε_m defined to predict the dehumidifier performances were related by a dimensionless parameter κ representing the difference between air inlet parameter and desiccant inlet iso-concentration line as:

$$\varepsilon_m = \varepsilon_h + \kappa\left(1 - \varepsilon_h - e^{-\mathrm{NTU}}\right) \tag{2.2}$$

The model was validated by both numerical simulation and their experimental results and the difference with the experimental results was within 20%. This model is relatively complex as compared to that of Stevens' and only for adiabatic dehumidifier/regenerator.

The analytical solution for internally-cooled dehumidifier is destined to be more complex than that for adiabatic ones due to the coupled heat and mass transfer between the fluids of air, solution and coolant. Such solution was not presented until Ren's work (Ren et al., 2007). Ren developed the analytical solution for internally-cooled dehumidifier based on their years' work on the heat and mass transfer between the falling film of desiccant solution and air. This model is applicable for four different flow configurations with parallel and counter flows between any two of the three fluids of air, desiccant solution and water. Like effectiveness-NTU model for adiabatic liquid-desiccant dehumidifier, assumptions of unity Lewis number and linearized equilibrium humidity ratio with temperature were assumed. And the assumption moves forward for linearized equilibrium humidity ratio with not only temperature, but also solution concentration. This is because the change of solution concentration is much larger than that of adiabatic dehumidifier and the effect of concentration change was considered. That is,

$$d\omega_e = c_1 dt_s + c_2 dX_s \tag{2.3}$$

where X_s is the concentration of the solution. The analytical solution was obtained by rearranging the one-dimensional governing equations into differential eigenvalue problem with three variables (two temperature differences and one humidity ratio difference):

$$\frac{d\mathbf{Y}}{d\mathrm{NTU}} = \mathbf{A} \cdot \mathbf{Y} \tag{2.4}$$

This differential eigenvalue problem can be solved analytically with given boundary conditions. The results of the analytical model were compared with the simplified model with average error less than 1% and maximum error less than 3%.

Although this model seems accurate, easy to use and fast, it is can just be called an analytical approach because there is no direct correlation expressing the performance of the dehumidifier as the effectiveness-NTU method does. And because linear approximation of equilibrium humidity ratio is adopted using the inlet and outlet parameters, iteration is necessary to obtain the converged results. Because the extreme values of the solution temperature may not appear at the inlet or outlet due to the coolant, special measure is necessary to find the vertex point for better accuracy. Furthermore, due to the intrinsic properties of the solution procedure, for dehumidifier with large size (or equivalently large NTU value), the term with $e^{\lambda NTU}$ would be too large and no solution can be obtained. This problem is encountered in our study.

2.3.4 Correlations of Heat and Mass Transfer Coefficents

The empirical correlations of heat and mass transfer coefficients are necessary for the commission of both the simplified and analytical models. These correlations can be developed either from the experimental data or from results of detailed model. The correlations of heat and mass transfer coefficients are generally presented in terms of Nusselt number and Sherwood number. Many correlations of mass transfer coefficient of adiabatic liquid-desiccant dehumidifier have been proposed and were summarized by Jain and Bansal (2007). However, the empirical correlations of heat and mass transfer coefficients for internally-cooled liquid-desiccant dehumidifier are scarce.

The few existing correlations for heat and mass transfer coefficients are summarized in Table 2.3. These correlations can be divided into two categories according to how the heat and mass transfer coefficients are derived.

Table 2.3 Empirical correlations of heat and mass transfer coefficients

Data source	Correlation	Type	Desiccant
(Mesquita et al., 2006)	$Nu = \frac{h_c \lambda_a}{d_{eq}} = 7.54$ For laminar flow $h_D = \frac{h_c}{\rho_a c_{p,m} Le^{2/3}}$	All flow configurations; plate type;	All
(Hassan and Hassan, 2009)	$Nu = \frac{h_c \lambda_a}{d_{eq}} = 1.86(\mathrm{Re}\,\mathrm{Pr})^{1/3}\left(\frac{d_{eq}}{L}\right)^{1/3}$ For laminar flow $Nu = 0.023\,\mathrm{Re}^{0.8}\,\mathrm{Pr}^{n}$ For turbulant flow $h_D = \frac{h_c}{c_{p,m}}$ with $Le = 1$	All flow; tube type	All
(Jain and Bansal, 2007)	$J_D = 0.023\,\mathrm{Re}^{-0.17}$ $4000 < \mathrm{Re} < 60000$ $h_D = J_D \rho_a v_a Sc^{-2/3}$ $h_c = h_D c_{p,m} Le^{2/3}$	All flow configurations; Circular-tube type	All
(Rahamah et al., 1998)	$Nu = 0.00641\,\mathrm{Pr}^{1.84}\,\mathrm{Re}^{0.9}\left(\frac{H}{0.6}\right)^{-0.69}\left(\frac{f_s}{0.0033}\right)^{n}$ $Sh = 0.00641 Sc^{1.84}\,\mathrm{Re}^{0.9}\left(\frac{H}{0.6}\right)^{-0.69}\left(\frac{f_s}{0.0033}\right)^{n}$	Parallel-flow; plate type	CaCl2
(Yin et al., 2009; Yin and Zhang, 2010)	$Sh = kSc^{0.33}\,\mathrm{Re}^{1.56}$ $k = 0.004513 \times 76.456 t_s^{-2.991}$ for dehumidification $k = 0.0046767 \times 5.52 t_s^{-3.36}$ for regenration	Parallel-flow; Plate type	LiCl

In the first category, the mass transfer coefficient can be derived from the existing heat transfer coefficient according to heat and mass transfer analogy, as done by Mesquita et al. (2006) and Hassan and Hassan (2009). These correlations are applicable for cases where the empirical mass transfer coefficient is absent. Because the effect of mass transfer on the coefficient of heat transfer is not considered, the accuracy of these correlations is limited. However, the application of these correlations is necessary for cases that no empirical mass transfer coefficient is available.

In the second category, the mass transfer coefficient is obtained by the experimental data (Yin et al., 2009; Yin and Zhang, 2010) or by numerical calculations directly, as done by Rahamah et al. (1998). The correlations for regeneration by Yin & Zhang (2009; 2010) are different which may be the writing error. The heat transfer coefficient is derived according to the heat and mass transfer analogy. The heat and mass transfer coefficients derived this way are more reliable than those of the first class and are preferred whenever available. The problem is with correlations of this class is that they are depends on the configurations and dimensions of the dehumidifier as well as desiccant material for certain correlations.

2.4 Design Methods for Equipment of Air-conditioning Systems

2.4.1 Cooling Load Calculation Method for Chiller Design

A method for cooling load calculations is fundamental for the design of air-conditioning systems. A trade-off among consistency, accuracy and simplicity is usually needed for selecting the design method. It should provide relatively consistent and accurate peak cooling loads for sizing the capacity of individual cooling components in different buildings. On the other hand, its calculation approach should be relatively simple, conceptually clear and computationally efficient.

A great number of developments and contributions (McQuiston and Spitler, 1992; ASHRAE, 1993; 2005) have been made for nonresidential design cooling calculations. Rudoy and Duran (1975) compared the total equivalent temperature difference/time averaging (TETD/TA) method and the transfer function method (TFM). They generated cooling load temperature differential (CLTD) and cooling load factor (CLF) data based on data produced by the TFM on a group of representative applications. The CLTD simplifies the calculation process by using tabulated data. It was concluded that the CLTD method can produce relatively accurate cooling loads consistent with those the TFM can achieve as compared to results generated by TETD/TA. Consequently, the CLTD/CLF procedure was published in Cooling and Heating Load Calculation Manual (Rudoy and Cuba, 1979). Subsequent studies (Harris and McQuiston, 1988; Sowell, 1988a; 1988b; 1988c; McQuiston and Spitler, 1992) substantially improved the CLTD/CLF method by better categorization schemes for zone types and the conductive transfer function (CTF) coefficients of walls and roofs, and a better factor, the solar cooling load (SCL), for solar load through windows. The improved technical data for the CLTD/SCL/CLF method, and the transfer function method and its associated design data were published in references (McQuiston and Spitler, 1992).

Design cooling load calculations have been historically based on steady periodic near-extreme heat sources so that the iterative calculations in estimating the initial conditions do not need to be performed. All the above methods do not utilize this periodic feature, and hence they need the tedious daily periodic calculations for determining the initial conditions of a building system. Jin (1986) presented a daily periodic response method in 1986 to avoid these tedious calculations while utilizing the principle of superposition in design cooling load calculations. It uses 24-hour response factors to compute the cooling loads. The author directly derived the periodic response factors from response coefficients. Spitler et al. (1997; 1999a; 1999b) described a radiant time series cooling load calculation procedure with essential periodic response factors in 1997 and 1999. The procedure uses the same periodic response function in 24 hours as that presented by Jin (1986), but further classifies heat gains from different heat sources into convective and radiant heat. Splitting heat gains into the two categories largely simplifies the calculation procedure of cooling loads due to different internal heat sources. This is because the radiant heat gains from all the internal heat sources only needs to be converted to cooling load once. It also greatly reduces the number of tabulated zone response factors of cooling loads to radiant heat gain due to the same reason. The RTS with 24 term response coefficients should produce more accurate results than the above mentioned three methods. The reason is that the TETD/TA method highly depends on subjective inputs, that the TFM provides much less accurate coefficients with only three or four zone weight factors derived from a very limited number of average building conditions, and that the CLTD/CLF method approximately derived response factors from a set of pre-assumed operation conditions.

All the above four methods associated with the tables of pre-calculated response data can be used only for continuous air-conditioning operation. The space air transfer function (SATF) method was originally intended for estimating the heat extraction rate when the space air temperature is allowed to vary in an acceptable range (ASHRAE, 1993; McQuiston and Parker, 1994). This method associated with z-transfer factors may be combined with the TFM or CLTD/SCL/CLF method to compute the intermittent design cooling load. However, it may not be possible to integrate the SATF method into the RTS method because the former needs the iterative calculations for determining the initial conditions while the latter does not.

In addition, the SATF method requires the additional response factors of cooling loads to a change in the space air temperature to be developed. Lin and Xu (2008) used a similar way to calculate the intermittent cooling load. They recalculated the response factors of cooling loads to space air temperature for several typical buildings, and then used them to determine the intermittent cooling load profile on a design day. These additional response factors may not be necessary because the response factors of cooling loads to radiant heat gain, which have been available for the TFM and RTS methods, have already contained the enough dynamic information needed. In the other words, the additional response factors can be directly obtained from the transfer function coefficients available in the different calculation method, rather than by recalculation.

Moreover, these addition response factors may largely increase the number of tables if the effect of different important parameters, such as external wall properties and area, on these factors is reasonably described. Otherwise, the calculation accuracy has to be lost if the tables showing the effect are omitted for simplicity. The current SATF method selects the latter, i.e. derived the additional response factors from typical average room configurations, which cannot reflect the effect of many important design parameters on the response factors. This could obviously result in large errors when a building under consideration is actually different from the one based on which the response factors are derived.

2.4.2 Design Method for Liquid-Desiccant Dehumidifier

The design of dehumidifier and regenerator greatly affects the performance of liquid desiccant system. A simple and easy-to-use design method is required either in the form of empirical correlations or in the form of nomograph. Analytical solution of the dehumidifier may be most appropriate. However, although the effectiveness-NTU method has been proposed for adiabatic dehumidifier (Stevens et al., 1989; Kinsara et al., 1996), few such easy-to-use methods are found in the literature for the internally-cooled/heated dehumidifier/regenerator.

From the literature, the performance of the liquid-desiccant dehumidifier can be represented by two non-dimensional characteristic parameters: the dehumidification effectiveness ε_m and the enthalpy effectiveness ε_h, which are defined as (Stevens et al., 1989; Jain and Bansal, 2007):

$$\varepsilon_m = \frac{\omega_{a,i} - \omega_{a,o}}{\omega_{a,i} - \omega_e} \tag{2.5}$$

$$\varepsilon_h = \frac{h_{a,i} - h_{a,o}}{h_{a,i} - h_e} \tag{2.6}$$

where ω_e and h_e are equilibrium humidity ratio and air enthalpy in equilibrium with solution at inlet conditions, respectively. Except the analytical solution by Stevens et al. (1989), several empirical correlations for dehumidification effectiveness of different type have been developed and summarized by Jain and Bansal (2007). These correlations are functions of the operating parameters and are valid only for certain type of dehumidifier within limited range. Jain and Bansal (2007) compared the results of different correlations and claimed that the variations ranged from 10-50% for decreasing ratio of liquid to gas flow rate.

Zografos and Petroff (1991) provided curves for the selection of the indirect-evaporative-cooled liquid desiccant dehumidifier using their numerical results. These curves were developed based on ARI design conditions and constant solution and water flow rates and are therefore not suitable for design with other conditions.

Khan (1998) attempted to develop a simple method for the prediction of the dehumidification effectiveness. His model is quite similar to that of Stevens'(1988) by replacing the term that related to desiccant solution with cooling water. The heat transferred to the solution and the concentration change of the solution were ignored in the model and the heat and mass transfer were assumed to be happened only between the air and cooling water, just like what happens in the cooling tower. This correlation tends to under-predict the dehumidification.

Thus, the development of proper correlation of the dehumidification and enthalpy effectiveness are still in need for the design of internally-cooled dehumidifier.

2.5 Summary

In conclusion, the studies on dehumidification technologies and especially the liquid desiccant dehumidification are reviewed. The studies on liquid desiccant systems mainly focus on the three fields of development of advanced liquid desiccant air conditioner, numerical modeling and studying of the heat and mass transfer process in the liquid desiccant conditioner, and the application of the liquid desiccant dehumidifier in the air-conditioning system. However, the COP of system investigated is still not satisfactory, except for those solar-driven systems. The condensing heat of chiller is not utilized in most of the systems, and the cooling energy of the exhaust air is also not effectively harvested. Therefore, an air-conditioning system has high energy efficiency is still in need.

Furthermore, problem remains for the design of air-conditioning system. An accurate design cooling load calculation method for intermittent cooling is not available by current ASHRAE recommended RTS method. A method compatible with RTS method for intermittent cooling load calculation is also on demand.

All these research outcomes will also provide theoretical basis and guidance for this study.

CHAPTER 3 METHODOLOGY

A methodology is presented to reach the objectives of this project. The methodology consists of six parts as following:

(1) The methodology starts by modeling of components of liquid desiccant air-conditioning system for numerical simulation and developing of a simulation platform for air-conditioning systems. The models of key components, including dehumidifier/regenerator, chiller with heat recovery are to be developed. The simplified numerical model for dehumidifier/regenerator with four flow configurations is utilized and a robust solution of the model is to be developed to prevent divergence. A detailed semi-theoretical model for chiller with recovery condenser is to be developed because the simplified chiller model is no longer applicable due to installation of the recovery condenser. The models for heat pump and total heat exchanger are to be selected from existing models. The models for other components, including cooling tower, cooling coil and heat exchanger, included in TRNSYS are to be used directly. FORTRAN subroutines of the models are written and introduced into TRNSYS for numerical simulations and analysis.

(2) New thermodynamic concepts about exergy and a method based on them for exergy analysis are to be developed to a) correct faulty calculations in

the conventional exergy analysis in HVAC engineering for certain conditions, and b) rationally quantify the real exergy gain for the desired function of equipment or system, and each exergy destruction or loss caused by each factor. The new exergy analysis method is to be exemplified by two typical processes in liquid desiccant system and is then applied for the analysis of standard air-conditioning system with DOAS using liquid desiccant. A novel integrated liquid desiccant air-conditioning system with DOAS is to be developed finally, utilizing the analytical results of the standard system.

(3) A new method for intermittent cooling load calculation is then developed for rational sizing of chiller in the proposed system. Accurate design cooling load prediction is the prerequisite of system design and analysis. However, the current radiant time serials (RTS) method with the assumption of periodic weather conditions is not suitable for intermittent operation of air-conditioning system in most commercial buildings. The new method for intermittent cooling load calculation shall properly determine the additional cooling load due to intermittent operation by a new set of time series. This time series called as overall periodic transfer coefficient will be obtained by available coefficients of radiant time series and conduction time series in RTS method.

(4) An effectiveness-NTU model of internally-cooled liquid desiccant dehumidifier is then developed for engineering design and an iterative design method using this simplified model for the design of proposed system is also

developed. The easy-to-use model is necessary because the numerical model is incapable for the hand design of dehumidifier/regenerator. This model is characterized by two performance indices of the dehumidifier/regenerator: mass transfer effectiveness and enthalpy effectiveness. Their correlations with non-dimensional parameters of numbers of transfer units of heat and mass, ratio of mass flow rates are determined by regression of results by numerical model. An Excel design tool is to be developed for design of the proposed system. With the cooling load rationally calculated by last phase, the proposed system can then be easily designed using the Excel design tool. The energy performance of the system can then be investigated in the next step.

(5) The energy and thermal performance of the proposed system is then to be investigated and compared with the standard liquid desiccant system with DOAS. This is to be accomplished by an example application of the system for a typical office building in hot and humid climate of Hong Kong. The annual and monthly energy performances of the proposed system are to be presented. The energy saving potential of the proposed system as compared to the standard system is to be identified. The effect of weather conditions, including outdoor dry-bulb temperature, humidity ratio, and space sensible heat ratio (SHR), on the performance of key components and system is to be investigated to provide insight information about the application of the proposed system to guide the operation of the proposed system at varied conditions.

(6) Sensitivity analyses of the independent operation parameters of the proposed system are to be conducted to evaluate the impact of these parameters on the performance of system and therefore find their optimal values to guide the optimal system design. The independent parameters to be studied are the independent operation parameters, including condensing temperature of chiller, flow rates of solution, cooling water and hot water. The optimal values of these parameters at varied weather conditions are to be determined according to the results of analysis.

CHAPTER 4 MODELING OF COMPONENTS

The models of primary components for numerical simulation of liquid desiccant dehumidification system are presented in this chapter. The models are: (1) a simplified numerical model with robust solvation procedure for four flow configurations of dehumidifier; (2) a detailed semi-theoretical model for chiller with condensing heat recovery; (3) a simplified regression model for heat pump; and (4) the effectiveness-NTU model for membrane enthalpy exchanger. The accuracy of these models is validated by either catalogue data or experimental results. These models provide the basis for development of simulation platform on TRNSYS for numerical study.

4.1 Introduction

A simulation platform for air-conditioning system is to be developed based on TRNSYS. Yet the models and corresponding subroutines of primary components of liquid desiccant dehumidification system, including internally-cooled liquid desiccant dehumidifier, chiller with heat recovery, total heat exchanger and heat pump, are missing and have to be developed or selected. This is the objective of this chapter.

The internally cooled dehumidifier has many advantages over the adiabatic dehumidifier, such as less entrainment and reduced pump power drawn to pump the solution. The models of internally-cooled dehumidifier are reviewed in Chapter 2, including the detailed numerical model, simplified numerical model and analytical model. The detailed numerical model divides the computation domain into two-dimensional grids. Although it gives most accurate results of the component, it is time consuming and not suitable for system performance prediction because iterations are necessary for the solvation of the system. Although the analytical model by Cheng (2007) is fast and accurate enough for engineering application, it is incapable of solving the dehumidifier with large size. The reason is that the term e^{NTU} would become extremely large and the solvation of inverse of matrix would fail. The simplified one-dimensional numerical model is therefore a trade-off selection.

The simplified one-dimensional numerical model for different flow configurations has already been proposed (Yin and Zhang, 2010). However, its solvation procedure is unstable. For cases with small liquid desiccant flow rate and/or large component size, divergence occurs. In this study, a robust solvation procedure is developed to guarantee the stability of model by two measures: (1) local linearization of mass transfer term to compensate for the lag of calculation of this term, and (2) multi-grid method which successively splits the calculation domain from coarse grid to fine grid and thus provides good initial value to prevent divergence. This solvation procedure is applicable for all the cases, even with extreme operation parameters and/or infinite component size.

Heat recovery chiller provides great opportunities for energy savings when both cooling and heating are required simultaneously. Many chiller models, either simplified (Hydeman and Gillespie, 2002) or detailed (Bourdouxhe et al., 1999; Jin and Spitler, 2002), exist to predict the performance of the chiller. However, the installation of recovery heat exchanger after the compressor excludes the simplified regression models used in TRNSYS. Detailed chiller model with the consideration of each component shall be applied. The fact is that the existing detailed chiller models do not incorporate the recovery heat exchanger. A detailed semi-theoretical model for chiller with heat recovery is to be developed and presented in this chapter.

The above mentioned chiller model is also suitable for heat pump. However, it is complicated for use because not only performance data is required, but also the detailed configuration data of evaporator and condenser which are usually unavailable. Since only the overall performance of heat pump is the concern, a simplified model is more appropriate. The DOE model based on regression function is to be adopted (Hydeman and Gillespie, 2002). Although it is developed for chiller simulation, it is applicable for heat pump because they are the same in nature.

Total heat exchanger can effectively recover both sensible and latent heats, and is adopted in the proposed system. The effectiveness-NTU model developed by Zhang and Niu (2002) for membrane enthalpy exchanger is briefly introduced. The model is presented here because it is necessary for system analysis in the following chapter.

4.2 Simplified Numerical Model of Internally-cooled Liquid Desiccant Dehumidifier

4.2.1 Configurations of Liquid Desiccant Dehumidifier

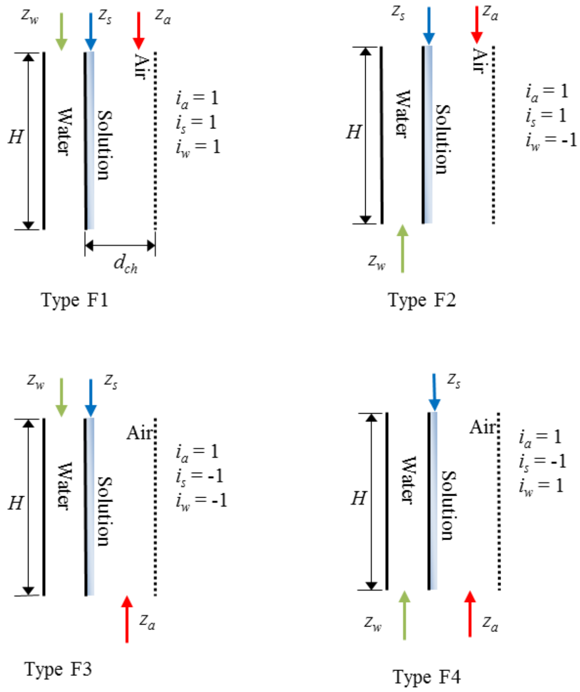

Figure 4.1 Schematic view of four flow configurations of internally-cooled dehumidifier

For internally-cooled dehumidifier with three fluids flowing inside the unit, there are at least 13 arrangements of its flow configurations of counter-flow, cross-flow and parallel-flow. Four flow configurations are considered in this project. The schematic views of the configurations are shown in Figure 4.1.

The air, solution and water are represented by a, s and w, respectively. The solution always falls from the top to bottom. The process air or scavenging air flows in contact with the solution either in parallel or counter-current. The cooling water flows in a separate channel to remove heat released by absorption. The height, width and channel depth of the dehumidifier are H, W and d_{ch}, respectively. Because the mathematical models of dehumidifier and regenerator are the same, only dehumidifier is discussed in the following section for simplicity.

4.2.2 Mathematical Model of Dehumidifier

The assumptions for mathematic modeling of the heat and mass transfer process in dehumidifier are as follows

1. All the three fluids are full-developed flow and in steady state. Thus there is no velocity gradient in the channel;
2. The local heat and mass transfer coefficients are uniform throughout the unit;
3. Thermodynamic and mass equilibrium exists at interface between air and solution;
4. The conduction and diffusion effects in the flow films are negligible due to forced flow.

In addition, multi-coordinate axes, z_a, z_s and z_w, originated from their inlet of air, solution and water are introduced. This coordinate system can make the governing equations and boundary conditions of all the four flow patterns as shown in Figure 4.1 to be uniform, so as to facilitate the expression and computer programing.

Mass balance between the air and solution is given by

$$\frac{d\omega_a}{d\bar{z}_a} = i_a \frac{h_D A}{m_a}(\omega_s - \omega_a) \tag{4.1}$$

where h_D is the mass transfer coefficient, kg/(m^2·s); ω is the humidity ratio (kg/kg). A is the total heat and mass transfer area of a (m^2). The bar over symbol z stands for normalized position of dehumidifier by $\bar{z}$=z/H.

According to the heat and mass transfer analogy, the relation between the mass transfer coefficient h_D and heat transfer coefficient h_c is (Oberg and Goswami, 1998)

$$h_D = \frac{h_c}{c_{p,m} Le^{2/3}} \tag{4.2}$$

where $c_{p,m} = c_{p,a} + \omega_a c_{p,v}$ is the specific heat of moist air, kJ/(kg·K); $c_{p,a}$ and $c_{p,v}$ are the specific heat of dry air and water vapor, respectively kJ/(kg·K). Le is the Lewis number. The heat transfer coefficient is determined by (Hassan and Hassan, 2009)

$$\mathrm{Nu} = \frac{h_c \lambda_a}{d_{eq}} = 1.86\,\mathrm{Re}^{1/3}\,\mathrm{Pr}^{1/3}\left(\frac{d_{eq}}{H}\right)^{1/3} \tag{4.3}$$

where Nu, Re and Pr are the Nusselt number, Reynolds number and Prandtl number of air, respectively; λ_a is the thermal conductivity of air, kW/(m·K); d_{eq} is the equivalent diameter of the channel that equals to $2d_{ch}$.

Energy balance on the air is expressed by

$$m_a dh_a = i_a h_c A(t_s - t_a) d\bar{z}_a + i_a h_D A(\omega_s - \omega_a) h_{v,t_a} d\bar{z}_a \tag{4.4}$$

where h_a is the enthalpy of air, kJ/kg; $h_{v,ta}$ is the enthalpy of water vapor at air temperature t_a calculated by $h_{v,ta} = h_{fg,0} + c_{p,v}t_a$. $h_{fg,0}$ is the evaporation heat of water at 0°C and is equal to 2500 kJ/kg.

The above equation can be rearranged as

$$\frac{dt_a}{d\bar{z}_a} = i_a \frac{h_D A C_a}{m_a}(t_s - t_a) \tag{4.5}$$

with $C_a = Le^{2/3} + \frac{c_{p,v}}{c_{p,m}}(\omega_s - \omega_a)$

Energy balance on the water is given by

$$\frac{dt_w}{d\bar{z}_w} = i_w \frac{U_w A}{m_w c_{p,w}}(t_s - t_w) \tag{4.6}$$

where U_w is the overall heat transfer coefficient, kW/m^{2}K .

Energy balance on the three streams is expressed by

$$d(m_s h_s) + i_w m_w c_{p,w} dt_w + i_a m_a dh_a = 0 \tag{4.7}$$

The mass conservation between the solution and air may be expressed by

$$dm_s = -i_a m_a d\omega_a \tag{4.8}$$

The differential of enthalpy of solution ($h_s = c_{p,s}t_s$), can be calculated, with the partial differential term of solution temperature neglected,

$$dh_s \approx c_{p,s} dt_s + t_s X_s \frac{\partial c_{p,s}}{\partial X_s} \tag{4.9}$$

Substituting Equation (4.8) and (4.9) into Equation (4.7) yields

$$dt_s = -i_w \frac{m_w c_{p,w}}{m_s c'_{p,s}} dt_w - i_a \frac{m_a c_{p,m}}{m_s c'_{p,s}} dt_a - i_a \frac{m_a C_h}{m_s c'_{p,s}} d\omega_a \tag{4.10}$$

with

$$C_h = h_{v,T_a} + \left(X_s \frac{\partial c_{p,s}}{\partial X_s} t_s \right) - \left(c_{p,s} T_s + h_d \right) \tag{4.11}$$

$$c'_{p,s} = c_{p,s} + X_s \frac{\partial c_{p,s}}{\partial X_s} \tag{4.12}$$

Equations (4.1), (4.5), (4.6) and (4.10), together with correlation of $\omega_s = f(t_s, X_s)$, are the governing equations for modeling heat and mass transfer in a dehumidifier.

The boundary conditions are given by

$$\begin{aligned} &\text{At } \bar{z}_a = 0, \;\; t_a = t_{ai}, \omega_a = \omega_{ai} \\ &\text{At } \bar{z}_s = 0, \;\; t_s = t_{si}, \; X_s = X_{si}, \; m_s = m_{si} \\ &\text{At } \bar{z}_w = 0, \;\; t_w = t_{wi} \end{aligned} \tag{4.13}$$

4.2.3 A Robust Numerical Solution to the Model

(1) Convergence Problem of Conventional Solution Procedure

The above equation set is usually discretized by finite difference method and solved from top to bottom or bottom to top for a fixed grid, assuming the unknown parameters at the boundary (top or bottom). This numerical approach is simple and straightforward. However, divergence may occur if the solution flow rate is small as compared to those of water and air or if the grid is relatively coarse.

One factor causing for the divergence is the improper treatment of the mass transfer term in Equations (4.1). In the discretization of the differential equations, the source term with regard to ω_s is conventionally treated as constant and is taken as the value of the last point k. For instance, for flow type F3, the Equation (4.1) is discretized as:

$$\frac{\omega_{a,k+1} - \omega_{a,k}}{\Delta \bar{z}} = -\frac{h_D A}{m_a}\left(\omega_{s,k} - \omega_{a,k}\right) \tag{4.14}$$

Problem arises from this measure of treatment. Because the solution equilibrium humidity ratio ω_s has nonlinear relationship with solution temperature and concentration and is indirectly related with the air humidity ratio, using the result of last point may cause the lag of this source term. This lag could become the key to the failure of numerical solution. Due to the small flow rate of solution as compared to those of air and water, a small difference of ω_s at the k^{th} node can lead to large solution temperature change at the $(k+1)^{th}$ node. This large solution temperature change will result in even larger change of ω_s and solution temperature at $(k+2)^{th}$ node, which leads to instable numerical calculations and divergence, as shown in Figure 4.2.

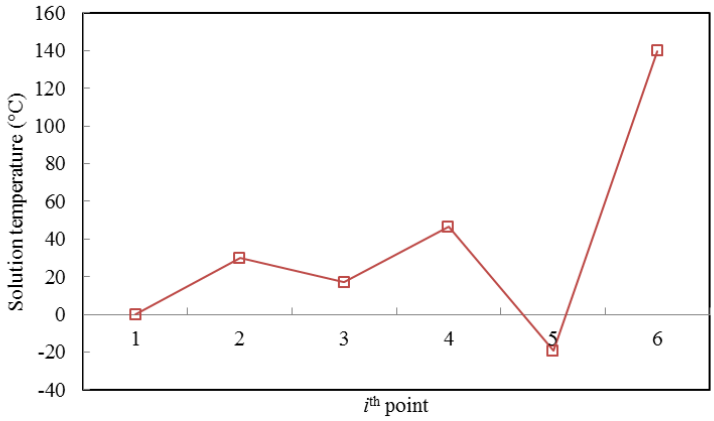

Figure 4.2 Illustration of divergence of solution for dehumidifier

Another reason of divergence is that the fixed-grid partitioning method divides the computation domain into arbitrary number of small segments. Such partitioning method may result in divergence if the initial values of unknown parameter profiles are poor (Shrivastava, 2004).

Two measures are adopted to solve the divergence problem of conventional numerical solution approach.

The first measure is to locally linearize the mass transfer term related to equilibrium humidity ratio of solution in Equation (4.1). Local linearization is generally used to handle the source term in the governing equations, which assumes that the source term can be regarded as the linear function of the variables within its small variation range (Tao, 2001). Thus, the equilibrium humidity ratio can be expressed as

$$\omega_s = c + e_t t_{s,k} + e_X X_{s,k} \tag{4.15}$$

where c is a constant. e_t and e_X are the slopes of humidity ratio variation with the two parameters, t_s and X_s, respectively, and can be regarded as constant within small variation of t_s and X_s. They are defined as

$$e_t = \frac{\partial \omega_s}{\partial T_s} \qquad e_X = \frac{\partial \omega_s}{\partial X_s} \tag{4.16}$$

Thus, the expression of equilibrium humidity ratio at the $(k+1)^{th}$ node may be expressed by

$$\begin{aligned} \omega_{s,k+1} &= (\omega_{s,k} - e_t t_{s,k} - e_X X_{s,k}) + e_t t_{s,k+1} + e_X X_{s,k+1} \\ &= (\omega_{s,k} - e_t t_{s,k} - i_a e_X \frac{h_D A_s}{m_s} \omega_{a,k}) + e_t t_{s,k+1} + i_a e_X \frac{h_D A_s}{m_s} \omega_{a,k+1} \end{aligned} \tag{4.17}$$

The lag of calculation of this term is effectively compensated by above treatment.

The second measure is to use multi-grid partitioning approach to provide more rational initial field for iteration and to accelerate convergence. This numerical approach will be described after the discretization of governing equations.

(2) Discretized Form of the Governing Equations

Although three coordinates are used for the three fluids, the theoretical model of dehumidifier is still one-dimensional for single fluid. Its computation domain can be discretized into m segments in the z direction.

Depending on the flow directions of the three streams in different flow patterns, the node numbers at the inlet and outlet of the k^{th} segment may be expressed by

$$
\begin{aligned}
kxi &= \begin{cases} k, & i_x = 1 \\ m-(k+1), & i_x = -1 \end{cases} \\
kxo &= \begin{cases} k+1, & i_x = 1 \\ m-k, & i_x = -1 \end{cases}
\end{aligned} \tag{4.18}
$$

where *kxi* and *kxo* stand for the node numbers of the k^{th} element for fluid x accounted from its inlet. Subscript x can be replaced by a for air, s for solution and w for water. Thus, k = 0 represents the inlet of all the streams and $k = m$ the outlet of all the streams. This naming scheme is adopted to represent the four different flow patterns by single set of expressions.

Locally linearizing the expression of ω_s, the governing equations can be discretized by

$$\omega_{a,kao} - \omega_{a,kai} = \mathrm{NTU}\Delta\bar{z}\left(\omega_{s,ksi} + \frac{e_t\left(t_{s,kso} - t_{s,ksi}\right)}{2} + \frac{e_X \frac{m_a}{m_s} X_s - 1}{2}\omega_{a,kao} - \frac{e_X \frac{m_a}{m_s} X_s + 1}{2}\omega_{a,kai} \right) \tag{4.19}$$

$$t_{a,kao} - t_{a,kai} = \mathrm{NTU}C_a\Delta\bar{z}\left(\frac{t_{s,kso} + t_{s,ksi}}{2} - \frac{t_{a,kao} + t_{a,kai}}{2} \right) \tag{4.20}$$

$$t_{w,kwo} - t_{w,kwi} = \mathrm{NTU}_w\Delta\bar{z}\left(\frac{t_{s,kso} + t_{s,ksi}}{2} - \frac{t_{w,kwo} + t_{w,kwi}}{2} \right) \tag{4.21}$$

$$t_{s,kso} - t_{w,ksi} = -\frac{m_w c_{p,w}}{m_s c_{p,s}}\left(t_{w,kwo} - t_{w,kwi}\right) - \frac{m_a c_{p,a}}{m_s c_{p,s}}\left(t_{a,kao} - t_{a,kai}\right) - \frac{m_a C_h}{m_s c_{p,s}}\left(\omega_{a,kao} - \omega_{a,kai}\right) \tag{4.22}$$

$$\omega_{s,kso} - \omega_{s,ksi} = e_t\left(t_{s,kso} - t_{s,ksi}\right) + e_X \frac{m_a}{m_s} X_s\left(\omega_{a,kao} - \omega_{a,kai}\right) \tag{4.23}$$

Rearranging the above equations yields

$$\mathbf{AX} = \mathbf{B} \tag{4.24}$$

where **X, A** and **B** are matrix given by.

$$\mathbf{X}=\left[t_{w,kwo}, t_{s,kso}, t_{a,kao,}\omega_{a,kao}\right]^{\mathrm{T}} \tag{4.25}$$

$$\mathbf{A}=\begin{bmatrix} \left(1+\dfrac{\mathrm{NTU}_w\Delta\bar{z}}{2}\right), & \dfrac{\mathrm{NTU}_w\Delta\bar{z}}{2}, & 0, & 0 \\ 0, & -\dfrac{\mathrm{NTU}\Delta\bar{z}}{2}e_t, & 0, & \left[1-\dfrac{\mathrm{NTU}\Delta\bar{z}}{2}\left(e_X\dfrac{m_a}{m_s}X_s-1\right)\right] \\ 0, & -\dfrac{\mathrm{NTUC}_a\Delta\bar{z}}{2}, & \left(1+\dfrac{\mathrm{NTUC}_a\Delta\bar{z}}{2}\right), & 0 \\ \dfrac{m_w c_{p,w}}{m_s c_{p,s}}, & 1, & \dfrac{m_a c_{p,a}}{m_s c_{p,s}}, & \dfrac{m_a C_h}{m_s c_{p,s}} \end{bmatrix} \tag{4.26}$$

$$\mathbf{B}=\begin{bmatrix} \left(1-\dfrac{\mathrm{NTU}_w\Delta\bar{z}}{2}\right)t_{w,kwi}+\dfrac{\mathrm{NTU}_w\Delta\bar{z}}{2}t_{s,ksi} \\ -\dfrac{\mathrm{NTU}\Delta\bar{z}}{2}e_t t_{s,ksi}+\left[1-\dfrac{\mathrm{NTU}\Delta\bar{z}}{2}\left(e_X\dfrac{m_a}{m_s}X_s+1\right)\right]\omega_{a,kai}+\mathrm{NTU}\Delta\bar{z}\,\omega_{s,ksi} \\ \dfrac{\mathrm{NTUC}_a\Delta\bar{z}}{2}t_{s,ksi}+\left(1-\dfrac{\mathrm{NTUC}_a\Delta\bar{z}}{2}\right)t_{a,kai} \\ \dfrac{m_w c_{p,w}}{m_s c_{p,s}}t_{w,kwi}+t_{s,ksi}+\dfrac{m_a c_{p,a}}{m_s c_{p,s}}t_{a,kai}+\dfrac{m_a C_h}{m_s c_{p,s}}\omega_{a,kai} \end{bmatrix} \tag{4.27}$$

The above four equations can be solved by Gaussian elimination method (Press, 1992) to obtain the outlet parameters of each segment.

(5) Multi-grid Approach for Numerical Solution

Multi-grid approach is characterized by successive partitioning of the whole computation domain, with each segment equally divided into 2 in each partitioning step (Tao, 2001). In this approach, the iteration starts from the coarsest grid of only one segment. The converged results in the last level of grid serve as the initial field in the next level of denser grid. The final solution is obtained when the difference between the solutions in two adjacent levels of grids meets the convergence criterion. The advantage of the multi-grid approach is to provide an appropriate initial field that can effectively ensure computation stability and convergence.

The variables in the governing equations are represented by $t_{a,j,k}$, $t_{s,j,k}$, $t_{w,j,k}$, $\omega_{a,j,k}$, $X_{s,j,k}$, $m_{s,j,k}$. Subscript k refers to the node number and j refers to the level of grids divided. The total number of segments divided is

$$m = j^2 \tag{4.28}$$

The schematic for multi-grid approach and its numbering scheme is shown in Figure 4.3. It starts from grid with a single element (j = 0, m =1, $\Delta\bar{z}$ =1). The outlet variables $\mathbf{X}_{0,1} = \mathbf{X}_{\text{old}} = [t_{w,0,1}, t_{s,0,1}, t_{a,0,1}, \omega_{a,0,1}]^T$ can be calculated directly with the Equation (4.24) and boundary conditions $\mathbf{X}_{0,0} = [t_{w,0,0}, t_{s,0,0}, t_{a,0,0}, \omega_{a,0,0}]^T$. The first subscript of $\mathbf{X}$ stands for the level of grid and the second for the node number.

The calculated results can serve as initial value for next level of grid with two segments (j = 1, m =2, $\Delta\bar{z}$ =0.5): $t_{w,1,2} = t_{w,0,1}$, $t_{s,1,2} = t_{s,0,1}$, $t_{a,1,2} = t_{a,0,1}$, $\omega_{a,1,2} = \omega_{a,0,1}$, $X_{s,1,2} = X_{s,0,1}$, $m_{s,1,2} = m_{s,0,1}$, and $\mathbf{X'}_{\text{old}} = [t_{w,1,2}, t_{s,1,2}, t_{a,1,2}, \omega_{a,1,2}]^T$. For stream with i_x = -1, the unknown parameters at the new nodes can be predicted by $t_{x,1,1} = 0.5(t_{x,1,0}+ t_{x,1,2})$. The parameters for each segment, $\mathbf{X}_{1,1}$ and $\mathbf{X}_{1,2}$ ($\mathbf{X}_{\text{new}}$), can be determined by Equation (4.24). The calculated results of the dehumidifier $\mathbf{X}_{\text{new}}$ is then compared with the initial assumptions $\mathbf{X'}_{\text{old}}$. If the difference is larger than the tolerance, $\mathbf{X}_{1,1}$ and $\mathbf{X}_{1,2}$ ($\mathbf{X}_{\text{new}}$) are recalculated with the updated results as the initial field until convergence is reached. The converged result of $\mathbf{X}_{\text{new}}$ is compared with the result by the last level of grid $\mathbf{X}_{\text{old}}$. If the difference exceeds the tolerance, the field should be further partitioned to denser grids (j = 2, m =4,

$\Delta\bar{z}$ =0.25). The above partitioning procedure repeats until the convergence criterion abs($\mathbf{X}_{new}$- $\mathbf{X}_{old}$)/ $\mathbf{X}_{new}$ < tolerance.

The algorithm of multi-grid approach for the numerical solution of dehumidifier model is shown in Figure 4.3. A FORTRAN program is written for the performance evaluation of the dehumidifiers with different flow patterns.

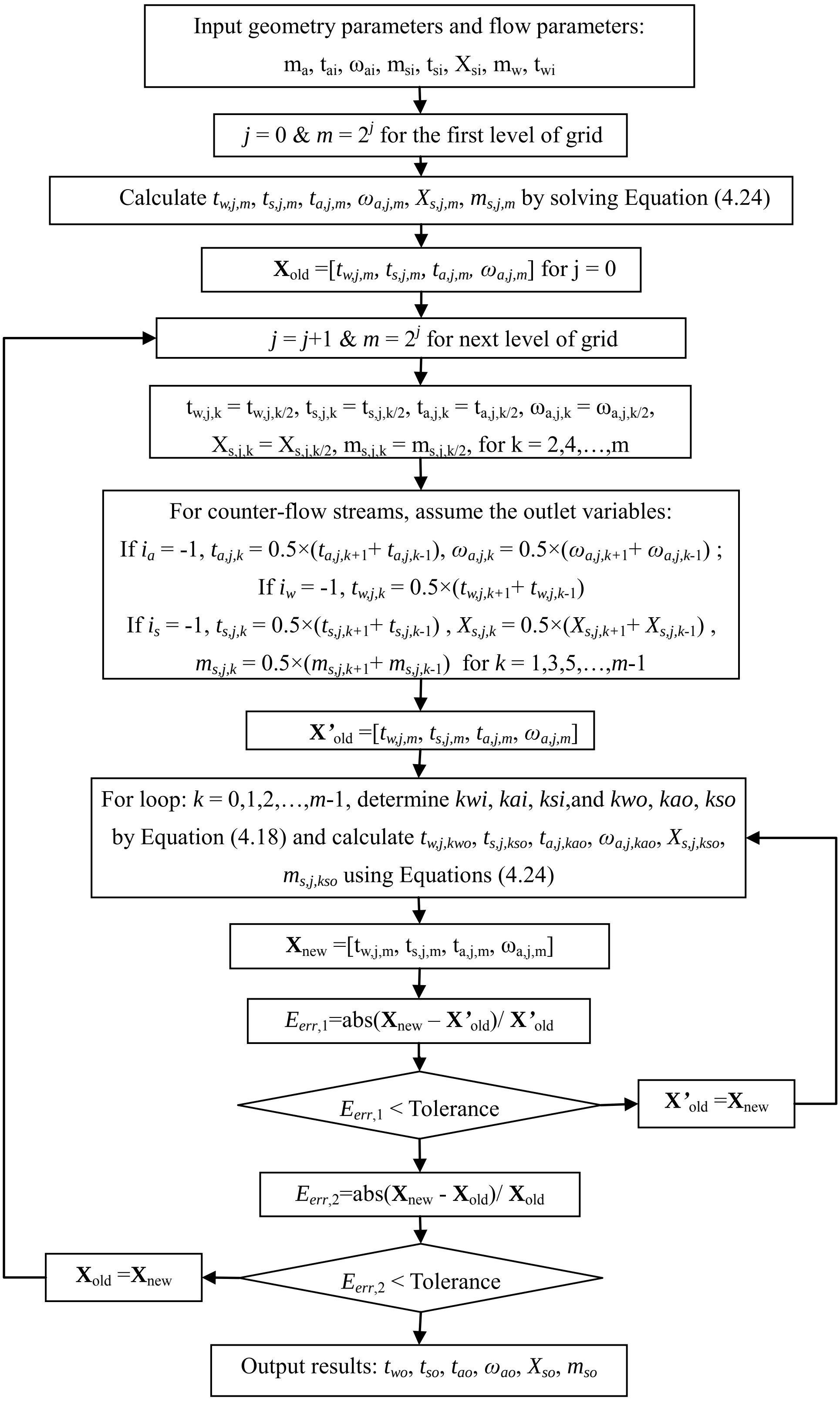

Figure 4.3 Algorithm of multi-grid approach for numerical solution of dehumidifier model

4.2.4 Validation of the Model

In order to validate the theoretical model and numerical approach, the calculated results are compared with the results of detailed variable thickness model developed by Mesquita (2006). The dimensions of the dehumidifier are listed in Table 4.1.

Table 4.1 Dimensions of the dehumidifier for validation

Height	0.46 m
Width	0.98 m
heat transfer coefficient through plate	0.17 kW/(m2·K)
Air channel depth	5.5 mm
Water channel depth	4.5 mm

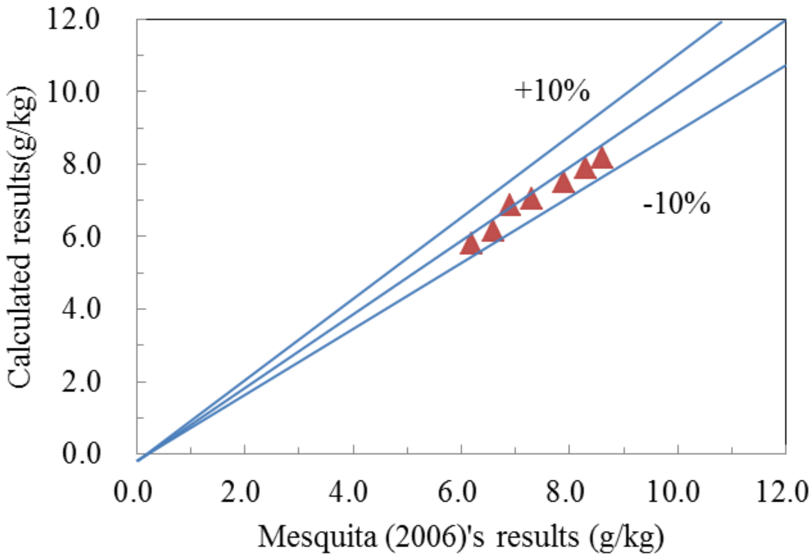

Figure 4.4 Comparison of the calculated dehumidification rates with Mesquita (2006)'s results

The comparison between the dehumidification rates by this study and by Mesquita (2006) is shown in Figure 4.4. It is noticed that the differences of dehumidification rates between the simulated results and Mesquita's results are less than 7% and the average difference is 4.8%. The difference may be caused by the inaccurate mass transfer coefficient used in this study. The larger difference occurs at smaller outlet air humidity ratio because a small absolute difference can result in large relative difference when the absolute value of air humidity ratio is small.

4.3 Semi-theoretical Model of Chiller with Heat Recovery

4.3.1 Description of Chiller with Heat Recovery

The schematic of a heat recovery chiller and its thermodynamic cycle are shown in Figure 4.5. Part of the condensing heat of the refrigerant is recovered by the recovery heat exchanger (process 2-5). The state of refrigerant leaving the recovery heat exchanger can be in superheated or saturated two-phase region depending on the heat demand in the system. The other part of condensing heat is rejected to the cooling water or air in the primary condenser (process 5-3).

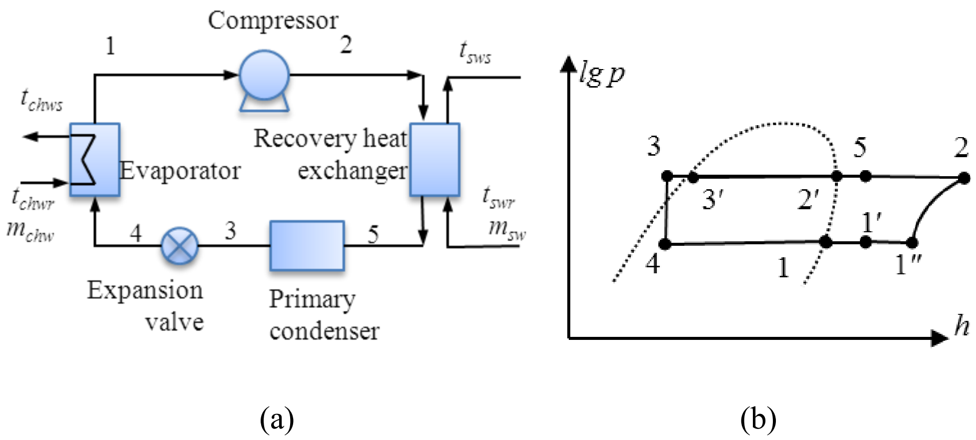

Figure 4.5 (a) Schematic of operating cycle and (b) pressure-enthalpy diagram for thermodynamic cycle of heat recovery screw-chiller at part-load

4.3.2 Models for Components

(1) Model of Twin-screw Compressor

The model described by Bourdouxhe et al. (1999) for twin-screw compressor is adopted here. The twin-screw compressor may be described by five parameters: full-load refrigerant volume flow rate at the compressor inlet V_s, leakage area $A_{leakage}$, the constant portion of electro-mechanic losses W_{loss}, the electro-mechanic loss factor proportional to the internal power α, the pressure jump of the by-passed refrigerant at part-load Δp_{pump}. These parameters can be identified from compressor/chiller performance data using the identification program by Bourdouxhe et al. (1999).

The screw compressor is a variable-volume ratio compressor whose built-in (internal) pressure ratio π_i can always match the varied system pressure ratio π. The internal work W_{in} of the variable-volume ratio compressor can be calculated by:

$$W_{in} = \frac{\gamma}{\gamma - 1} p_1 \left(V_s - V_{pump}\right)\left[\pi^{(\gamma-1)/\gamma} - 1\right] + V_{pump} \Delta p_{pump} \qquad (4.29)$$

with $\pi = \dfrac{p_2}{p_1}$

where γ is the isentropic coefficient of the refrigerant, p_1 the evaporating pressure (Pa), p_2 the condensing pressure (Pa), V_{pump} the diverted refrigerant volume flow rate (m^3/s).

The refrigerant mass flow rate can be determined by

$$m_R = \frac{1}{v_{1'}}\left(\left(V_s - V_{pump}\right) - A_{leakage}\sqrt{p_1 v_{1'}}\,\pi^{(\gamma-1)/(2\gamma)}\sqrt{\gamma\left(\frac{2}{\gamma+1}\right)^{(\gamma+1)/(\gamma-1)}}\right)$$

(4.30)

with $v_{1'} = \frac{\zeta r t_{1'}}{p_1}$

where $v_{1'}$ is the specific volume after heating (m^3/kg); $t_{1'}$ is the temperature after heating (℃).

The temperature after heating can then be reevaluated by

$$t_{1'} = t_1 + \frac{W_{loss} + \alpha W_{in} + V_{pump}\Delta p_{pump}}{c_{p,R} m_R} \quad (4.31)$$

The internal power and refrigerant mass flow rate should be calculated again with this updated temperature until it reaches the converged value.

The power consumed by the compressor is

$$W_{comp} = W_{loss} + \alpha W_{in} + W_{in} \quad (4.32)$$

The enthalpy of refrigerant leaving the compressor is

$$h_2 = h_1 + \frac{W_{comp}}{m_R} \quad (4.33)$$

The temperature of refrigerant leaving the compressor is

$$t_2 = t_1 + \frac{h_2 - h_{2'}}{c_{p,R}} \tag{4.34}$$

(2) Detailed Model of Primary and Recovery Heat Exchanger

The recovery heat exchanger is connected directly with compressor to produce hot water. The refrigerant at its outlet may be superheated vapor, or to two-phase mixture depending on the rate of heat to be recovered. The primary condenser after the recovery heat exchanger ejects the remaining part of condensation heat and cools the refrigerant to sub-cooled state.

If the refrigerant leaving the recovery heat exchanger is superheated vapor, the heat recovered is

$$q_{rec} = m_R(h_2 - h_5) \tag{4.35}$$

The remaining condensing heat is the sum of the de-superheating section $q_{cd,sh}$, two-phase section $q_{cd,tp}$ and sub-cooling section $q_{cd,sc}$:

$$q_{cd} = q_{cd,sh} + q_{cd,tp} + q_{cd,sc} \tag{4.36}$$

$$\begin{cases} q_{cd,sh} = m_R(h_5 - h_{2'}) \\ q_{cd,tp} = m_R(h_{2'} - h_{3'}) \\ q_{cd,sc} = m_R(h_{3'} - h_3) \end{cases} \tag{4.37}$$

where subscript 2' and 3' is the dry and liquid saturated refrigerant, respectively.

If the refrigerant leaving the recovery heat exchanger is in two-phase section, the heat recovered is the summation of heat in both de-superheating section $q_{rec,sh}$ and two-phase section $q_{rec,tp}$:

$$q_{rec} = q_{rec,sh} + q_{rec,tp} \tag{4.38}$$

$$\begin{cases} q_{rec,sh} = m_R(h_2 - h_{2'}) \\ q_{rec,tp} = m_R(h_{2'} - h_5) \end{cases} \tag{4.39}$$

The remaining condensing heat becomes the sum of the two-phase section $q_{cd,tp}$ and sub-cooling section $q_{cd,sc}$:

$$q_{cd} = q_{cd,tp} + q_{cd,sc} \tag{4.40}$$

$$\begin{cases} q_{cd,tp} = m_R(h_5 - h_{3'}) \\ q_{cd,sc} = m_R(h_{3'} - h_3) \end{cases} \tag{4.41}$$

With the known condensing heat in each section, the heat transfer effectiveness for each section can be determined by:

$$\varepsilon = \frac{q}{C_{\min}(t_{R,i} - t_{fld,i})} \tag{4.42}$$

where C_{min} is minimum heat capacity of the refrigerant and cooling fluid (water or air). Subscript i represent the inlet condition of each segment.

The NTU of each segment can therefore be determined with known heat transfer effectiveness. The calculation of NTU for different sections and different type heat exchangers are different. The NTU for the single phase de-superheating or sub-cooling section of shell-and-tube condenser is

$$\mathrm{NTU} = -\left(1 + C_r^2\right)^{-1/2} \ln\left(\frac{E-1}{E+1}\right) \quad \text{with}\, E = \frac{2/\varepsilon - (1 + C_r)}{\left(1 + C_r^2\right)^{1/2}} \tag{4.43}$$

The NTU for the single phase de-superheating or sub-cooling section of air-cooled condenser is

$$\mathrm{NTU} = \begin{cases} \dfrac{1}{C_r - 1} \ln\left[\dfrac{\varepsilon - 1}{\varepsilon C_r - 1}\right] & C_r < 1 \\ \dfrac{\varepsilon}{\varepsilon - 1} & C_r = 1 \end{cases} \tag{4.44}$$

The NTU for the two phase section is

$$\mathrm{NTU} = -\ln(1 - \varepsilon) \tag{4.45}$$

Accordingly, the relative areas for recovery heat exchanger and primary condenser, x_{sh}, x_{tp}, x_{sc}, can therefore be determined respectively by:

$$x = \frac{C_{\min}\mathrm{NTU}}{UA} \tag{4.46}$$

where U is heat transfer coefficient for specific section, A is the total heat transfer area of the primary condenser or recovery heat exchanger .

The sum of the relative areas in all the three sections of recovery heat exchanger or primary condenser should satisfy the following equation:

$$x_{sum} = x_{sc} + x_{tp} + x_{sh} \equiv 1 \tag{4.47}$$

If the x_{sum} calculated for recovery heat exchanger is larger or smaller than 1, which means the value of h_5 is over-predicted or under-predicted, the state of refrigerant leaving the recovery heat exchanger should be adjusted by bisection method until the above criterion is satisfied. The same measure applies to the calculation the primary condenser by adjusting the condensing temperature or condenser air flow rate based on the control strategy.

Finally, the temperature of cooling fluid leaving each section of recovery heat exchanger and primary condenser can be calculated by

$$t_{fld,o} = t_{fld,i} + \frac{\varepsilon C_{\min}\left(t_{R,i} - t_{fld,i}\right)}{m_{fld} c_{p,fld}} \tag{4.48}$$

(3) Model of Expansion Valve

The expansion valve reduces the temperature and pressure of the refrigerant from the condenser and is also responsible for maintaining the pressure level of refrigerant in the evaporator. The expansion process across the valve is regarded as isenthalpic:

$$h_3 = h_4 \tag{4.49}$$

(4) Detailed Evaporator Model

A shell-and-tube flooded evaporator is adopted here. Since the refrigerant vapor above the tube bundle is almost saturated, one zone model for two-phase mixture is acceptable. With assumed evaporating temperature t_{ev}, heat transferred in evaporator is

$$q_{ev} = m_R (h_1 - h_4) \tag{4.50}$$

The NTU of the evaporator equals

$$\mathrm{NTU}_{ev} = \frac{U_{ev} A_{ev}}{m_{chw} c_{p,w}} \tag{4.51}$$

The effectiveness of heat transfer is

$$\varepsilon_{ev} = 1 - \mathrm{e}^{-\mathrm{NTU}_{ev}} \tag{4.52}$$

The evaporating temperature t_{ev} can therefore be recalculated by

$$t_{ev} = t_{chwr} - \frac{q_{ev}}{\varepsilon_{ev} m_{chw} c_{p,w}} \tag{4.53}$$

If the difference between this calculated value and initially assumed value of t_{ev} is larger than tolerance, the above approach should be repeated until the criterion is satisfied.

The chilled water supply temperature t_{chws} can then be calculated by

$$t_{chws} = t_{chwr} - \frac{q_{ev}}{m_{chw} c_{p,w}} \tag{4.54}$$

(5) Capacity Factor of Chiller

The detailed condenser and evaporator models and semi-theoretical compressor model requires the configuration data of condenser & evaporator and performance data of chiller to be implemented. In order to predict the performance of chiller in the same series, a non-dimensional parameter called capacity factor is introduced.

The capacity factor is defined as the ratio of the capacity required to the capacity of the reference chiller at the same condition:

$$f_{cap} = \frac{q_{ev}}{q_{ev,0}} \tag{4.55}$$

The reference chiller here is the chiller of which the performance data and configuration data are used for simulation. To predict the performance of a chiller with capacity not equal to that of the reference chiller, the flow rates of chilled water, cooling water should be divided by the capacity factor as the input for simulation. The calculated electricity use by reference chiller should be multiplied by capacity factor to give the final result.

4.3.3 An Algorithm for Modeling

With the characteristic parameters and configuration data of chiller with recovery condenser, the operating variables can be evaluated with the given input data of chilled water flow rate m_{chw}, return temperature t_{chwr}, and supply temperature set-point $t_{chws,sp}$, as well as the cooling water flow rate m_{sw}, its return temperature t_{swr}, and the outdoor air temperature t_a

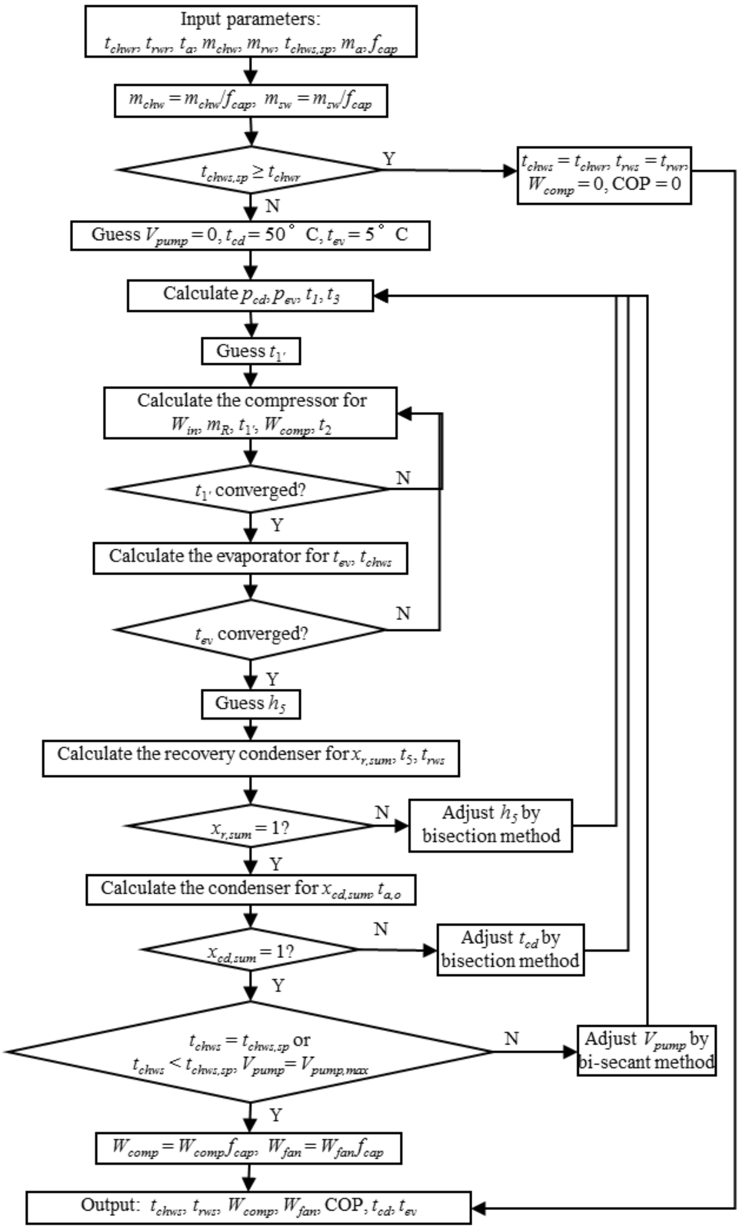

Figure 4.6 Algorithm for chiller with heat recovery

An algorithm for modelling of chiller with heat recovery is described below. Algorithms for two different control schemes, maintaining constant condenser air flow rate m_a or condensing temperature $t_{cd,sp}$, are presented.

(1) Constant air flow rate through condenser

The solution algorithm for control by constant air flow rate through condenser is shown in Figure 4.6. With this control scheme, the maximum and minimum possible condensing temperature can be easily obtained by setting air flow rate to zero or its maximum. If head pressure control is adopted, the minimum condensing temperature of chiller at given operating condition is hard to determine. By constant air flow rate control, both evaporating and condensing temperatures are allowed to change in their operation range. The algorithm begins by assuming the evaporating temperature, condensing temperature and pumping pressure.

First, the evaporating temperature is to be determined. Assume the temperature after heating $t_{1'}$, and the internal cooling load and refrigerant mass flow rate can be determined. The value of temperature after heating can then be updated until it reaches convergence. With the known refrigerant mass flow rate, the cooling load, chilled water supply temperature and re-evaluated evaporating temperature can be determined. If this re-evaluated evaporating temperature does not agree with the assumed or last calculated one, repeat the above calculation until convergence is reached.

Then, the state of refrigerant leaving the recovery heat exchanger is to be determined so as to calculate the temperature of water leaving it. This is achieved by iterative method with an initial assumption of refrigerant enthalpy h_5 leaving the recovery heat exchanger. The state of refrigerant leaving the recovery heat exchanger can be determined when h_5 is known. The heats transferred in each section of recovery heat exchanger can therefore be calculated. And the relative area of each section can be determined. If the sum of the relative area $x_{rec.sum}$ do not equal to 1.0, the assumed value of h_5 is adjusted by bisection method and the relative area of each section is re-evaluated. The cooling water leaving temperature t_{sws} can then be determined when h_5 is finally determined.

Next, the condensing temperature is to be determined. The heat transferred in each section of the primary condenser can be determined with the known h_5 and h_3. The relative areas of each section of primary condenser are calculated using the same method as that for recovery heat exchanger. The sum of the relative areas of each section $x_{cd,sum}$ should equal 1.0. If the difference exceeds a specified tolerance, the condensing temperature t_{cd} will be adjusted by bisection method. The compressor, recovery heat exchanger and primary condenser are recalculated until convergence is reached.

Finally, the throttle rate of the chiller is to be determined. The performance of chiller is by now determined with the assumed refrigerant flow rate by-passed at part-load, V_{pump}. The chilled water supply temperature t_{chws} is to be compared with its set point $t_{chws,sp}$. If the difference exceeds the tolerance, the value of V_{pump} is updated by secant method and the above calculations are repeated. If $t_{chws} < t_{chws,sp}$ with the maximum value of V_{pump} corresponding to the minimum cooling load of the chiller, it means that cooling load is less than the minimum capacity of the chiller. No further iteration is required and the chiller should be cycled by on/off control.

(2) Constant condensing pressure

Constant condensing pressure operation is the most popular operation mode of chiller. While it is suitable for performance prediction of chiller, it is incapable of determine the lowest possible condensing temperature for chiller optimization.

The algorithm is similar to that mentioned above. But instead of assuming condensing temperature, the value of air flow rate through condenser should be assumed and then determined by bisection method through iteration. The other parts of the algorithm are the same.

4.3.4 Validation of the Model

The model of chiller was verified by the catalog data of an air-cooled screw chiller, Trane RTAD 100 (Trane, 2002). Figure 4.7 presents the comparison between the model calculated cooling capacities and COPs and the measured ones. It is shown that the diviation of the calculated value from the measured ones is within ±5% which is acceptable for energy analysis.

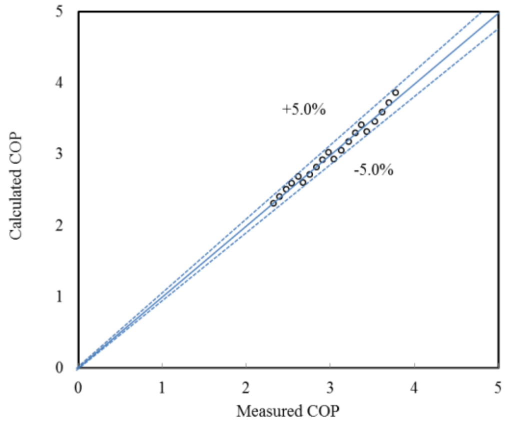

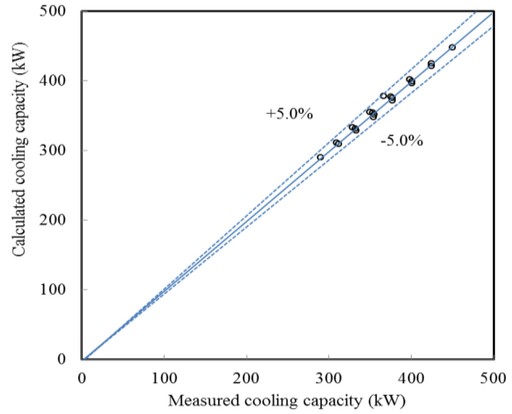

Figure 4.7 Comparison between the calculated and measured cooling capacities and COP of the air-cooled chiller RTAD 100

4.4 Simplified Regression Model of Heat Pump

The DOE model based on regression functions is used, which relate the heating capacity and power consumption to the entering source water temperature and leaving hot water temperature as well as part-load ratio (Hydeman and Gillespie, 2002). They are given by

$$\text{CAPFT} = a_1 + b_1 t_{hws} + c_1 t_{hws}^2 + d_1 t_{swi} + e_1 t_{swi}^2 + f_1 t_{hws} t_{swi} \tag{4.56}$$

$$\text{EIRFT} = a_2 + b_2 t_{hws} + c_2 t_{hws}^2 + d_2 t_{swi} + e_2 t_{swi}^2 + f_2 t_{hws} t_{swi} \tag{4.57}$$

$$\text{EIRFPLR} = a_3 + b_3 \text{PLR} + c_3 \text{PLR}^2 \tag{4.58}$$

$$W = W_{rated} \times \text{CAPFT} \times \text{EIRFT} \times \text{EIRFPLR} \tag{4.59}$$

with $\text{PLR} = \dfrac{Q_h}{Q_{h,rated}\text{CAPFT}}$

where CAPFT is the heat pump capacity as a function of hot water supply temperature t_{hws} (°C) and source water inlet temperature t_{swi} (°C); EIRFT is chiller efficiency as a function of the two temperatures; EIRFPLR is chiller efficiency as a function of part-load ratio PLR. W the power consumed by the heat pump (kW), $Q_{h,rated}$ the rated heat pump capacity (kW), W_{rated} the rated power consumption (kW), *a, b, c, d, e, f* regression coefficients.

The model is validated by the data of heat pump selected: scroll-type McQuay TGZ Templifier water heater (McQuay, 2009). The coefficients of the fitting equations based on the catalogue data are listed in Table 4.2. The calculated COP and the COP provided by the manufacture are shown in Figure 4.8. The maximum error between them is 1.4% for limited operation conditions.

Table 4.2 Coefficients for the performance fitting equations of the heat pump

Coefficient	CAPFT	EIRFT	EIPFPLR
a	0.37642	0.84399	0.04411957
b	-0.00107	0.00598	0.64036703
c	2.01E-05	0.000356306	0.31955532
d	0.01794	-0.0187	
e	0.000286	0.000396203	
f	-0.00018	-0.000625703	

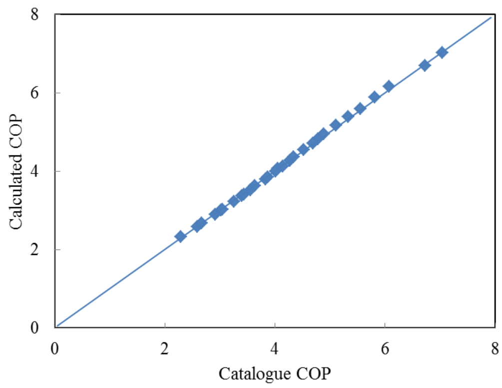

Figure 4.8 Validation of heat pump model

4.5 Effectiveness-NTU Model of Membrane Enthalpy Exchanger

The theoretical model of cross-flow membrane enthalpy exchanger developed by Zhang and Niu (2002) had been validated by their experimental results and is used here. It is analogous to the Effectiveness-NTU method of heat exchanger (Incropera, 2002). The effectiveness of sensible heat transfer and mass transfer for cross-flow type are:

$$\varepsilon_s = 1 - \exp\left[\frac{\exp\left(-\mathrm{NTU}^{0.78} C_r\right) - 1}{\mathrm{NTU}^{-0.22} C_r}\right] \tag{4.60}$$

$$\varepsilon_l = 1 - \exp\left[\frac{\exp\left(-\mathrm{NTU}_l^{0.78} C_{r,l}\right) - 1}{\mathrm{NTU}_l^{-0.22} C_{r,l}}\right] \tag{4.61}$$

with

$$\mathrm{NTU}_l = \beta \cdot \mathrm{NTU} \tag{4.62}$$

where NTU is the number of heat transfer units; C_r is the heat capacity ratio of two air streams; $C_{r,l}$ is the mass flow rate ratio of two air streams. The parameter β is the ratio of number of transfer units for moisture to that for sensible heat, and can be determined by the properties of the membrane and its configuration (Zhang and Niu, 2002). Subscript s stands for sensible heat transfer, and l for the latent heat.

The temperatures and humidity ratios of the supply and exhaust air at the outlet can be determined by

$$\begin{aligned} t_{as,o} &= t_{as,i} - \frac{1}{m_{as} c_{p,a}} \varepsilon_s C_{\min} \left(t_{as,i} - t_{ae,i} \right) \\ \omega_{as,o} &= \omega_{as,i} - \frac{1}{m_{as}} \varepsilon_l C_{l,\min} \left(\omega_{as,i} - \omega_{ae,i} \right) \end{aligned} \tag{4.63}$$

$$\begin{aligned} t_{ae,o} &= t_{ae,i} + \frac{1}{m_{ae} c_{p,a}} \varepsilon_s C_{\min} \left(t_{as,i} - t_{ae,i} \right) \\ \omega_{ae,o} &= \omega_{ae,i} + \frac{1}{m_{ae}} \varepsilon_l C_{l,\min} \left(\omega_{as,i} - \omega_{ae,i} \right) \end{aligned} \tag{4.64}$$

where $C_{l,\min}$ is the minimum of mass flow rate of two air streams; $C_{\min}$ is the minimum of heat capacity rate of two air streams. Subscript *as* stands for supply air, *ae* for exhaust air, *i* for inlet, and *o* for outlet.

4.6 Summary

The models and their numerical solutions of primary components used for air-conditioning system with DOAS of liquid desiccant are developed or introduced in this chapter for performance prediction.

The internally cooled/heated dehumidifier/regenerator is the core of the liquid desiccant system. A simplified numerical model for dehumidifier/regenerator with four flow patterns is adopted in this study. A robust numerical solution for the model is developed by adoption of two measures: the locally linearization of mass transfer term and multi-grid approach. The model is validated using existing experimental data.

A detailed semi-theoretical model of chiller with heat recovery is developed to evaluate both cooling and heat recovery capacities of the chiller. It is a semi-theoretical model because although the models of condenser and evaporator are theoretical, the model of compressor still needs the performance data. Algorithms of the chiller with two different operation schemes are presented. The model is validated by catalogue data.

A simplified regression model of heat pump based on the DOE model for chiller is presented and verified. The effectiveness-NTU model of membrane enthalpy exchanger is also introduced for system analysis and design in the following chapters.

With all these component models, the simulation platform can be developed by TRNSYS. The performances of the components and air-conditioning system can then be simulated, which is work of the following chapters.

CHAPTER 5 A NEW METHOD OF EXERGY ANALYSIS FOR THE THERMODYNAMIC DEVELOPMENT OF HVAC SYSTEMS

New thermodynamic concepts about exergy and a method based on them for exergy analysis are presented in this chapter to correct faulty calculations in the conventional exergy analysis in HVAC engineering for certain conditions. They are also aimed in rational quantifying the real exergy gain for the desired function of equipment or system, and each exergy destruction or loss caused by each factor. The new method is illustrated by exergy analysis of two typical components in liquid desiccant system and is then applied for the analysis of standard air-conditioning system with DOAS using liquid desiccant. A novel integrated air-conditioning system is finally developed, utilizing the analytical results of the standard system.

5.1 Introduction

The exergy of a system is the maximum useful work possibly extracted from it if it could be reversibly brought into equilibrium with a given environment. In contrast to energy analysis, the approach of exergy analysis based on second law of thermodynamics is superior in finding the most efficient way of energy use and identifying real losses in the useful work or energy.

It is critical in exergy analysis to rationally evaluate the thermodynamic performance of equipment and system and compare different thermodynamic systems for the same purpose. “Simple” or “universal” and “rational” or “functional” exergy efficiencies have been widely used in HVAC engineering until now (Torio, 2009). The simple exergy efficiency is defined as the ratio of total exergy outputs to total exergy inputs (Shukuya and Hammache, 2002), ignoring the desired purpose for which the equipment is used. Some of the process outputs that may not be beneficial for the desired purpose are included in the efficiency. For instance, the water condensed from the process air and the return chilled water are both outputs from wet cooling coils, but cannot really make any contribution to the cooling and dehumidification of space. This is because the condensed water is eventually released out of the system, and the leaving chilled water will return back to the chiller. Hence, the simple exergy efficiency can only show the degree of thermodynamic perfectness of thermal processes (Szargut, 1988). However, it cannot truly indicate the percentage of the real desired exergy gain to the truly used exergy.

To overcome the weakness mentioned above, the rational exergy efficiency has been presented and defined as the ratio of the desired exergy gain to the exergy consumed (Shukuya and Hammache, 2002; Tsatsaronis, 2007). The efficiency only takes into account the net exergy output desired for the purpose of equipment and system and the net exergy input. Still using the cooling coils as an example, the net exergy gain of the process air is equal to the exergy difference between the process air at the inlet and outlet of the unit. The consumed exergy in the cooling coils is equal to the exergy difference between the supply and return chilled water. The water condensed in the process of cooling coils is considered as a loss for the function of cooling and dehumidification. When the temperature of incoming process air is lower than or equal to the environment or reference temperature, the rational exergy efficiency can show the percentage of the desired exergy output obtained from the consumed exergy input. It can further evaluate the percentage of exergy output unbeneficial for the cooling and dehumidification of space, and that of exergy destruction due to the other irreversible processes. Thus, the above three values together can also indicate the degree of thermodynamic perfectness of a process in cooling coils.

However, the rational exergy efficiency defined above becomes irrational when the temperature of process air at the inlet of cooling coils is higher than the environment temperature. For instance, if the temperatures of process air at the inlet and outlet of cooling coils are symmetric to the environment temperature, the net exergy gain desired for the cooling and dehumidification of space is equal to zero, according the current definition of the rational exergy efficiency. The reason causing this unreasonable result is that the process air at the inlet and outlet of cooling coils has different types of exergy in reality. The process air at a temperature higher than the environment temperature has “heat”-exergy and otherwise has “cold”-exergy. Subtracting these two different types of exergy each other leads to an unreasonable result. Similarly, there are the other two types of exergy that should be distinguished for dehumidification and humidification. A working medium at moisture content lower than the environment moisture content should have “dry”-exergy, and otherwise “wet”-exergy.

Different types of exergy should be separately treated in arithmetical calculations when the function of equipment is taken into account because they may be beneficial or unbeneficial for the required function of equipment. For instance, the heat-exergy of process air at the inlet of cooling coils is unbeneficial for the function of cooling. The heat-exergy of process air has to be removed before the process air can obtain any cold-exergy to achieve the purpose of cooling. This means the same amount of cold-exergy as that of heat-exergy brought by the process air may have to be consumed in the cooling coils. Therefore, exergy, which is unbeneficial for the required function of HVAC equipment or system, may have to be considered as exergy destruction rather a useful exergy input. Consequently, the exergy input and output should be classified into two types of exergy, beneficial or good and unbeneficial or bad for the required function of equipment or system.

In addition to the above mentioned weaknesses, results from the both current methods of exergy analysis cannot provide an insight to exergy destructions caused by various factors even though the rational exergy efficiency is better than the simple one sometimes in this aspect. This could be a serious barrier to identification of the important factors causing exergy destructions, and in turn to the thermodynamic improvement of HVAC systems. The objective of this chapter is therefore to present the new concepts and method of exergy analysis in order to identify the primary thermodynamic disadvantages and the factors causing them. This should be helpful for the improvement of existing HVAC systems. Application of the new concepts and method to analysis of the standard HVAC system with liquid desiccant dehumidification results in a novel HVAC system of high energy performance.

5.2 Calculation of exergy in air, water and desiccant solution

As described above, there are generally four types of exergy in HVAC engineering for cooling, heating, dehumidification and humidification. A fluid at a temperature either higher or lower than the environment temperature possesses either heat-exergy or cold-exergy. The same equation can be used to compute either heat-exergy or cold-exergy. The calculated exergy should be cold-exergy when the temperature of fluid is lower than the environment temperature, and otherwise heat-exergy. Similarly, the same equation can be adopted to calculate either wet-exergy or dry-exergy, depending on if the moisture content of a fluid is higher or lower than the environment moisture content. Hence, we will only present the symbol of cold- or dry-exergy in those equations that can be used for the calculation of cold- or heat-exergy and dry- or wet-exergy.

When the temperature of air, water or desiccant solution is lower than the reference temperature, its cold-exergy, e^c, can be calculated by

$$e^c = c_p \left(T - T_0 - T_0 \ln \frac{T}{T_0} \right) \tag{5.1}$$

where e is specific exergy rate (kJ/kg), c_p is the specific heat capacity of fluid (kJ/kg-K), T is the temperature of fluid (K), superscript c stands for cold and subscript 0 for the reference state, which is the environment condition in this study.

If the humidity ratio of air is lower than the environment humidity ratio, the dry-exergy of air, $e^d{}_a$, can be calculated by (Szargut, 2005)

$$e_a^d = R_a T_0 \left[(1 + 1.608\omega) \ln \frac{1 + 1.608\omega_0}{1 + 1.608\omega} + 1.608\omega \ln \frac{\omega}{\omega_0} \right] \tag{5.2}$$

where R_a is the specific ideal gas constant for air (0.287 kJ/kg-K) , ω is the humidity ratio (kg water/kg dry air).

The latent heat of evaporation is needed when water evaporates into air. This chemical exergy of water is considered as wet-exergy here, and can be calculated by (Szargut, 2005)

$$e_w^w = -R_v T_0 \ln \varphi_0 \tag{5.3}$$

where R_v is the specific ideal gas constant of water vapor (0.4615 kJ/kg-K), φ_0 is the relative humidity ratio of the reference state ($0<\varphi_0\leq 1$).

When the equilibrium humidity ratio of saturated air on the surface of desiccant solution is lower than the humidity ratio of the reference state, its dry-exergy, $e^d{}_s$, can be calculated by (Szargut et al., 1988)

$$e_s^d = n_{\mathrm{LiCl}}\bar{e}_{\mathrm{LiCl}} + n_{\mathrm{H2O}}\bar{e}_{\mathrm{H2O}} + RT_0\left(n_{\mathrm{H2O}}\ln a_{\mathrm{H2O}} + n_{\mathrm{LiCl}}\ln a_{\mathrm{LiCl}}\right) \tag{5.4}$$

where a is the activity of the water or solute in the solution, n is the mole number of water of solute per kg solution, R is the universal gas constant (8.3145×10^{-3} kJ/mol-K). The last term in Equation (5.4) is a free energy change due to the mixing of water (H2O) and solid solute (LiCl). It is an exergy loss due to the irreversible process of solution formation, and must be negative. The standard chemical exergy, $\bar{e}_{\mathrm{LiCl}}$, of lithium chloride at 298.15 K and 101.325 kPa is 70.7 kJ/mol (Szargut et al., 1988). For engineering application, this chemical exergy at other conditions is approximately equal to the standard chemical exergy (Szargut et al., 1988). The mole chemical exergy of water can be calculated by

$$\bar{e}_{\mathrm{H2O}} = -RT_0 \ln \varphi_0 \tag{5.5}$$

The activity of water in the solution can be calculated by (Palacios-Bereche et al., 2010)

$$\ln a_{\mathrm{H_2O}} = -\phi\cdot v\cdot m\cdot M_{\mathrm{H2O}} \tag{5.6}$$

where v is the dissociation number and equals 2 for LiCl solution, m is the molarity of the solution which is defined as the number of moles of solute per kilogram solvent, M_{H2O} is the mole mass of the water (0.018 kg/mol), ϕ is the osmotic coefficient of water and is determined by

$$\phi = 1 + \sum_{i=1}^{6} c_i m^{i/2} \text{ with } c_i = \sum_{j=0}^{2} c_{ij} T^{-j} \tag{5.7}$$

where coefficients c_{ij} are determined by an approach described by (Kim and Ferreira, 2006), and they are given in Table 5.1 for LiCl; And T is the reference temperature in exergy analysis.

Table 5.1 Coefficients c_{ij} for determining the osmotic coefficient

c	0	1	2
c1j	-1.09612	8.5546E1	-7.7034E4
c2j	-0.56944	5.9212E3	1.3582E5
c3j	4.73256	-2.1071E3	4.1792E4
c4j	-1.41436	2.0761E2	1.1693E5
c5j	-0.41688	4.3272E2	-9.9952E4
c6j	9.781E-2	-7.5604E1	1.4281E4

The activity, a_{LiCl}, of LiCl in the solution can be calculated by

$$\ln a_{\mathrm{LiCl}} = v\left(\ln m + \ln \gamma^{\pm}\right) \tag{5.8}$$

where the activity coefficient, $\gamma^{\pm}$, of LiCl can be determined by (Kim and Ferreira, 2006)

$$\ln \gamma^{\pm} = \sum_{i=1}^{6} \left(1 + \frac{2}{i}\right) c_i m^{i/2} \tag{5.9}$$

The exergy rate, E, of any fluid stream is needed in exergy analysis and can be computed by

$$E_{i,j}^{k}(p_j) = m_i \, e_{i,j}^{k}(p_j) \tag{5.10}$$

where m is a mass flow rate of fluid, e is specific exergy, subscript i is the type of fluid, using a for air, w for water, and s for solution, j is the location of equipment or system, using i for input or at inlet, and o for output or outlet, k is exergy type, using c for cold, h for heat, d for dry, and w for wet, and p is the thermal property of a fluid, such as temperature and humidity ratio. For simplicity of expressions, independent property p in expression of E will be omitted when the specific exergy only depends on single variable.

5.3 Principle of new method for exergy analysis

A new method for exergy analysis is intended to rationally quantify the real exergy gain for the desired function of equipment or system, and each exergy destruction or loss caused by each factor. Equations in exergy analysis highly depend on thermal process, required function and the state of fluids involved. It would be tedious to present all mathematic equations for all possible components in different operation conditions. Hence, the principle of the new method for exergy analysis will be illustrated here by two example units: sensible heat exchanger and desiccant dehumidifier. It should not be difficult to establish the equations of exergy analysis for other processes by following the principle described in this section.

Any exergy efficiency for a desired evaluation can be logically and rationally defined and easily determined based on the physical meaning of above parameters calculated. For instance, the rational exergy efficiency, ψ_r, may be defined as the ratio of real exergy gain and beneficial exergy consumption or net input, i.e.

$$\psi_r = \frac{\Delta E^g_{k,o}}{\Delta E^g_{k,i}} \tag{5.11}$$

where $\Delta E^g_{k,o}$ is the real or effective exergy gain (kW) of the equipment or system k. $\Delta E^g_{k,i}$ is the net beneficial exergy input or beneficial exergy consumption of component or system k.

Equation (5.11) only take into account the input exergy beneficial for the desired function and considers the other input exergy as a loss in the process.

Hence, the value of this rational exergy efficiency may not fully reflect the perfectness of the process. Therefore, the overall rational exergy efficiency is introduced and defined by the ratio of the output exergy beneficial for the desired function to the total exergy input as follows

$$\psi_{or} = \frac{\Delta E_{K,o}^{g}}{\sum_{l=1}^{L} \Delta E_{K,i}^{l}} \tag{5.12}$$

where subscript *or* means overall rational, K is given equipment, i is input; L is the total number of different type exergy inputs including those unbeneficial for the desired function of the equipment. On the other hand, the overall exergy destruction coefficient may also be defined as the total exergy destruction to the total exergy input as follows

$$\psi_{od} = \frac{\sum_{j=1}^{J} \Delta E_{K,j}^{b}}{\sum_{l=1}^{L} \Delta E_{K,i}^{l}} \tag{5.13}$$

where combination of Δ and superscript b means exergy destruction, subscript j is different kinds of exergy destructions, and J is the total number of exergy destructions in the equipment.

5.3.1 Sensible heat exchanger (HE)

A sensible heat exchanger is used generally for either cooling or heating in air-conditioning. An air-to-water counter-flow heat exchanger for cooling is taken as an example here. There may be three scenarios in the temperature variation of two fluid streams referring to the environment temperature, t_0. First, all the temperatures of two fluids involved in the heat exchanger are lower than or equal to the environment temperature. Then, all the equations in the conventional rational exergy analysis can be used, and all the exergy involved should be cold-exergy. Hence, they will not be tediously presented here. Second, warm process air at an inlet temperature ($t_{a,i}$) higher than the environment temperature (t_0) is cooled down to a temperature ($t_{a,o}$) lower than the environment one while all the temperatures of cool water are lower than or equal to the environment one, as shown in Figure 5.1(a). Third, the two fluid streams cross the environment temperature somewhere inside the heat exchanger, as shown in Figure 5.1(b).

In the second case, heat carried by the warm air above the environment temperature has to be removed before the air can obtain any cold energy. The same amount of cold energy provided by the water needs to be used to eliminate this heat. According to heat balance, the water temperature ($t_{w,x}$) at point x of the heat exchanger, where the warm air reaches the environment temperature, may be computed by

$$t_{w,x} = t_{w,o} - \frac{m_a c_{p,a}}{m_w c_{p,w}} (t_{a,i} - t_0) \tag{5.14}$$

where m is mass flow rate (kg/s), c_p is specific heat (kJ/kg °C), subscripts a and w are air and water, subscripts i and o are inlet and outlet, and 0 is reference.

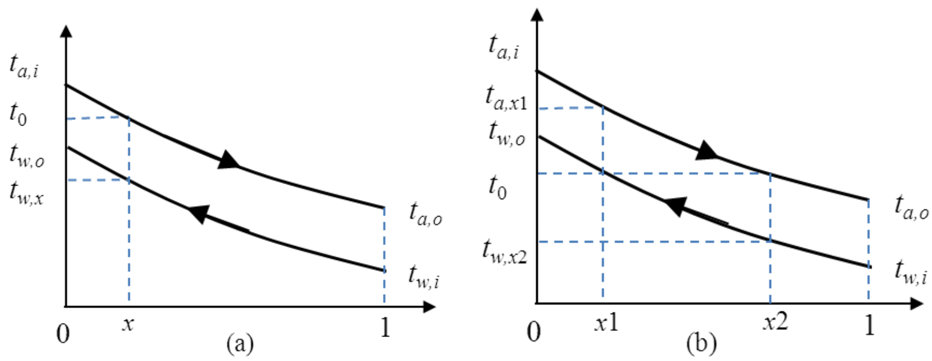

(a) warm air crosses the reference state at point x, (b) two fluids cross the reference state at point x_1 and x_2

Figure 5.1 Temperature variation of two fluids in a counter-flow heat exchanger

The exergy input of the warm air, which is unbeneficial for cooling, should be considered as waste exergy or exergy destruction rather than a useful exergy input. An amount of exergy used in the counteraction of heat and cold energy should be considered as exergy destruction, and can be computed by

$$\Delta E^{b}_{HE,ch} = E^{h}_{a,i} + (E^{c}_{w,x} - E^{c}_{w,o}) \tag{5.15}$$

where combination of *Δ* and superscript *b* means exergy destruction, subscript *HE* is heat exchanger, and *ch* means exergy loss caused by the counteraction of heat and cold energy. Because the warm air crosses the reference temperature in the heat exchanger, the real cold-exergy gain by the process air should be the cold-exergy of outlet air. It can be expressed by

$$\Delta E^{g}_{HE,o} = E^{c}_{a,o} \tag{5.16}$$

where combination of *Δ*, superscript *g* and subscript *o* means beneficial exergy gain. The net cold-exergy input is only provided by the water, and can be given by

$$\Delta E^{g}_{HE,i} = E^{c}_{w,i} - E^{c}_{w,o} \tag{5.17}$$

where combination of *Δ*, superscript *g* and subscript *i* means net exergy input. The thermodynamic irreversibility in a process of heat exchanger may be also due to the limited size of heat exchanger as well as the mismatched heat capacities of warm and cold fluids. Although it is possible to separate the exergy destructions caused by these two factors, it will not be discussed here because this study mainly focuses on the thermodynamic development of DOAS systems. The remaining exergy destruction may be expressed by

$$\Delta E^{b}_{HE,sc} = E^{c}_{w,i} - E^{c}_{w,x} - E^{c}_{a,o} \tag{5.18}$$

where subscript *sc* means exergy loss in the subsequent cooling process due to the two above mentioned remaining factors.

Thus, the total exergy destruction in the heat exchanger may be computed by

$$\Delta E^{b}_{HE} = \Delta E^{b}_{HE,ch} + \Delta E^{b}_{HE,sc} \tag{5.19}$$

The above equations indicate the percentage of exergy destructions caused by different factors can be clearly and accurately quantified, which may be more useful for us to identify primary thermodynamic losses easily in an HVAC system and hence improve it with clear intentions.

Figure 5.1(b) shows that in the third case, the warm air crosses the environment temperature, t_0, at point x_2 while the cool water at point x_1. It can be observed that heat transfer conditions in the two sections between points x_1 and x_2 and between point x_2 and the inlet of cool water are similar to those in the second case. Hence, all the equations and physical explanations described above for the second case should be applicable to these two sections. Because one more section is added in the third case, both subscripts i for inlet of air and o for outlet of water should be replaced by x_1 and x by x_2 in Equations (5.14), (5.15) and (5.18). Equation (5.19) only gives the total exergy destruction in the two sections rather than in the entire heat exchanger.

In the section between the inlet of the warm air and point x_1, there is the transmission of heat-exergy from the warm air to cool water. An exergy destruction in this section (represented by sh) is caused by a temperature difference between the two fluids,

$$\Delta E^{b}_{HE,sh} = (E^{h}_{a,i} - E^{h}_{a,x1}) - E^{h}_{w,o} \tag{5.20}$$

The air temperature at point x_1 where the water temperature reaches the reference temperature is calculated by

$$t_{a,x} = t_{a,i} - \frac{m_w c_{p,w}}{m_a c_{p,a}} (t_{w,o} - t_0) \tag{5.21}$$

The total exergy destruction in the heat exchanger with two fluid streams crossing the environment temperature is the sum of all three types of exergy destruction and is computed by

$$\Delta E^b_{HE} = \Delta E^b_{HE,ch} + \Delta E^b_{HE,sc} + \Delta E^b_{HE,sh} \tag{5.22}$$

5.3.2 Liquid Desiccant Dehumidifier (DEH)

Liquid desiccant dehumidifier with parallel-flow between desiccant solution and water and counter-flow between desiccant solution and air is considered here because it is one of the most concerned components in the system and both heat and mass transfers are involved in it. The desired function of DEH is to dehumidify as well as cool down the process air if sufficient cooling is provided. To avoid tedious describing some unnecessary equations for the exergy analysis of the equipment, only realistic conditions occurring in this component are considered.

Generally, the concentration X_i and temperature $t_{s,i}$ of desiccant solution at the inlet is higher than those (X_o and $t_{s,o}$) of desiccant solution at the outlet: $X_i > X_o$ and $t_{s,i} > t_{s,o}$. The humidity ratio $\omega_{a,i}$ of the process air at the inlet is higher than that ($\omega_{a,o}$) at the outlet and equal to or lower than that (ω_0) of the reference air: $\omega_{a,o} < \omega_{a,i} \le \omega_0$. The temperature $t_{a,i}$ of the process air at the inlet is usually equal to or lower than that of the reference air: $t_{a,i} \le t_0$. The temperature $t_{w,i}$ of cooling water at the inlet is lower than that ($t_{w,o}$) at the outlet and the reference temperature: $t_{w,i} < t_{w,o}$ and $t_{w,i} < t_0$.

For any working medium, we should have the following expressions

$$E_m^c(t_m) = 0 \qquad t_m \ge t_0$$
$$E_m^h(t_m) = 0 \qquad t_m \le t_0 \tag{5.23}$$

The above two equations mean that the cold exergy rate of any working medium should be equal to zero when its temperature is higher than or equal to the reference temperature and that the heat exergy rate of any working medium should be equal to zero when its temperature is lower than or equal to the reference temperature.

The net beneficial exergy gain by the process air through a desiccant dehumidifier is the summation of net dry exergy and cold exergy gains for the desired functions of dehumidification and cooling. Through a dehumidifier, the humidity ratio of air should decrease, and the air temperature should increase first and then decrease. When $t_{a,i} < t_0$, the cold-exergy of the inlet air is counteracted by the heat-exergy of the solution because the air temperature is raised to the level higher than the reference temperature. Hence, the beneficial exergy gain may be computed by

$$\Delta E_{DEH,o}^{g} = \Delta E_a^{d,g} + \Delta E_a^{c,g} = (E_{a,o}^d - E_{a,i}^d) + E_{a,o}^c \tag{5.24}$$

The process air in the desiccant dehumidification process may lose its cold exergy if difference between the exergy rates at the outlet and inlet is negative.

The net beneficial exergy input by desiccant solution and cooling water may be expressed by

$$\Delta E_{DEH,i}^{g} = (E_{s,i}^d - E_{s,o}^d) + (E_{s,i}^c - E_{s,o}^c) + (E_{w,i}^c - E_{w,o}^c) \tag{5.25}$$

Generally, the both solution temperatures at the inlet and outlet of DEH are higher than the reference temperature, i.e., $t_{s,i} > t_0$ and $t_{s,o} > t_0$. This means that the cold energy at these two points is equal to zero, which makes the second term on the right side of Equation (5.25) to be equal to zero.

The desiccant solution at a higher temperature at the inlet of dehumidifier is first cooled down primarily by cooling water to a temperature below the reference, and then is heated up by heat generated from dehumidification. In this heat transfer process, the cold-exergy of the cooling water is eventually counteracted by the heat existing in the inlet desiccant solution and generated during dehumidification. This exergy destruction is computed by

$$\Delta E_{DEH,w,ch}^{b} = E_{w,i}^{c} - E_{w,o}^{c} \tag{5.26}$$

A primary part of process in the dehumidifier is dehumidification besides removing the heat carried by the solution. Exergy destruction in this part of process should include the irreversibility of desiccant dehumidification, the limited capacity of the equipment, as well as unmatched thermal capacity rates among the three working streams., and it may be computed by

$$\Delta E_{DEH,tr}^{b} = (E_{s,i}^{h} + E_{a,i}^{h}) + \Delta E_{DEH,i}^{g} - \Delta E_{DEH,o}^{g} - (E_{w,o}^{h} + E_{s,o}^{h}) \tag{5.27}$$

where subscript *tr* means heat and mass transfer process. Note that the above exergy destruction also includes the heat exergy destruction in the solution and air due to counteract of heat and cooling energy. This exergy destruction can be separately computed when the temperature of solution and air can be found in the simulation of heat and mass transfer process.

5.4 Application of New Exergy Analysis Method

5.4.1 Description of Standard Liquid Desiccant System

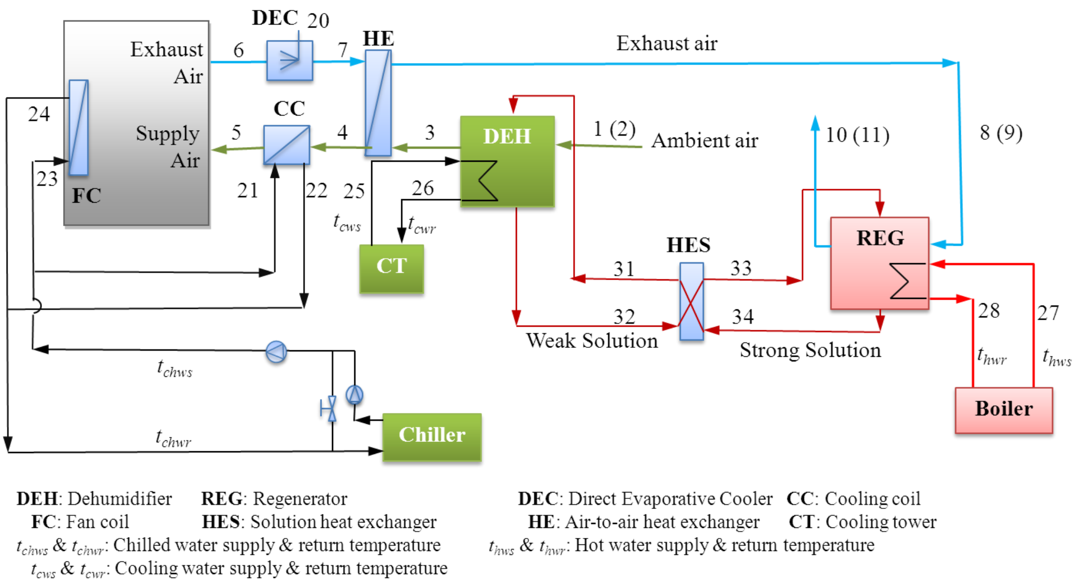

Figure 5.2 Schematic diagram of standard liquid desiccant system

Figure 5.2 presents the schematic diagram of the standard liquid desiccant system. Note that air state numbers in the brackets are kept for the novel proposed system so that the description of them can be easily followed. Hot and humid outdoor air at state 1 (2) is dehumidified by the internally-cooled dehumidifier (DEH). The process air is sensibly heated by heat released from water vapor absorption in the dehumidifier and may be hot at state 3 if the cooling water temperature is limited. The hot process air is cooled down first by the exhaust air through the sensible heat exchanger (HE) and then cooled down by the cooling coil (CC) to the supply condition at state 5. To cool down the process air as much as possible, a direct evaporative cooler (DEC) has been widely adopted in desiccant dehumidification systems to convert the latent heat of the exhaust air to sensible heat. The combination of DEC+HE recovers the sensible and latent heat of exhaust air in terms of sensible cooling energy. The exhaust air at state 6 is humidified and cooled to near saturation condition at state 7 in the direct evaporative cooler. The cooled exhaust air is heated by the process air in the heat exchanger (HE) and is then fed to the regenerator (REG). It removes water vapor released from the weak solution with the assistance of supplied heat in an internally heated regenerator, and is eventually exhausted into the ambient at state 11. The combination of DEH+HES+REG+Boiler forms the dehumidification subsystem of DOAS.

The fan coil (FC) installed in the zone handles only the sensible cooling load by chilled water at an elevated supply temperature (e.g. 13-18°C). The desiccant solution is cooled inside the dehumidifier by cooling water from cooling tower (CT) to remove heat from absorbed water vapor and sensible heat from the desiccant solution. A heat exchanger (HES) is used to recover heat in the concentrated solution leaving the regenerator. Hot water up to 65 °C is pumped to the regenerator for desiccant solution regeneration. The desired solution concentration leaving the regenerator can be controlled by regulating either hot water flow rate or temperature or both of them. The hot water is produced by boilers commonly used in the liquid desiccant systems (Torio et al., 2009).

5.4.2 Exergy Performance of Standard Liquid Desiccant System

For the calculation and analysis of the system, the following operation conditions are used here: $t_0 = t_1 = 30.89$°C; $\omega_0 = \omega_1 = 22.6$ g/kg; $t_6 = 24$°C; $\omega_6 = 9.2$ g/kg; $t_5 = 18$°C; $\omega_5 = 7.5$ g/kg; $t_{chws} = 16$°C; the flow rates of process and exhaust air are $m_{as} = m_{ae} = 0.5$ kg/s; the condensing temperature of chiller is t_{cd} =

46°C. The thermodynamic data for the standard LDCS are presented in detail in Table 5.2.

Table 5.2 Thermodynamic data for the standard system

Properties of air

Point	t_{db}	ω	m	h	e^c	e^h	e^d	e^w	e^t	E^t
	℃	**g/kg**	**kg/s**	**kJ/kg**	**kJ/kg**	**kJ/kg**	**kJ/kg**	**kJ/kg**	**kJ/kg**	**kW**
1	30.9	22.6	0.5	88.7			0		0	0.00
3	31.8	7.5	0.5	51		0.001	0.93		0.931	0.47
4	20.5	7.5	0.5	39.6	0.186		0.93		1.115	0.56
5	18	7.5	0.5	37.1	0.287		0.93		1.217	0.61
6	24	9.2	0.5	47.4	0.081		0.7		0.782	0.39
6s	17	12.1	0.5	47.6	0.336		0.401		0.736	0.37
7	17.7	11.8	0.5	47.5	0.304		0.431		0.735	0.37
7x	28.1	11.8	0.5	58.1	0.014		0.431		0.444	0.22
8	29	11.8	0.5	59	0.006		0.431		0.437	0.22
11	47.3	27.4	0.5	118.2		0.453		0.064	0.517	0.26
12	24	9.2	5	47.4	0.081		0.7		0.782	3.91
13	19.4	9.2	5	42.8	0.227		0.7		0.927	4.64

Properties of water & solution

Point	t_{db}	X_s	m	e^c	e^h	e^d	e^t	E^t
	℃	**kg/kg**	**kg/s**	**kJ/kg**	**kJ/kg**	**kJ/kg**	**kJ/kg**	**kW**
20	17.0		0.001	1.373			1.373	0.00
21	16.0		0.050	1.580			1.580	0.08
22	22.8		0.050	0.459			0.459	0.02
23	16.0		0.820	1.580			1.580	1.30
24	22.8		0.820	0.459			0.459	0.38
25	28.4		0.500	0.044			0.044	0.02
26	37.3		0.500		0.276		0.276	0.14
27	53.6		1.000		3.384		3.384	3.38
28	46.7		1.000		1.670		1.670	1.67
31	38.0	0.400	0.017	0.0	0.220	526.6	526.8	8.80
32	37.3	0.277	0.024	0.0	0.197	324.9	325.1	7.85
33	41.4	0.277	0.024	0.0	0.530	324.9	325.4	7.86
34	44.6	0.400	0.017	0.0	0.811	526.4	527.2	8.80

The flow rate, temperature of air, water and solution as well as humidity ratio and concentration of air and solution are listed. The corresponding specific cold/heat exergy and specific dry/wet exergy of the three fluids determined by their state properties are also presented. These values of exergies are essential for the new exergy analysis method to identify the effective exergy gain and exergy destructions in each process. Point 6s is the saturated state of the indoor air, and point 7x is the point at which the temperature of process air in HE equals to reference temperature, determined by Equation (5.12) with water replaced by exhaust air.

5.4.3 Rational Exergy Analysis of Standard Liquid Desiccant System

The types and amounts of exergies destructed or lost in each component of the standard liquid desiccant system are to be identified according to its function, using the new exergy analysis method introduced in section 5.3. This detailed investigation can provide insight information about how the useful energy input (beneficial exergy) is destructed in the system and can therefore guide the direction of development for an air-conditioning system with high thermodynamic perfection. The beneficial exergy gain ΔE^g, the exergy destructions due to exergy counteraction $\Delta E^b{}_{ch}$, process irreversibility $\Delta E^b{}_{tr}$, exhuast loss $\Delta E^b{}_{ls}$, the total exergy destruction ΔE^b, and the rational efficiency ψ_r of components, subsystem and whole system are determined and listed in Table 5.3.

The cooling coil (CC) in the system is to cool the process air by chilled water. In cooling coil, the input and output exergies of air and water are beneficial exergy because the temperatures of fluids are all below reference temperature and are beneficial for the function of process. This is similar to the first case of sensible heat exchanger described in section 5.3.1. The beneficial cold-exergy gain is the cold-exergy gain by air, 0.051 kW. The exergy destruction of CC is resulted from ineffectiveness of heat transfer process. The exergy destructed is 0.008 kW, which is relatively small as compared to beneficial exergy gain and thus the rational exergy efficiency of CC is 86.1%.

Table 5.3 Exergy gain, destruction, and efficiency of components of standard system

Equipment and system	ΔE^g	ΔE^b_{ch}	ΔE^b_{tr}	ΔE^b_{ls}	ΔE^b	ψ_r
	(kW)	(kW)	(kW)	(kW)	(kW)	(%)
Cooling coil (CC)	0.051		0.008		0.008	86.1%
Chiller (CH)	0.059		0.298	0.562	0.859	6.4%
DOAS-OA Cooling	0.051		0.306	0.562	0.868	5.6%
Heat exchanger (HE)	0.093	0.005	0.052		0.057	62.2%
Direct evaporative cooler (DEC)	0.112		0.065		0.065	63.2%
DOAS-OA Recovery	0.093	0.005	0.117		0.122	43.4%
Dehumidifier (DEH)	0.465	0.022	0.347		0.369	55.7%
Regenerator (REG)	0.949	0.037	0.978	0.259	1.273	42.7%
Solution heat exchanger (HES)	0.008		0.002		0.002	81.4%
Boiler (HP)	1.714		32.135		32.135	5.1%
DOAS-OA Dehumidification	0.465	0.059	33.462	0.259	33.780	1.4%
DOAS subsystem	0.609	0.063	33.820	0.820	34.704	1.7%
Indoor cooling subsystem	0.916		4.186	9.212	13.398	6.4%
Whole system	1.525	0.063	38.006	10.033	48.102	3.1%

The chilled water for cooling coil is provided by chiller (CH). In order to evaluate the performance of cooling subsystem of DOAS, the exergy gain and destruction of CH listed in Table 5.3 only stands for those for chilled water produced for cooling coil. The cold-exergy gain of chiller is the cold-exergy change of chilled water, which is 0.059 kW. The exergy destruction in chiller can be divided into two parts: (1) 0.298kW exergy destruction due to the irreversibility of the heat transfer, compression and expansion processes, and (2) 0.562kW exergy loss due to the release of hot air to the environment. The resulting exergy efficiency of chiller is 6.4%. It should be noticed that dominant part of exergy destruction is due to the exhuast heat-exergy loss. The utilization of this heat-exergy for heating should be able to improve the performance of system considerably.

The combination of CC+CH composes the cooling subsystem of DOAS. The beneficial exergy gain should be the beneficial exergy gain of CC and the exergy destruction should be the sum of them. The total exergy destruction in CC+CH is 0.868 kW and the rational exergy efficiency becomes 5.6%.

The heat exchanger (HE) before the cooling coil cools the process air by exhaust air. From Table 5.2, because the temperature of inlet air is higher than the reference temperature, it is similar to case 2 of sensible heat exchanger described in last section.

The heat-exergy of inlet process air is unbeneficial for the cooling process. The beneficial exergy gain should be the cold-exergy of outlet process air, which is 0.093 kW calculated by Equation (5.16). As mentioned above, the exergy destruction can be divided into two parts: (1) the heat-exergy and cold-exergy destructed in the heat-exergy removal process, which are 0.001 kW and 0.004 kW, respectively. The counteraction of heat-exergy and cold-exergy has double side-effect and should therefore be prevented; and (2) the cold-exergy exergy destructed in the subsequent cooling process is 0.052 kW due to limited component size. Because more exergy is destructed in the process, the rational exergy efficiency of HE is only 62.2%.

The direct evaporative cooler (DEC) converts the latent heat of exhaust air into sensible heat. Although the energy keeps constant in this process, it is an exergy destruction process in nature: part of the beneficial dry-exergy is destructed due to the irreversibility of evaporation and diffusion of water vapor. At the above operation condition, the beneficial cold-exergy gain by air is 0.112 kW. However, due to the irreversibility nature, the total beneficial exergy gain by air should be negative, which is -0.004 kW. The exergy destruction due to the irreversibility is 0.065 kW. In contrast to other components, the component size has side-effect on the performance of DEC. This is because the large component size will result in more perfection of evaporation process and more exergy destruction. In this application, the exergy destruction becomes 0.069 kW if the size of DEC is infinite. As compared to the exergy destruction of 0.065 kW for DEC with finite size, the negative amount of -0.004 kW is caused by the finite component size. This implies that no DEC should be adopted in order to prevent exergy destruction whenever dehumidification is needed.

DEC and HE work together to recover both the dry-exergy and cold-exergy of exhaust air. In this combination of DEC+HE, the beneficial exergy gain is only the beneficial exergy gain of HE, but the exergy destruction is the sum of the two components. Therefore, from Table 5.3, the rational exergy efficiency of this combination decreases to 43.4%, which is much lower than that of single component.

From Table 5.2, the dehumidifier (DEH) only dehumidifies the process air without cooling it, and the temperature water leaving DEH is higher than the reference temperature. The beneficial exergy gain is only the dry-exergy gain by air in DEH, which is 0.465 kW. The net beneficial exergy inputs are the cold-exergy change of water and dry-exergy change of solution. The other exergy variation should be classified as unbeneficial exergy gains. The three parts of exergy destructions are: (1) 0.022 kW cold-exergy of water destructed in the heat-exergy removal process; (2) 0.347 kW cold-exergy of water and dry-exergy of solution destructed in the dehumidification process. The total exergy destruction and loss are 0.369 kW. The rational exergy efficiency of DEH is 55.7%. It is noticed that the outlet water possesses a large amount of heat-exergy which is handled in the cooling tower and wasted. This heat-exergy can be used for the cases where low-quality heating is required, such as for the regeneration of desiccant solution described below.

The regenerator (REG) concentrates the weak solution by utilizing heat input. The beneficial exergy gain is the dry-exergy increase of solution, with a value of 0.949 kW. The net beneficial exergy input includes the heat-exergy changes of water and solutions, dry-exergy change of air. Because the temperature of inlet air is lower than reference temperature, its cold-exergy is unbeneficial input and will be destructed. The exergy destruction of 1.273 kW can also be divided into three parts: (1) 0.037 kW of cold-exergy and heat-exergy counteracted for air heating; (2) 0.978 kW of beneficial heat-exergy of water and dry-exergy of air destructed in the regeneration process due to irreversibility nature of the process and component size; and (3) 0.259 kW heat-exergy loss of air. The rational exergy efficiency of REG is therefore 42.7%. The air leaving REG also possesses considerable heat-exergy that is wasted and would otherwise be utilized. The heating of low-temperature air also consumes considerable amount of high-quality energy. In fact, it would be better to recover the wasted exergy of air leaving REG for the pre-heating of entering air.

The solution heat exchanger (HES) is used to recover the heat-exergy of solution leaving the regenerator to pre-heat the solution entering the regenerator. Because all the temperatures are above the reference temperature and are beneficial for heating, the input and output heat-exergies are beneficial input and output exergies, respectively. The beneficial exergy gain is the increase of heat-exergy of solution in HES, which is 0.008 kW. According to the first case of heat exchanger described in section 5.3.1, the exergy destruction occurred in HES is only caused by the limited size of component and unmatched heat capacity rates, which is 0.002 kW. The rational exergy efficiency is 81.4%.

Boiler produces hot water with heat-exergy. Therefore, the beneficial exergy gain of boiler should be the net heat-exergy change of hot water, which is 1.714 kW. The beneficial exergy input is the 33.85kW fuel-exergy consumption. Thus the exergy destruction is 32.135kW fuel-exergy consumed in the burning and heating process in boiler. Because high-quality fuel energy is used for low-quality heat energy producing, the rational exergy efficiency of boiler is only 5.1%.

The combination of DEH, HES, REG and Boiler forms the dehumidification subsystem of DOAS. The exergy destruction occurred in this subsystem equals to that occurred in the liquid desiccant subsystem plus the exergy destruction in boiler. Therefore, the total exergy destruction in the subsystem is 33.78 kW and the rational exergy efficiency drop sharply to 1.4%.

The indoor-cooling subsystem provides sensible cooling for the zone. It is composed by the cooling terminals installed in the zone and the chiller to produce chilled water. The beneficial exergy gain of the subsystem is 0.916 kW cold-exergy gain by the indoor air. The exergy destructions occurred in this subsystem include the exergy destructed in the chiller and cooling terminals due to irreversibility of the processes and exergy loss due to the release of heat-exergy to the environment. The total exergy destruction is thus 13.398 kW and the rational exergy efficiency of the subsystem is 6.4%.

For the whole system, the beneficial exergy gain is the cold-exergy and dry-exergy gains by the fresh air and indoor air, which is 1.525 kW. The exergy destruction is sum of all the exergy destructed or lost in the system, which is

48.014 kW. The rational exergy efficiency of the system is 3.1%, which is higher than that of the DOAS subsystem but lower than the indoor-cooling subsystem.

5.5 Development of a Novel System with Low Exergy Destruction

The identification of types and magnitudes of exergy destructions and losses in above analysis can guide the direction for performance improvement. A novel system with reduced exergy destructions and losses is to be developed by replacing the processes with large exergy destructions and by effectively utilizing the available waste exergy.

5.5.1 Identification of the largest exergy destruction and loss

From Table 5.3, the largest exergy destruction of the standard system occurs in the boiler, accounting for 94.4% of the total exergy destruction in the DOAS subsystem. This is primarily caused by producing low-quality energy hot water by using high-quality fuel energy in a boiler. The resulting rational exergy efficiency of boiler is merely 5.1%.

The way to improve the exergy efficiency is to replace the boiler by a component with low energy consumption if the desired heat-exergy is to be guaranteed for desiccant regeneration. Free heat-exergy with temperature high enough should be the best choice because no valuable fuel-exergy is to be consumed and the corresponding amount of heat-exergy destruction is small. However, the availability of qualified free exergy is usually restricted. For instance, the availability of waste heat from power plant or factory is limited to their nearby place; the solar energy is unstable and requiring space for installation. Thus, heat pump is therefore a good alternative.

From the exergy analysis of the standard system, there are three main locations where heat energy is released to the environment, including the energy from water leaving the dehumidifier, from air/water leaving condenser of chiller, and from air leaving the regenerator. In order to utilize other waste heat, the heat-exergy of air leaving the regenerator is more suitable for pre-heating the air entering the regenerator by simply installing a recovery heat exchanger after the regenerator. This can not only increase the heat-exergy input of air, but also reduce the heat-exergy input by water. In fact, in the standard system, due to the low exergy efficiency of the boiler, this amount of 0.23kW heat-exergy for air heating will have to be produced by 4.6 kW fuel exergy, which greatly reduce the system exergy efficiency by about 10%. Furthermore, the exergy of fresh air can also be possible heat source for heat pump. The advantage of using fresh air as a heat source is that it can harvest cold-exergy at the same time. These heat sources are to be analyzed below to find the most suitable one.

The quality level of the waste energy is evaluated by the log mean temperature of the medium water t_m, which is determined by

$$t_m = \frac{t_i - t_o}{\ln\left[(t_i + 273.15)/(t_o + 273.15)\right]} - 273.15 \tag{5.28}$$

The log mean temperature of the medium fluid, water or air, available amount of heat and the corresponding exergy provided by the heat sources are listed in Table 5.4. The first heat source is the condensing heat of chiller in the de-superheating section. The cooling flow rate of water is determined by assuming a 5°C drop of water. The degree of this heat energy is the highest, yet the amount of energy of far from regeneration requirement.

Table 5.4 Energy level and amount of varied heating sources

Heat source for heat pump	t_{in} (°C)	t_{out} (°C)	m (kg/s)	t_m (°C)	Q (kW)	E^h (kW)
Regeneration Requirement per zone	56.8	51.8	0.5	54.3	10.6	0.755
Condenser-desuperheater	44.5	39.5	0.5	43.7	3.1	0.123
Condenser-total	43.0	38.0	1.4	40.5	30.3	0.927
Dehumidifier	35.0	29.2	0.3	32.1	7.4	0.028
Fresh air	30.9	23.0	0.5*	26.9	4.7	0.063

* means the fluid rate is for air.

While the temperature of the condensing heat is slightly lower than that of de-superheating heat, the amount of condensing heat is adequate for regeneration. Therefore, partially recovering the condensing heat in the de-superheating section and two-phase section would be the best choice, providing adequate heating at the possibly highest degree level.

Another alternative is the absorption heat released in the dehumidifier. The flow rate and condition of water are from the results of cooling water for dehumidifier. Both the amount and level of energy of the heat obtained are less than those of condensing heat of chiller.

The other heat source comes from the heat released by cooling of the fresh air. Supposing the fresh air is cooled down from 30.9°C to 23°C, it is noticed that the energy level of this heat is the lowest. Furthermore, due to the low temperature and small heat transfer coefficient between air and refrigerant, the evaporating temperature and thus the COP of the heat pump would be low.

Thus, the heat partially recovered from condenser would be the best choice of heating source. The heat from dehumidifier would also be a possible alternative.

5.5.2 Identification of the unnecessary destructions

From Table 5.3, the exergy destruction occurred in the dehumidifier only accounts for 1.5% of total exergy destruction in the DOAS subsystem. Yet the related exergy destructions in regenerator and boiler account for 97.2% of total exergy destruction in the DOAS subsystem. The 98.7% of exergy destruction results from the dehumidification load on the dehumidification subsystem. Thus, the most effective and fundamental way to reduce exergy destruction is to reduce the dehumidification load on dehumidifier. Because the exhaust air possesses beneficial dry-exergy that is not effectively and efficiently utilized in the standard system by direct evaporative cooler and sensible heat exchange, the potential for improvement does exist.

The conversion of dry-exergy to cold-exergy is by no means an exergy efficient way to utilize the dry-exergy of exhaust air. Apart from the exergy destruction in the process, it converts highly valuable latent energy into less valuable sensible energy. More exergy is required to produce the same amount of dry-exergy than cold-exergy. From Table 5.3, while the rational exergy efficiency for cooling is 5.6%, the rational exergy efficiency for dehumidification subsystem is only 1.4%. If the dry-exergy of exhaust air can be recovered directly by the fresh air, the exergy destruction and exergy consumption can both be considerably reduced in the DOAS subsystem.

Thus, the combination of direct evaporative cooler and heat exchanger are an inefficient and ineffective way to recover the dry-exergy of the exhaust air. A good heat recovery system should recover not only the cold-exergy, but also the valuable dry-exergy. Total heat exchanger (membrane enthalpy exchanger or desiccant wheel) is a good alternative. Total heat exchanger installed before the dehumidifier can directly transfer dry-exergy from exhaust air to process air. This will successfully decrease the dry-exergy demand from the dehumidifier and the heat-exergy for regeneration as well. The heat exchanger installed before the cooling coil should still be kept to transfer cold-exergy from exhaust air to process air.

5.5.3 A novel system with high thermodynamic perfection

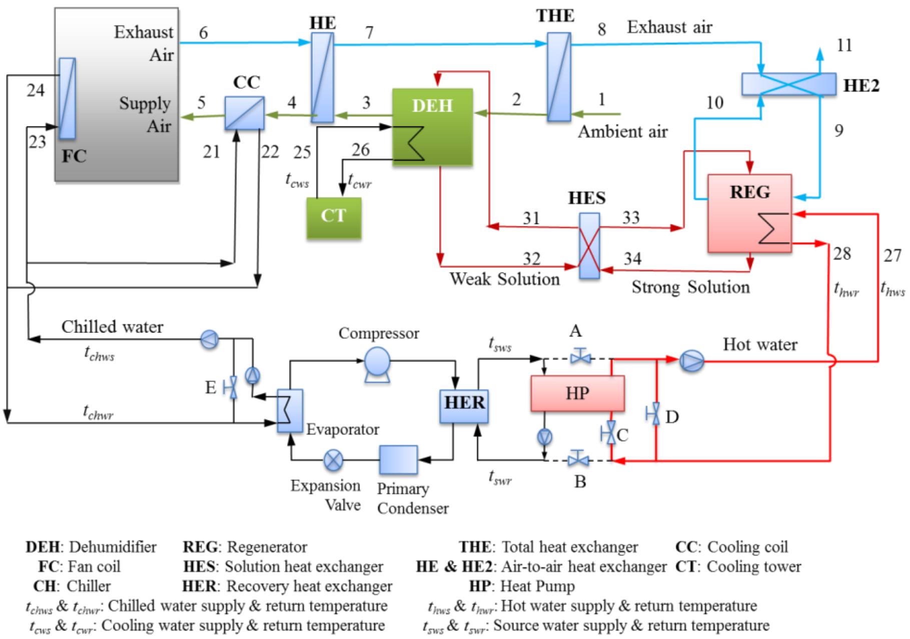

Figure 5.3 Proposed novel hybrid DOAS with liquid desiccant

A novel hybrid DOAS with liquid desiccant that may have less exergy destruction is proposed according to the exergy analysis results of the standard system, as shown in Figure 5.3. In contrast to the standard system, the new system intends to maximize the utilization of sensible and latent energy available in exhaust air, and waste heat at the condenser of chillers to reduce exergy destruction and losses.

The direct evaporative cooler in the standard system is replaced by total heat exchanger (THE) installed before the dehumidifier to recover valuable dry-exergy of exhaust air. Moreover, the arrangement of sensible heat exchanger (HE) and THE in the new system allows us to maximally utilize these cooling and dehumidification potentials. Either membrane enthalpy exchanger or desiccant wheel may be used for total heat recovering. A membrane enthalpy exchanger is considered in this study. Because the latent load on the dehumidifier is reduced, the size of dehumidifier, regenerator, cooling tower can be reduced and the corresponding pump power will decrease accordingly.

Furthermore, a high-efficiency heat pump is installed to replace the boiler for desiccant regeneration. According to the compassion of different heat source for heat pump, the waste heat from condensing heat of chiller, especially the desuperheating part, is the best choice. Therefore, a recovery heat exchanger (HER) is installed between the compressor and primary condenser to partially recovery the condensing heat at higher temperature. Because the temperature lift of the heat pump is small due to the elevated source water temperature, the COP and exergy efficiency of heat pump are supposed to be higher than that of chiller. Moreover, in the new system, for cases with low regeneration heat requirement, waste heat in the superheated section can be directly utilized without using the heat pump with the valve A & B on and valve C off.

To reduce the external exergy loss of the exhaust air, a sensible heat exchanger (HE2) is installed after the regenerator to recover the heat-exergy of the exhaust air leaving the regenerator.

The indoor cooling subsystem which handles the indoor sensible cooling load remains the same with the standard system.

5.6 Comparisons of Exergy Performance of the Two Systems

5.6.1 Exergy performance of the proposed system

The thermodynamic performance of the new system working at the same conditions as those with the standard system is presented in Table 5.5.

Table 5.5 Thermodynamic data for the new system

Properties of air										
Point	t_{db}	ω_a	m_a	h_a	e^c	e^h	e^d	e^w	e^t	E^t
	℃	**g/kg**	**kg/s**	**kJ/kg**	**kJ/kg**	**kJ/kg**	**kJ/kg**	**kJ/kg**	**kJ/kg**	**kW**
1	30.9	22.6	0.5	88.7	0.000		0.000		0.000	0.000
2	30.7	13.9	0.5	66.4	0.000		0.262		0.262	0.131
3	32.3	7.5	0.5	51.6		0.004	0.930		0.933	0.467
4	25.7	7.5	0.5	44.8	0.046		0.930		0.976	0.488
5	18.0	7.5	0.5	37.1	0.287		0.930		1.216	0.608
6	24.0	9.2	0.5	47.4	0.081		0.700		0.782	0.391
6x	29.2	9.2	0.5	52.7	0.011		0.700		0.712	0.356
7	30.7	9.2	0.5	54.2	0.000		0.700		0.700	0.350
8	30.8	17.9	0.5	76.5	0.000		0.073		0.073	0.036
9	47.8	17.9	0.5	94.0		0.469	0.073		0.542	0.271
10	52.0	24.3	0.5	115.1		0.736		0.009	0.745	0.372
11	35.1	24.3	0.5	97.4		0.030		0.009	0.038	0.019
12	24.0	9.2	5	47.4	0.081		0.700		0.782	3.908
13	19.4	9.2	5	42.8	0.227		0.700		0.927	4.636

Properties of water & solution								
Point	t_{db}	X_s	m	e^c	e^h	e^d	e^t	E^t
	℃	**kg/kg**	**kg/s**	**kJ/kg**	**kJ/kg**	**kJ/kg**	**kJ/kg**	**kW**
21	16.0		0.167	1.580			1.580	0.264
22	22.6		0.167	0.487			0.487	0.082
23	16.0		0.848	1.580			1.580	1.340
24	22.6		0.848	0.487			0.487	0.413
25	29.1		0.300	0.021			0.021	0.006
26	35.0		0.300		0.115		0.115	0.035
27	56.8		0.500		4.380		4.380	2.190
28	51.8		0.500		2.875		2.875	1.438
29	42.0		0.865		0.827		0.827	0.715
30	30.9		0.865		0.000		0.000	0.000
31	36.7	0.399	0.017		0.150	525.6	525.776	8.780
32	35.1	0.337	0.020		0.083	416.5	416.604	8.253
33	46.7	0.337	0.020		1.134	416.5	417.654	8.274
34	51.3	0.399	0.017		1.761	525.6	527.333	8.806

Because most of the components of the proposed system are identical to those of standard system, except for the total heat exchanger, the detailed analysis of exergy destruction in these components is not to be fully described here and the results are listed directly in Table 5.6.

Table 5.6 Exergy gain, destruction and efficiency of components of new system

Equipment and system	ΔE^g	ΔE^b_{ch}	ΔE^b_{tr}	ΔE^b_{ls}	ΔE^b	ψ_r
	kW	kW	kW	kW	kW	%
Cooling coil (CC)	0.120		0.063		0.063	65.7%
Chiller (CH)	0.183		0.353	1.814	2.167	7.8%
DOAS-OA Cooling	0.120		0.416	1.814	2.230	5.1%
Total heat exchanger (THE)	0.131		0.183		0.183	41.7%
Heat exchanger (HE)	0.021	0.007	0.012		0.019	52.7%
DOAS-OA Recovery	0.131	0.007	0.195		0.202	39.3%
Dehumidifier (DEH)	0.334	0.006	0.078		0.085	79.8%
Regenerator (REG)	0.526		0.127		0.127	80.5%
Solution heat exchanger (HES)	0.021		0.005		0.005	80.0%
Recovery heat exhanger (HER)	0.235	0.000	0.118	0.019	0.138	63.0%
Heat pump (HP)	0.753		3.969		3.969	15.9%
DOAS-OA Dehumidification	0.334	0.007	4.298	0.019	4.323	7.2%
DOAS subsystem	0.608	0.014	4.908	1.833	6.755	8.3%
Indoor cooling subsystem	0.927		2.506	8.480	10.986	7.8%
Whole system	1.535	0.014	7.414	10.313	17.741	8.0%

The total heat exchanger (THE) recovers both sensible and latent heat of the exhaust air. The beneficial exergy gain in THE is the cold-exergy and dry-exergy gain by fresh air, which is 0.131 kW. The irreversibility of this process is caused by the limited component size and construction, and this exergy destruction can be theoretically divided into two parts: (1) exergy destruction due to the heat transfer and (2) exergy destruction due to mass transfer. In this study, the exergy destruction is mainly caused by the second part of dry-exergy destruction, which is 0.183 kW, accounting for 99.99% of total exergy destruction in THE. In contrast to poor performance of DEC+HE to recover the dry-exergy and cold-exergy of exhaust air in the standard system, the combination of THE+HE in the new system is more effective. The beneficial exergy gain by process air in THE+HE of the new system reaches 0.152 kW, while that in DEC+HE of standard system is only 0.093 kW.

5.6.2 Exergy performance comparison and analysis

From the results of Because most of the components of the proposed system are identical to those of standard system, except for the total heat exchanger, the detailed analysis of exergy destruction in these components is not to be fully described here and the results are listed directly in Table 5.6.

Table 5.6, the proposed new system is clearly superior over the standard one. The rational exergy efficiency of the new system reaches 7.9%, while that of the standard system is only 3.1%. The fuel exergy consumed by the new system is 19.28 kW, which is 30.36 kW less than that by the standard system.

As compared to the high exergy destruction of 33.78 kW in the dehumidification subsystem of the standard system, the exergy destruction occurred in the dehumidification subsystem (DEH+HES+REG+HER+HP) of the new system is reduced by 87.2% to 4.323 kW. Because the beneficial exergy gain is constant and the exergy destruction is reduced, the rational exergy efficiency of dehumidification subsystem surges from 1.4% for the standard system to 7.2% for the new system. This increase can be explained by three reasons.

Firstly, the exergy destructions in dehumidifier and regenerator are reduced due to the decreased dehumidification load. This is the result of effective dry-exergy recovery equipment of total heat exchanger. This can be explained clearly by examination of the thermodynamic data of the new system in Table 5.5. The humidity ratio of process air leaving total heat exchanger decreased to 13.9 g/kg from 22.6 g/kg. The corresponding dry-exergy gain, recovered from the exhaust air, is 0.26kJ/kg. Thus only the dry-exergy of 0.67kJ/kg is to be derived from the dehumidifier. This decreased dehumidification load means decreased exergy destruction in DEH and REG.

Secondly, the exergy destruction in the hot water producing process is partly reduced due to the significantly reduced heat-exergy required for regeneration. In the standard system, the required heat-exergy for regeneration is 1.714 kW. However, it is reduced by 44% to 0.753 kW in the new system. The decrease of heat-exergy for regeneration results from the reduced dehumidification load and the recovery of waste heat-exergy of scavenging air. As mentioned in the last section, the air leaving the regenerator possesses large amount of heat-exergy which is released into the environment and wasted. By the installation of HE2 in the new system, the heat-exergy of 0.29kW can be recovered from the air leaving the regenerator. Therefore, for a component with given efficiency, boiler or heat pump, the exergy destruction should decrease proportionally.

Thirdly, the exergy destruction in the hot water producing process is also reduced by the adoption of heat pump utilizing the condensing heat of chiller. As compared to the low exergy efficiency of boiler (5.1%), the rational exergy efficiency of heat pump utilizing the chiller condensing heat triples to 15.9%.

Another appreciate fact is that the rational exergy efficiency of the chiller is improved from 6.4% to 7.8%. This improvement attributes to the installation of the recovery heat exchanger (HER) to recover the condensing heat of chiller. In this study with constant condensing temperature, the fan power of primary condenser would decrease consequently and thus the increase of rational exergy efficiency. The part of condensing heat recovered for desiccant regeneration also reduces the exhaust exergy loss of chiller and thus contributes to the improvement of exergy efficiency.

One problem with the new system is that the beneficial dry-exergy of scavenging air entering the regenerator is significantly decreased, which may increase the heat-exergy demand for regeneration. Because of the mass transfer in total heat exchanger, about 90% of dry-exergy of exhaust air is either transferred to the fresh air or destructed in the process. While the amount of dry-exergy input into the regenerator by air is 0.27 kW in the standard system, this value decreases by 88.7% to 0.037kW in the new system. It seems that this reduction is unbeneficial for regeneration. However, from the point view of dehumidification subsystem, although this reduction is beneficial for the performance of regenerator, it can contribute more to reduce the exergy destruction in the subsystem as mentioned above.

Another problem with the new system is that although the counteraction of heat-exergy and cold-exergy is reduced, but it still exists in HE and DEH. This irrational operation should be prevented. Yet the solvation of this problem requires the installation of other equipment, which may be uneconomic because the exergy destruction caused by this side-effect is only 0.011 kW, less than 0.2% of the total exergy destruction of DOAS subsystem.

In brief, the exergy performances of the components are highly interconnected. For the improvement of the system, the fundamental reason that causes the exergy destruction and fuel-exergy consumption should be found. All the efforts should be tried to reduce or even eliminate these exergy destructions.

5.7 Summary

A new method for exergy analysis is presented in this chapter to (1) rationally quantify the real exergy gain for the desired function of equipment or system, and each exergy destruction or loss caused by each factor, and (2) guide the development of HVAC system with thermodynamic perfection.

The new exergy analysis method is characterized by classifying the exergies of the fluids into dry-exergy, wet-exergy, cold-exergy and heat exergy, depending on the state of the fluid corresponding to the reference state. These exergies can then be determined as beneficial exergy gains or exergy destructions/losses, depending on the desired function of equipment or system. The new exergy analysis method is illustrated and exemplified by two typical components of liquid desiccant system, sensible heat exchanger and liquid desiccant dehumidifier. Other components and system can be analysis by the same principles.

The new exergy analysis method is applied to the standard air-conditioning system with DOAS using liquid desiccant. A novel integrated air-conditioning system with DOAS using liquid desiccant is then developed based on the analytical results.

The conclusions are as follows:

1) The new exergy analysis method can rationally quantify the real exergy gain and destructions of a process with temperature or humidity ratio crossing the reference state, which is incapable by traditional exergy analysis methods.
2) The new exergy analysis method can effectively determine the exergy

destructions caused by all the factors in a process or system, which guides the direction for improvement.

3) The proposed new system is definitely superior over the standard one in the exergy point of view, whose rational exergy efficiency is 8.0% as compared to 3.1% of the standard system.
4) The improvement comes from three ways identified by the exergy analysis of standard system: (1) the combination of total heat exchanger and sensible heat exchanger to recover the exergy of exhaust air; (2) the replacement of boiler by high performance heat pump which utilizes the condensing heat of chiller as heat source; and (3) the recovering of heat-exergy of air leaving the regenerator.
5) The direct evaporative cooler is an inefficient and ineffective way for dry-exergy recovery, and it should not be adopted and a total heat recover should be used whenever the system needs dehumidification
6) The exergy performances of the components are highly interconnected for complicated systems. The fundamental factors that cause the exergy destruction should be found, which could provide hints for system improvement. Efforts should concentrate on these fundamental factors to reduce or even eliminate exergy destructions.

CHAPTER 6 A NEW COOLING LOAD CALCULATION METHOD FOR INTERMITTENT COOLING BASED ON RTS METHOD

The design of the proposed system needs accurate determination of cooling load of the space. A new cooling load calculation method for intermittent cooling based on the RTS method is developed in this chapter to overcome the weakness of original method which is only suitable for continuous operation of the air-conditioning system. The new model is based on the principle of thermal network and the intermittent cooling load is calculated by response factors obtained from existing RTS factors.

6.1 Introduction

The RTS method currently recommended by ASHRAE Handbook is based on continuous operation. However, most of air-conditioning systems, if not all, in commercial buildings, are intermittently operated in practice. The application of the current RTS method to intermittent air-conditioning in nonresidential buildings could result in underestimated design cooling loads, and inconsistently sized air-conditioning systems. Improperly sized systems could deteriorate the performance of system operation and management. Therefore, a new method based on both the current RTS method and the principles of heat transfer has been developed.

6.2 RTS Equations in a Close-form

ASHRAE Fundamentals (ASHRAE, 2005) presents a RTS method in detail for cooling load calculations. The RTS approach may be further developed by combining relevant equations, and sorting and rearranging equations in a close-form (Chen and Yu, 2009). The close-form of the RTS approach can reduce the amount of calculations, and is useful for developing a new procedure to determine the intermittent peak cooling load.

Cooling loads may be classified by the driving heat sources, namely outdoor dry-bulb and wet-bulb temperatures, global solar radiation incident on the exterior surfaces of external building envelope, direct and diffuse solar radiation transmitted through windows, and internal heat. Equations for computing the first five cooling loads have been derived by Chen and Yu (2009), and will be directly presented without detailed derivations. Cooling loads driven by temperature difference between outdoor and space air temperatures may be computed by

$$q_{c,t_o}(k) = \sum_{j=0}^{23} g_{t_o,j}\left[t_o(k-j)_{24} - t_a(k-j)_{24}\right] \tag{6.1}$$

where

$$g_{t_o,0}(k) = r_{rw,c}\sum_{i=1}^{n_{rw}} c_{i,0}(UA)_i + r_{rw,c}\sum_{i=1}^{n_w}(UA)_{w,i} + m_a c_{pa} + \sum_{l=0}^{23} r_{ns,l}\, a_{(0-l)_{24}}$$

(6.2)

$$g_{t_o,j}(k) = r_{rw,c}\sum_{i=1}^{n_{rw}} c_{i,j}(UA)_i + \sum_{l=0}^{23} r_{ns,l}\, a_{(j-l)_{24}} \quad (j=1,\cdots,23) \tag{6.3}$$

with

$$a_0 = r_{rw,r} \sum_{i=1}^{n_{rw}} c_{i,0} (UA)_i + r_{rw,r} \sum_{i=1}^{n_w} (UA)_{w,i}$$
$$a_j = r_{rw,r} \sum_{i=1}^{n_{rw}} c_{i,j} (UA)_i \quad (j = 1, \cdots, 23) \tag{6.4}$$

The physical meaning of Equation (6.1) through (6.4) is that the total dynamic heat gain is equal to the product of the overall heat conductance UA and the temperature difference, $t_o - t_a$, between outdoor and indoor air at discrete time k. However, when and how much heat is transferred into the space is determined by the dynamic characteristics of a building, which is quantitatively represented by conduction time factors $c_{i,,j}$. and non-solar radiant time factors $r_{ns,j}$. Subscript 24 indicates the number of hours in a periodic design period over 1 – 24 hr. This means that $k - j$ should be replaced by a positive value 24 + ($k - j$) whenever $k - j < 0$. In the equations, a space under consideration has n_{rw} types of roofs and/or walls, and n_w types of windows. Since the convective ratio $r_{rw,cv}$ for roofs and walls is equal to that $r_{w,cv}$ for windows, $r_{rw,cv}$ can replace $r_{w,cv}$ for the reason of simplicity, and $r_{rw,r}$ is the radiant heat ratio. Only a part of the cooling load from infiltration and ventilation ($m_a\ c_{pa}\ (t_o - t_a)$) is included because the other part depends on outdoor moisture content w_o, and will be computed separately. Subscript w represents window. Space air temperature t_a is assumed to be constant in the current RTS method, and will be considered as a variable in this study when the air-conditioning system is not working.

Latent cooling load, $q_{c,vl}$, caused by infiltration and/or ventilation is expressed by

$$q_{c,vl}(k) = m_a h_l \left[w_o(k) - w_a \right] \tag{6.5}$$

where h_l is the average latent heat per unit kg dry air, w is the humidity ratio of moist air, and subscripts o and a are outdoor and indoor air, respectively.

Cooling load due to total solar radiation incident on the exterior surface of walls and roofs may be given by

$$q_{c,E_t}(k) = \sum_{j=0}^{23} g_{E_t,j} E_t (k-j)_{24} \tag{6.6}$$

with

$$g_{Et,j} = \frac{r_{rw,cv}}{h_o} \sum_{i=1}^{n_{rw}} c_{i,j} (UA)_i \alpha_i + \sum_{l=0}^{23} r_l a_{(j-l)_{24}} \tag{6.7}$$

where

$$a_j = \frac{r_{rw,r}}{h_o} \sum_{i=1}^{n_{rw}} c_{i,j} (UA)_i \alpha_i \qquad (j = 0, \cdots, 23) \tag{6.8}$$

where E_t is total solar irradiance incident on the exterior surface of walls and roofs; h_o is convective heat transfer coefficient at the exterior surface of walls and roofs; α_i is the absorbtivity of the exterior surface of wall or roof i; r_l is solar radiant time series; and subscript E_t means cooling loads due to total solar irradiance E_t.

Heat gains due to both diffuse and direct solar radiation, q_s, transmitted through windows may be expressed by

$$q_s(k) = \sum_{i=1}^{n_w} A_{w,i} (IAC)_i \left[< SHGC >_i \; E_d(k) + SHGC_i(\theta(k)) \; E_b(k) \right] \tag{6.9}$$

where A is area (m^2); (IAC) the inside shading attenuation coefficient; $< SHGC >$ the diffuse solar heat gain coefficient; $SHGC(\theta(k))$ the direct solar heat gain coefficient as a function of solar incident angle θ; E solar irradiance incident on the exterior surface of a window, subscript w represents window, d and b are diffuse and beam solar irradiance, and i is the ith window.

Cooling loads from the direct solar radiation through windows may be expressed by

$$q_{c,E_b}(k) = \sum_{j=0}^{23} g_{E_b,j} SHGC^*(\theta(k-j)_{24}) E_b(k-j)_{24} \tag{6.10}$$

with

$$g_{E_b,o} = r_{sb,cv} \sum_{i=1}^{n_w} A_{w,i}(IAC)_i R_{b,i} + \left[r_{sb,r} \sum_{i=1}^{n_w} A_{w,i}(IAC)_i R_{b,i} \right] r_{s,0} \tag{6.11}$$

$$g_{E_d,j} = \left[r_{sb,r} \sum_{i=1}^{n_w} A_{w,i}(IAC)_i R_{b,i} \right] r_{s,j} \tag{6.12}$$

where r_s is solar RTS. When a window does not have blinds, $(IAC) = 1$, $r_{sb,cv} = 0$, and $r_{sb,r} = 1$, and otherwise $(IAC) < 1$, $r_{sb,cv} = 0.37$, and $r_{sb,r} = 0.63$ (ASHRAE, 2005), R_b is the normalized *SHGC* values of a window given by Chen and Yu (2009), $SHGC^*$ is the representative solar heat gain coefficient, and subscript E_b is direct solar irradiance.

Diffuse solar heat gain has the same fraction of the convective cooling load as that ($r_{rw,c}$) from conductive heat gains. Cooling loads due to this heat gain may be expressed by

$$q_{c,E_d}(k) = \sum_{j=0}^{23} g_{E_d,j} E_d(k-j)_{24} \tag{6.13}$$

with

$$g_{E_d,o} = r_{rw,cv} \sum_{i=1}^{n_w} A_{w,i}(IAC)_i \langle SHGC \rangle_i + \left[r_{rw,r} \sum_{i=1}^{n_w} A_{w,i}(IAC)_i \langle SHGC \rangle_i \right] r_{ns,0}$$

(6.14)

$$g_{E_d,j} = \left[r_{rw,r} \sum_{i=1}^{n_w} A_{w,i}(IAC)_i \langle SHGC \rangle_i \right] r_{ns,j} \tag{6.15}$$

where subscript E_d is diffuse solar radiation transmitted through windows.

Heat gain from occupants can be divided into latent and sensible components. The latent heat gain directly becomes instant cooling load. The sensible heat gain can be added to sensible heat gains from the other internal heat sources, such as lights differently installed and electrical equipment. Similarly, this part of cooling loads may be also expressed in a close-form as follows

$$q_{c,h_i}(k) = \sum_{i=1}^{n_{h_i}} [r_{h_i,cv,i} + r_{ns,0} - r_{ns,0} r_{h_i,cv,i}]\, q_{h_i,i}(k) + \sum_{j=1}^{23} r_{ns,j} \sum_{i=1}^{n_{h_i}} (1 - r_{h_i,cv,i})\, q_{h_i,i}(k-j)_{24}$$

(6.16)

Equation (6.16) means that the number of sensible heat sources is n_{hi}, the convective portion of each heat source i is $r_{hi,cv}$, and the nonsolar RTS values, $r_{ns,j}$, should be used to estimate cooling loads from the radiant portion ($1-r_{hi,cv,i}$) of this each heat source i.

6.3 RTS-based Model in Intermittent Air-conditioning

In the intermittent operation of an air-conditioning system, the space air temperature in Equation (6.1) should vary when the air-conditioning system is not working. This causes heat storage during night, and the stored heat then releases later, which results in additional cooling loads over those computed in continuous operation. This part of cooling loads cannot be estimated by the current RTS method because all the given technical data depends on the assumption of constant space air temperature. A model to be developed is based on the RTS method so as to utilize the advantages of RTS method and the available technical data associated with it (ASHRAE, 2005).

Five assumptions are adopted in modeling of intermittent air-conditioning as follows:

1. The both temperatures at the interior surfaces of the internal envelope and the external envelope with heat storage are uniform, separately.

2. The heat storage capacity of space air can be neglected.
3. Heat loss through the external envelope is only caused by temperature difference between the indoor air and the outdoor air, and the loss of radiant heat through the external envelope can be neglected.
4. The variation of the indoor space air temperature in the adjacent spaces is the same as that of the space air temperature under consideration.
5. The governing equations of heat transfer in a space are linear, and hence the principle of superposition can be applied in calculations.

Actually, the last four assumptions are either explicitly or implicitly adopted in the current RTS method. The first assumption is used only for convenient establishing a thermal network, and would not really impact the resultant model.

Utilizing the method for describing a general thermal network of space (Chen and Athienitis, 1993; Chen, 2003), a thermal model based on the first and second assumptions may be established, as shown in Figure 6.1. Nodes *a*, *i*, *e*, *v*, *w* and *r* represent the space air, the interior surface of the internal and external envelopes, the exterior surface of the internal and external envelopes, and the reference, respectively. The overall heat transfer coefficient between nodes is indicated by thermal admittance *y*, and the overall heat conduction through massive internal and external envelopes is described by general thermal admittance Y_i and Y_e. Subscripts 1 and 3 are wall self-admittance, and 2 is wall transfer admittance. T_o and T_{aa} are independent heat sources, the outdoor air temperature and the air temperature in the adjacent space. $Q_{c,sh}$ is cooling load due to solar radiation, internal heat sources, and infiltration and ventilation. Q_c is cooling supplied by air-conditioning system for an assumed constant space air temperature.

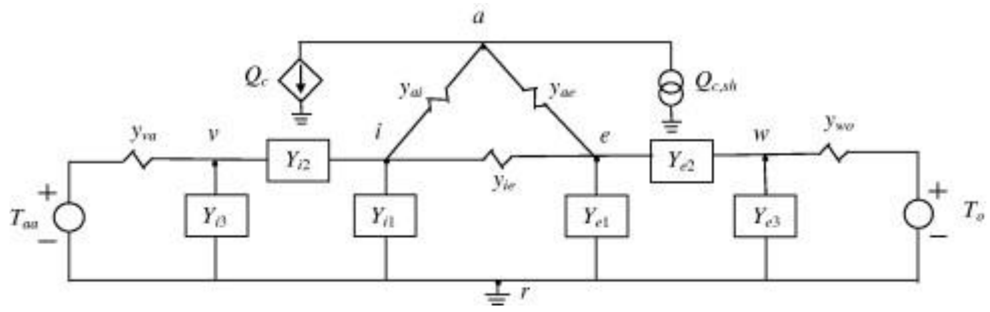

Figure 6.1 Thermal network of a space

Intermittent cooling loads may be derived from cooling loads in continuous operation. An amount of cooling that should be supplied in continuous operation is not provided during the unoccupied hours in intermittent air-conditioning. It is imagined that continuous operation is first carried out. Then supply convective heat to the space during unoccupied hours, which is equal to the calculated cooling load in continuous operation. The overall result of the above operation is actually intermittent air-conditioning. Figure 6.2 shows the additional heat transfer processes in the imagined operation of delivering the convective heat into the space.

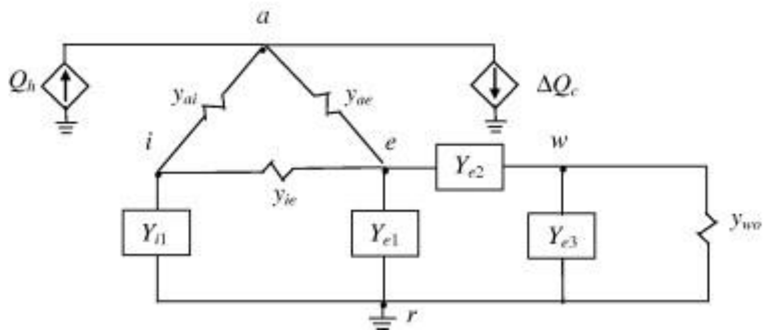

Figure 6.2 Additional thermal network for intermittent operation

Heat balance at node *a* in Figure 6.2 may be expressed in the Laplace domain by

$$Q_h(s) - \Delta Q_c(s) = Y_{st}(s)\Delta T_a(s) + Y_{tf}(s)\Delta T_a(s) \qquad (6.17)$$

where Y_{st} is the heat storage thermal admittance combining two self-admittances Y_{i1} and Y_{e1}; $Y_{tf}(s)$ the overall transfer admittance of the external envelope from node a through nodes e, w and r; ΔT_a the variation of space air temperature due to convective heat supplied; Q_h is convective heat supplied to the space, which is equal to the cooling load computed for continuous air-conditioning; ΔQ_c is the additional cooling load to be removed in intermittent air-conditioning; and s is the Laplace variable. Although these two admittances can be derived from the thermal network in Figure 2, the derivation may not be necessary. This is because only the concept of Equation (6.17) is needed, while the resultant coefficients can be computed directly from the available RTS coefficients.

The inverse Laplace transform of the multiplication of two image functions in the Laplace domain results in the convolution of the respective original functions (Doetsch, 1974). Then, the inverse Laplace transform of image Equation (6.17) yields the following original equation:

$$q_h(t) - \Delta q_c(t) = \int_0^t y_{st}(\tau)\Delta t_a(t-\tau)\,d\tau + \int_0^t y_{tf}(\tau)\Delta t_a(t-\tau)\,d\tau \qquad (6.18)$$

where t is time; q_h, y_{st}, Δt_a and y_{tf} are the original functions corresponding to the respective image functions Q_h, Y_{st}, ΔT_a and Y_{tf} in the image Equation (17). For hourly cooling load calculations, the two convolutions can be written in the discrete form of response factors, which can be further equivalently converted to the periodic form as follows:

$$q_h(k) - \Delta q_c(k) = \sum_{j=0}^{23} y_{st,j} \Delta t_a (k-j)_{24} + \sum_{j=0}^{23} y_{tf,j} \Delta t_a (k-j)_{24} \quad (6.19)$$

where k is discrete time; subscript 24 indicates that the periodic time length is 24 hours; according the physical meaning of y_{st} and y_{tf} in Equation (6.18), $y_{tf,j}$ is equal to overall conduction time series $g_{to,j}$ in Equation (6.1), which can be computed by Equations (6.2) to (6.4); and $y_{st,j}$ is overall RTS coefficients. $y_{st,j}$ is positive when space air temperature at the current time k is not equal to zero, indicating heat stored into the envelope, and negative when space air temperature at the current time k is equal to zero, indicating heat released into the space driven by the air temperature at the other hours. The space air temperature variation $\Delta t_a(k)$ should be equal to zero during the occupied hours.

6.4 Approach to Determine the Additional Cooling Loads

The radiant time series is the periodic transfer response of the space zone to the unit impulse of radiant heat incident on the interior surface. The equivalent amount of heat incident on the same interior surfaces of the space may be driven by space air temperature Δt_a:

$$q_{r,imp} = UA \Delta t_a \quad (6.20)$$

where $q_{r,imp}$ is the impulse of radiant heat input at the initial time; and UA is the overall heat conductance between the space air and the interior surface of the space. The above equation implies that the amount of heat equivalent to $q_{r,imp}$ is incident on the interior surfaces when $\Delta t_a = q_{r,imp} / UA$. Hence, the RTS coefficients responding to the impulse of space air temperature can be directly derived from those due to the impulse of radiant heat.

Heat storage difference between the interior surfaces of the internal and external envelopes is neglected here because they are not distinguished in the RTS method either. This implies that the radiant heat transfer conductance y_{ie} is infinite. From Figure 6.2, the overall heat conductance UA may be expressed by

$$UA = y_{ai} + y_{ae} = h_c(A_i + A_e) \tag{6.21}$$

where h_c is convective heat transfer coefficient over the interior surface; A_i the interior surface area of the internal envelope; A_e the interior surface area of the external envelope excluding windows because heat storage capacity of windows is negligible.

To derive the RTS coefficients responding to the impulse of space air temperature, consider that the impulse of internal radiant heat input, $q_{r,imp}$, acts at the current time k. This will cause a change in space air temperature, Δt_a, which is equal to $1/UA$. The heat release at the current time due to $q_{r,imp}$ should be equal to the nonsolar radiant time coefficient at the current time, i.e. $r_{ns,0}$. The radiant time coefficient of heat storage should be the complement to that of heat release, i.e. 1- $r_{ns,0,}$ based on energy conservation. Then, the radiant time coefficient of heat storage responding to the impulse of space air temperature, Δt_a, should be equal to (1- $r_{ns,0}$)/(1/UA). The other radiant time series responding to the impulse of space air temperature at the other hours for heat release at the current hour, $y_{st,j}$ (j > 0), can be similarly derived. Therefore, the RTS coefficients responding to the impulse of space air temperature for the first discrete convolution on the right side of Equation (6.19) can be determined by

$$\begin{aligned} y_{st,0} &= UA(1 - r_{ns,0}) \\ y_{st,j} &= -UA\, r_{ns,j}, \quad j > 0 \end{aligned} \tag{6.22}$$

where $r_{ns,j}$ is nonsolar RTS coefficients.

In intermittent air-conditioning, precooling is usually adopted to satisfy the required space air temperature at the first occupied hour with a reasonable system size. A general operation schedule for air-conditioning system may be assumed to be as follows: the precooling hour is n_1, the air-conditioning system is operated between n_1+1 and n_2-1, but not from 1 to n_1-1 and from n_2 to 24. The number of equations with the varying space air temperature $\Delta t_a(k)$ should be equal to the number of the hours without air-conditioning. According to Equation (6.19), the space air temperature during the hours without air-conditioning may be expressed by

$$\mathbf{A}\Delta\mathbf{T} = \mathbf{B} \tag{6.23}$$

with

$$\Delta\mathbf{T} = \left[\Delta t_a(n_2) \;\; \Delta t_a(n_2+1) \;\; \cdots \;\; \Delta t_a(24) \;\; \Delta t_a(1) \;\; \cdots \;\; \Delta t_a(n_1-1)\right]^T$$

$$\mathbf{A} = \begin{bmatrix} a(0) & a(23) & \cdots & a(n_2) & a(n_2-1) & \cdots & a(n_2-n_1+1) \\ a(1) & a(0) & \cdots & a(n_2+1) & a(n_2) & \cdots & a(n_2-n_1+2) \\ \vdots & \vdots & \cdots & \vdots & \vdots & \cdots & \vdots \\ a(24-n_2) & a(24-n_2-1) & \cdots & a(0) & a(23) & \cdots & a(24-n_1+1) \\ \vdots & \vdots & \cdots & \vdots & \vdots & \cdots & \vdots \\ a(24-n_2+n_1-1) & a(24-n_2+n_1-2) & \cdots & a(n_1-1) & a(n_1-2) & \cdots & a(0) \end{bmatrix}$$

$$\mathbf{B} = \left[b(n_2) \;\; b(n_2+1) \;\; \cdots \;\; b(24) \;\; b(1) \;\; \cdots \;\; b(n_1-1)\right]^T$$

where **ΔT**, **A** and **B** are the vector of space air temperature, coefficient matrix and vector, respectively. Both the equations and the variables $\Delta t_a(k)$, respectively corresponding rows and columns, are arranged in the order of the unoccupied hours, starting from n_2 to n_2+1, …24, 1,… n_1-1. The index of entries in vectors **ΔT** and **B** is expressed by the hour index. The physical meaning of coefficients in matrix **A** is the overall periodic response factor, and their index can be computed by

$$j = \begin{cases} k - k' & k \ge k' \\ 24 + k - k' & k < k' \end{cases} \tag{6.24}$$

where k is the current hour for the equation under consideration, and k' is the other hours. Examination of matrix **A** shows that the index of all the principal diagonal entries is equal to zero. The summation of the two indexes of any pair of entries that are symmetrical to the principal diagonal is equal to 24 or 0. Note that 24 is the number of hours in a day, and hence it is the same as 0 for the index of the periodic transfer coefficients. The entries of matrix **A** and vector **B** can be computed by

$$\begin{aligned} a(0) &= g_{t_o,0} + (1 - r_{ns,0})\,UA \\ a(j) &= g_{t_o,j} - r_{ns,j}\,UA \qquad j = 1,2,\cdots,23 \end{aligned} \tag{6.25}$$

$$b(k) = q_h(k) - a(k - n_1)\,\Delta t_a(n_1) \tag{6.26}$$

where discrete time k takes all the hours without air-conditioning, i.e. n_2, n_2+1, …, 24, 1, 2, …,n_1-1. For simplicity, the space air temperature at the precooling hour n_1 is assumed to be 0.5°C higher than the constant room air temperature, i.e. $\Delta t_a(n_1)$ = 0.5 °C.

The simultaneous equation (6.23) can be solved by available numerical methods. However, any numerical approach to solving more than four simultaneous equations is generally tedious for manual calculation and difficult for spreadsheet programming. From the results of EnergyPlus simulations, we noticed that there is a sharp increase of the space air temperature in the first two or three hours after the air-conditioning system is shut down and then the space air temperature increases slowly in the following hours. Therefore, the average space air temperature may be used one hour later after air-conditioning system is shut down at hour n_2. Thus, only two variables, $\Delta t_a(n_2)$ and $\Delta t_a(n_2+1)$, are unknown. However, the number of heat balance equations is still equal to the number of the hours without air-conditioning. This will produce conflicts among these simultaneous equations. The best approach to solving these conflict equations is the least square method. A simpler alternative method is to compute the average coefficients from these equations to generate two simultaneous equations first, which can be easily solved. The most simplified approach is to directly use the two equations at the first two unoccupied hours immediately after the air-conditioning system is shut down since they should be important equations due to the largest variation of the space air temperature at these two hours. The two equations are given by

$$
\begin{aligned}
&a(0)\Delta t_a(n_2) + \left[\sum_{j=n_2-n_1+1}^{23} a(j)\right]\Delta t_a(n_2+1) = b(n_2) \\
&a(1)\Delta t_a(n_2) + \left[a(0) + \sum_{j=n_2-n_1+2}^{23} a(j)\right]\Delta t_a(n_2+1) = b(n_2+1)
\end{aligned}
\tag{6.27}
$$

The air-conditioning system will be operated to maintain the required space air temperature from hour n_1+1 to n_2-1. An additional cooling load $\Delta q_c(k)$ due to the release of heat stored during the unoccupied hours can be calculated after the space air temperature variations are calculated by

$$
\Delta q_c(k) = UA\sum_{j=1}^{23} r_{ns,j}\ \Delta t_a(k-j)_{24} \tag{6.28}
$$

Note that the variation of the space air temperature is equal to 0 during the hours from n_1+1 to n_2-1.The total hourly intermittent cooling load $q_{c,t}(k)$ at hour k can finally be obtained by the summation of this additional cooling load $\Delta q_c(k)$ and the cooling load $q_c(k)$ calculated by the conventional RTS method based on continuous operation, given by Equations (6.1) to (6.16), i.e.

$$q_{c,t}(k) = q_c(k) + \Delta q_c(k) \tag{6.29}$$

6.5 Model Validation

The primary objective of this study is to develop a method for direct, reasonable and consistent estimating the peak cooling load in intermittent air-conditioning. Therefore, additional cooling load increase Δq_c computed by the new method, rather than absolute cooling loads estimated by the current RTS method, will be examined and validated in this section.

6.5.1 Zone configurations and properties

A typical zone in different types of office buildings located in Hong Kong at the latitude of 22.33° and the longitude of 114.18° is considered for the validation of the new method. Table 6.1 shows the configurations and properties of a zone used in calculations.

Table 6.1 Zone configurations and properties

Item	Particulars
Floor dimension (L × W)	6 × 4 m
External wall dimension (L × H)	6 × 3 m
Zone orientation	West-facing
Window	Uncoated double-glazed
Ratio of window to external wall	10%, 50%, 90%
Zone construction	See Table 22 on page 30.29 (ASHRAE, 2005)
Indoor convective transfer coefficient	3.08 W/(m2K)

A west-facing zone has one external envelope on one side, and uncoated double-glazed window with 3mm clear type pane and 6 mm air space. The window is type 5a given in Table 13 of Chapter 31 in ASHRAE Handbook (ASHRAE, 2005). Three window sizes, 10%, 50% and 90% of the external envelope, are adopted in calculations. The detailed zone construction including external wall, ceiling, internal partitions and floor is referred to the information given in Table 22 of Chapter 30 on page 30.29 in ASHRAE Handbook (ASHRAE, 2005).

6.5.2 Operation conditions

Table 6.2 indicates the operation conditions of intermittent air-conditioning used in calculations. The latent load is not considered because it cannot be stored, and hence it should be approximately equal to that in continuous operation. For the similar reason, the infiltration and ventilation rate is set to zero. Hourly solar irradiance on July 21 is generated with the clear sky solar radiation model given by ASHRAE (2005). Hourly outdoor dry-bulb temperatures are calculated by EnergyPlus using the maximum dry-bulb temperature and daily temperature range.

Table 6.2 Operation conditions

Item	Particulars
Operation day	July 21
Extreme dry-bulb temperature	32.9 °C
Daily temperature range	4.5 °C
Indoor air temperature	24 °C
Cooling schedule	7:00 – 21:00
Pre-cooling hour	6:00 – 7:00
Indoor set-point in pre-cooling hour	24.5 °C
Ventilation/infiltration	0 m^3/s
Lighting heat	1 kW
The convective heat of lighting	0.36

The operation schedule described in Table 6.2 means that precooling hour n_1 is 6, and shutting down hour n_2 is 22. The space air temperature is assumed to be precooled to 24.5 °C for simplicity, which is 0.5 ℃ higher than the required space air temperature.

6.5.3 Calculation Procedure

The calculation procedure consists of two major steps. First, hourly cooling loads are computed, using Equations (6.1) through (6.16). The close form of the RTS equations presented in this paper allows us to avoid many unnecessary repeated multiplications, and hence makes the method more computationally efficient. Besides, the overall wall conduction time series (CTS) $g_{to,j}$ computed in the first step can be reused for calculating the additional cooling load. In addition to CTS provided in ASHRAE Handbook (2005), the PRF/RTF Generator software developed by Iu (2006) may be used to obtain more accurate CTS. The latter measure is adopted for determining CTS in this study.

In the second step, the hourly cooling loads in the continuous air-conditioning mode are needed in the hours without air-conditioning in the intermittent operation, and the CTS coefficients of the external walls and roof are also needed. These values have been computed in the first step. Then, the following calculation procedure is used to calculate intermittent cooling loads.

1. The RTS coefficients responding to the impulse of space air temperature may be easily computed, using Equation (6.22). The nonsolar RTS can be found in AHSRAE Handbook (2005).
2. Heat balance equations based on Equations (6.23) should be established, and then simultaneously solved by any numerical method (Mathews, 1992) for the space air temperature during the hours without air-conditioning. It may be difficult to program the numerical method into a spreadsheet. Hence, the simplified Equation (6.27) may be adopted using spreadsheet for cooling load calculations.
3. Calculate the additional cooling loads Δq_c(k) due to intermittent air-

conditioning, using Equation (6.28), and then determine the total hourly cooling loads, using Equation (6.29), in the operation hours.

6.5.4 Comparison of Computed Cooling Loads

A FORTRAN computer program with the above-described procedure has been developed. Both the new program and EnergyPlus (EERE, 2008) are used to compute a number of cases based on zone properties in Table 6.1 and operation conditions in Table 6.2. The effect of four important parameters on the peak cooling loads in intermittent air-conditioning is analyzed. These parameters are orientation, window-to-wall-ratio (WWR), and building heat storage capacity, i.e. building weight.

Figure 6.3 shows the variation of hourly cooling loads in continuous and intermittent air-conditioning of a west-facing space with lightweight, medium-weight and heavyweight envelope. The WWR of the external envelope is 50%. Examination of Figure 6.3 shows that the absolute cooling loads computed by the RTS-based method and EnergyPlus are somehow different, and the values generated by the former are generally higher than those by the latter. This means the peak cooling loads calculated by the RTS-based method is on the safe side for sizing air-conditioning systems. The difference of computed cooling loads should be primarily due to inherent features of the RTS method and the method used by EnergyPlus, which is out of the scope of this study. As expected, the cooling loads in intermittent air-conditioning are always higher than those in continuous operation because of heat stored in the building during the hours without air-conditioning. The additional cooling loads due to intermittent operation is larger at the first few hours immediately after air-conditioning is started and becomes smaller in the subsequent hours.

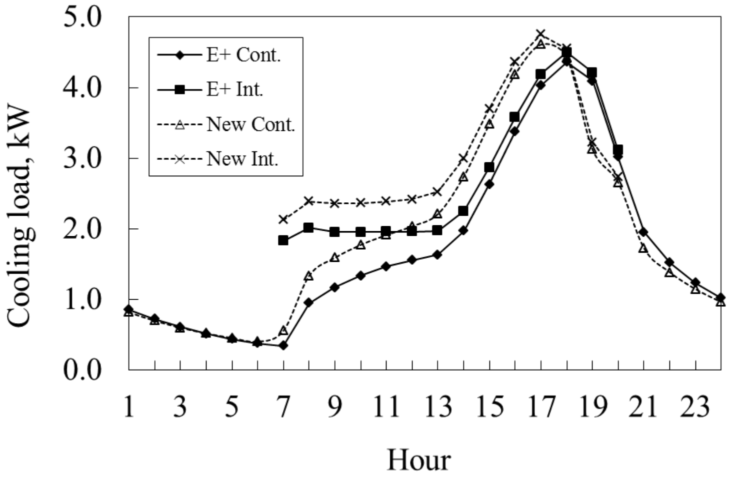

(a) Light-weight envelope

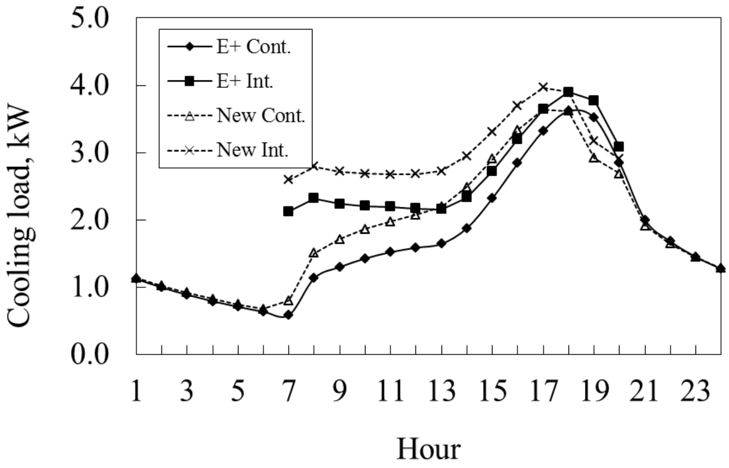

(b) Medium-weight envelope

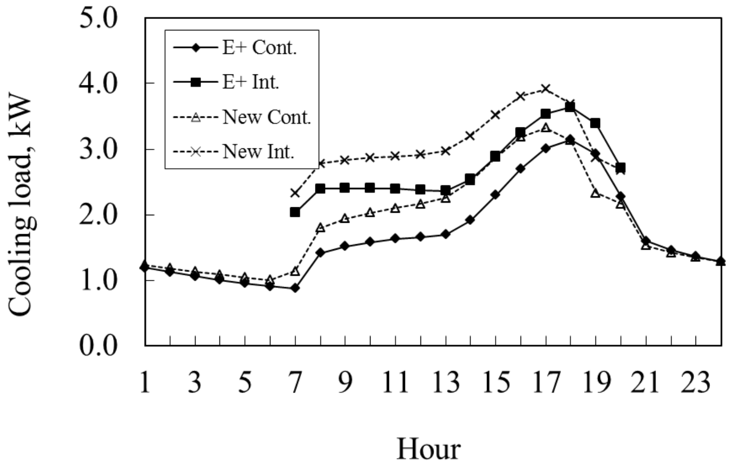

(c) heavy-weight envelope

Figure 6.3 Hourly cooling loads computed by EnergyPlus and new method for different envelope type

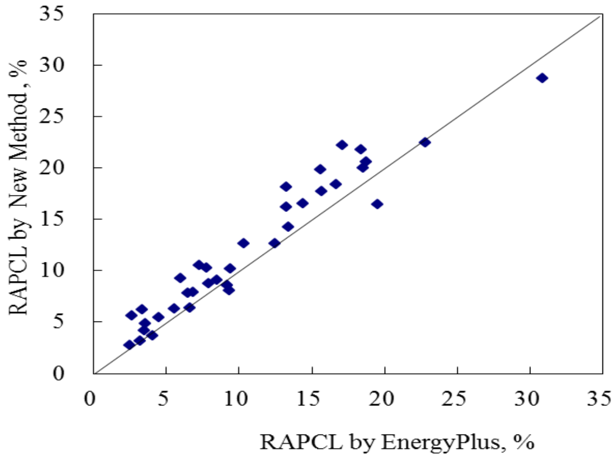

Figure 6.4 Comparison of the RAPCLs calculated by new method and EnergyPlus

Figure 6.4 shows the relative additional peak cooling loads (RAPCL) due to a change from continuous to intermittent operation, computed by EnergyPlus and the new method. The RAPCL is defined as the ratio of the additional peak cooling load (APCL) caused by intermittent operation to the total cooling load in continuous operation, which are computed by the same method or computer program. The solid line shows the relative addition peak cooling loads (RAPCL) generated by EnergyPlus. All the dots represent the RAPCL computed by the new RTS-based method, corresponding to those by EnergyPlus under the same conditions. Examination of Figure 6.4 indicates that the RAPCLs generated by the new method agree well with those simulated by EnergyPlus. The root mean square deviation (RMSD) between the RAPCLs computed by the two methods is 1.8%. The deviation of the RAPCL generated by the new method varies between −3.0% and 5.0% from that given by EnergyPlus, and the mean deviation is 1.35%. The error should be primarily caused by two sources. As mentioned previously, the first source should be differences in the inherent features of the two calculation methods. Unlike the simulation method, the design method need make reasonable assumptions to simplify the calculation procedure so as to make a balance among accuracy, consistence and simplicity in design calculation. The second one should be the neglecting of the loss from internal radiant heat. This is why the overall deviation of the RAPCL computed by the RTS method is positive, which is 1.35%. This factor could be further taken into account by the ratio of the interior surface of the external envelopes to the total interior surface and the ratio of the inward heat conductance from the interior surface of the external envelope to the overall heat conductance.

Table 6.3 indicates how zone orientation, WWR and building weight impact the RAPCL due to a change from continuous operation to intermittent operation.

Table 6.3 RAPCL computed by the new method

WWR	Wall type	RAPCL in eight orientations, %							
		N	NE	E	SE	S	SW	W	NW
10%	Light	4.19	13.46	12.63	11.81	6.27	3.71	3.70	3.39
	Medium	10.30	15.27	16.46	13.46	10.18	8.93	8.58	8.36
	Heavy	22.19	29.47	28.69	27.86	21.75	20.51	20.58	20.24
50%	Light	6.25	9.80	8.07	10.12	5.44	3.16	3.15	3.19
	Medium	10.49	15.33	14.26	13.57	9.08	7.96	8.76	8.21
	Heavy	19.84	24.34	22.44	22.85	18.35	18.17	17.74	17.49
90%	Light	5.59	8.46	6.41	8.14	4.84	2.79	2.76	2.80
	Medium	9.24	12.91	12.61	11.42	7.94	7.17	7.83	7.74
	Heavy	18.16	21.48	20.01	20.39	16.49	16.60	16.18	15.98

It can be observed that the largest RAPCL always occurs in the zone facing-east. The reason is that the peak cooling loads in the east-facing zone occur earlier than in the other orientation zones when intermittent operation most impacts the additional cooling loads. The RAPCL in heavier buildings is generally higher than that in lighter buildings when the other conditions remain the same. On an average, the intermittent peak cooling load increases approximately by 6% for the lightweight envelope, by 10% for the medium weight, and by 20% for the heavyweight. It can also be seen that the additional peak cooling loads generally increase with decrease of WWR.

6.5.5 Verification of the Simplified Method

Figure 6.5 presents a comparison between the RAPCLs obtained by the accurate new method and the most simplified new method. The former needs to accurately solve the simultaneous Equation (6.23), which is difficult to do by spreadsheet or hand calculation. The latter only needs direct solving the two simultaneous Equations (6.27). The solid line at the slope of 45° represents the RAPCLs computed by the former while all the dots indicate those corresponding loads generated by the latter under the same conditions. It can be observed that the RAPCLs obtained by these two methods well agree each other. The RMSD of the RAPCL is about 0.44%. Therefore, the most simplified method should be acceptable for intermittent cooling design.

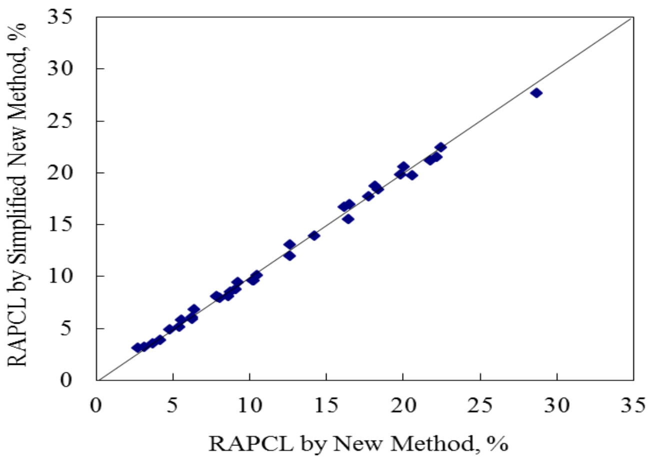

Figure 6.5 RAPCLs computed by the simplified and accurate methods

6.6 Summary

In this chapter, a new method based on both the current RTS method and the principles of heat transfer has been developed for intermittent peak cooling load calculations. The new method can utilize the technical data available in the current RTS method to compute zone responses to a change in space air temperature without the need for regenerating the new data. It simplifies the RTS calculation by the derived equations in a close form, and only needs one more step after the conventional RTS calculations. Both the overall RTS coefficients and the hourly cooling loads computed in the RTS procedure can be utilized to estimate the additional cooling loads due to a change from continuous to intermittent operation.

A large number of simulations with different building constructions, WWR and zone orientations are conducted. The results show that the peak cooling load in intermittent operation may be 2.5–30% larger than that in continuous operation. The additional peak cooling load increases with increase of building weight and with decrease of WWR. It also varies with different orientations, and may reach its highest in east-facing zones.

The RAPCLs generated by the new method and EnergyPlus well agree each other. The RMSD of the RAPCL computed by the new method and EnergyPlus is about 1.8%. The deviation of the RAPCL varies from −3.0% to 5.0%, and the mean deviation is 1.35%. This should be accurate enough for air-conditioning engineering design.

The additional peak cooling loads due to a change from continuous to intermittent operation could be very large and should not be ignored. The simple measure of multiplying the peak cooling load of continuous operation by a certain factor cannot provide reasonably accurate and consistent design cooling loads. The reason is that different factors, such as zone orientation, WWR and building weight, significantly impact the additional peak cooling load.

CHAPTER 7 DESIGN METHOD AND TOOL FOR THE PROPOSED SYSTEM

With the design cooling load, the system can then be rationally designed. This chapter presents the procedure and tool for the design of the proposed system. Because the numerical model of the dehumidifier/regenerator proposed in Chapter 4 is not suitable for design application due to its complexity and numerous calculations, an effectiveness-NTU model for design of dehumidifier and regenerator is developed in this chapter by regression of results calculated by the numerical model. Because of the coupled performance of the dehumidifier and regenerator with other units, iterative approach is adopted for design of the dehumidifier and regenerator. A design procedure and Excel tool are developed in this chapter as well.

7.1 Introduction to Design of Proposed System

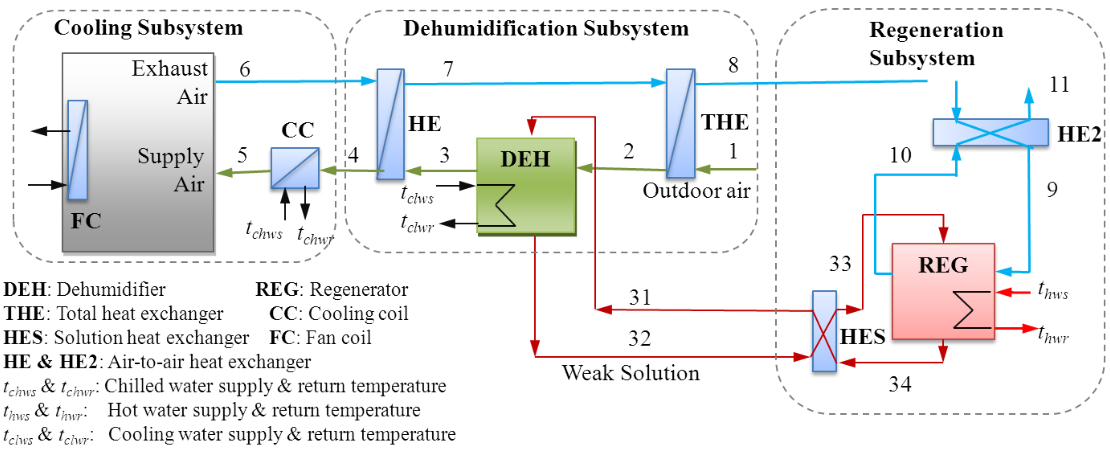

Figure 7.1 Schematic of the proposed system for design

The proposed system is featured by its decoupled temperature and humidity control and by effective harvesting the waste energy available. Depending on the purpose of the components, the system can be split into three subsystems of dehumidification, cooling, and regeneration, as shown in Figure 7.1. The dehumidification subsystem includes components of total heat exchanger, dehumidifier and sensible heat exchanger (HE). The cooling subsystem includes components of cooling coil, fan coil and chiller. The regeneration subsystem is composed of regenerator, air heat exchanger (HE2) and solution heat exchanger (HES).

The design of dehumidifier and regenerator in the dehumidification and regeneration subsystems is the key of whole design process. Yet the numerical model for dehumidifier and regenerator presented in Chapter 4 is complex and requires too much calculation and is therefore not suitable for the design process. An effectiveness-NTU model for the design of internally cooled dehumidifier and internally heated regenerator is preferable. Correlations that directly present the relationship between the performances and dimensions as well as operation parameters are expected. Although such models for adiabatic dehumidifier/regenerator exist (Stevens et al., 1989), models for internally cooled/heated ones are rare in the literature. Khan (Khan, 1998) proposed a simplified model for internally-cooled dehumidifier using the analogy to the effectiveness-NTU model for adiabatic dehumidifier by Stevens (1989), assuming that the solution temperature equals to that of the water. The effect of solution flow rate on the performance of the dehumidifier/regenerator is thus ignored. However, the solution flow rate does noticeably influence the performance of the dehumidifier/regenerator when the mass ratio of solution to air is less than 1/40 (Heinzen et al., 2007). Thus, the development of an effectiveness-NTU model with improved accuracy is the main objective of this chapter for the ease of design.

Even with the effectiveness-NTU model, the design of the dehumidifier and regenerator is not straightforward because their performances are affected by other heat and mass transfer units. The inlet air and solution temperatures for the dehumidifier and regenerator are both unknown for the design of the units at the beginning. Iteration procedure is therefore required to determine their dimensions.

The chiller, heat pump and cooling tower can only be sized when the dehumidification and regeneration subsystems are sized. With regard to the design of chiller, the design cooling load includes not only the sensible cooling load of the space, but also the sensible cooling load of the fresh air imposed on the cooling coil. The space sensible cooling load can be calculated by intermittent cooling load calculation method introduced in previous chapter. The sensible cooling load of the fresh air is also affected by the design of total heat exchanger, dehumidifier and sensible heat exchanger (HE). Only when all the heat and mass transfer units have been designed can the chiller be properly sized.

In this study, an effectiveness-NTU model for internally cooled dehumidifier and internally heated regenerator with flow type F3 is developed. It correlates the heat and mass transfer effectiveness with non-dimensional operation parameters. The coefficients in the correlations are determined by regression of the numerical results for a vast amount of cases. The effects of solution inlet and outlet temperature on the performance of dehumidifier and regenerator are analyzed to validate the feasibility of the decoupled design of dehumidifier and regenerator. The procedures for design of dehumidifier/regenerator and sizing of the chiller and heat pump are introduced in detail. An Excel design tool is developed for engineers to design the proposed system simply by inputting design conditions.

7.2 Simplified Method for Design of Dehumidifier

7.2.1 Effectiveness-NTU Model for Dehumidifier/Regenerator

To predict the performance of the dehumidifier, two performance indices, mass transfer effectiveness and enthalpy effectiveness are introduced. The mass transfer effectiveness is defined as

$$\varepsilon_m = \frac{\omega_{a,i} - \omega_{a,o}}{\omega_{a,i} - \omega_e} \tag{7.1}$$

And the enthalpy effectiveness is defined as

$$\varepsilon_h = \frac{h_{a,i} - h_{a,o}}{h_{a,i} - h_e} \tag{7.2}$$

where ω_e is the saturated humidity ratio of the air in equilibrium with the desiccant solution at water inlet temperature $t_{w,i}$ and solution inlet concentration $X_{s,i}$; h_e is the saturated air enthalpy at temperature $t_{w,i}$ and humidity ratio ω_e. The outlet air conditions can be determined by the two indices of effectiveness.

Correlations that relate the two indices of effectiveness and influencing non-dimensional parameters are proposed for the dehumidifier/regenerator with flow type F3. The correlation for enthalpy effectiveness is proposed based on the theoretical expression of the effectiveness and NTU by Khan (1998). A fitting term that takes the effect of solution flow rate into account is included. The effectiveness of enthalpy for both dehumidifier and regenerator can be given by:

$$\varepsilon_h = \frac{1-\exp\left[-\left(1-C_r^*\right)\mathrm{NTU}_t\left(a_0 + a_1\dfrac{m_{s,i}}{m_a}\right)\right]}{1-C_r^*\exp\left[-\left(1-C_r^*\right)\mathrm{NTU}_t\left(a_0 + a_1\dfrac{m_{s,i}}{m_a}\right)\right]} \tag{7.3}$$

where a_0 and a_1 are regression coefficients; $m_{s,i}/m_a$ is the mass ratio of the solution at inlet to air. C_r* is an equivalent heat capacity ratio defined analogous to the capacitance ratio used in sensible heat exchanger:

$$C_r^* = \frac{m_a c_{\mathrm{sat}}}{m_w c_{p,w}} \tag{7.4}$$

where c_{sat} is the saturation specific heat defined as the derivative of the enthalpy of saturated air in equilibrium with solution at temperature of water and concentration of solution:

$$c_{\mathrm{sat}} = \frac{dh_e}{dt_w} = \frac{h_{e,t_{w,i},X_{s,i}} - h_{e,t_{w,o},X_{s,o}}}{t_{w,i} - t_{w,o}} \tag{7.5}$$

The NTU_t for indirect heat transfer between air and water is determined by:

$$\mathrm{NTU}_t = \frac{\mathrm{NTU}_w \mathrm{NTU}_m \mathrm{Le}}{\mathrm{NTU}_w + \mathrm{NTU}_m C_r^* \mathrm{Le}} \tag{7.6}$$

where Le is the Lewis number which is usually assumed to be unity (Stevens et al., 1989). The NTU_m for mass transfer between air and solution and NTU_w for heat transfer between water and solution are defined as:

$$\mathrm{NTU}_m = \frac{h_D A}{m_a}, \quad \mathrm{NTU}_w = \frac{U_w A}{m_w c_{p,w}} \tag{7.7}$$

Similar to the expression for the enthalpy effectiveness, the mass transfer effectiveness can be expressed as:

$$\varepsilon_m = \begin{cases} \dfrac{1-\exp\left[-\left(1-C_r^*\right)\mathrm{NTU}_m\left(b_0+b_1\dfrac{m_{s,i}}{m_a}\right)\right]}{1-C_r^*\exp\left[-\left(1-C_r^*\right)\mathrm{NTU}_m\left(b_0+b_1\dfrac{m_{s,i}}{m_a}\right)\right]}\left(b_2\dfrac{t_{a,i}}{t_{w,i}}\right) & \left(C_r^* \neq 1\right) \\ \dfrac{\mathrm{NTU}_m\left(b_0+b_1\dfrac{m_{s,i}}{m_a}\right)}{1+\mathrm{NTU}_m\left(b_0+b_1\dfrac{m_{s,i}}{m_a}\right)}\left(b_2\dfrac{t_{a,i}}{t_{w,i}}\right) & \left(C_r^* = 1\right) \end{cases} \tag{7.8}$$

where b_0, b_1, b_2 are regression coefficients; $t_{a,i}$ is the inlet air temperature.

Compared to the enthalpy effectiveness, a term with the inlet temperature ratio of air to water is included in the expression of mass transfer effectiveness because this ratio has evident effect on the effectiveness, especially when the ratio departs far from one.

The values of coefficients in the above effectiveness correlations are obtained by regression from the results calculated by the numerical model described in Chapter 4. A total of 9,000 cases are calculated with varied operating conditions and different dimensions for dehumidifier and regenerator, respectively. The operation range of $m_{s,i}/m_a$ is [0.03,0.10], and the range of m_w/m_a is [0.2, 2.2]. The resulting values of coefficients are listed in Table 7.1. The average errors for both correlations of dehumidifier and regenerator are less than 5%.

Table 7.1 Coefficients in the correlations of effectiveness

		Coefficients			Error	
		0	1	2	Avg. Error	R^2
Dehumidifier	a	1.481	-5.298	-	3.6%	0.994
	b	0.87	-0.42	1.039	1.8%	0.986
Regenerator	a	-	27.584	-	3.4%	0.847
	b	-	10.439	1.102	4.1%	0.94

The results of enthalpy effectiveness calculated by Equation (7.3) and by the model of Khan are compared with those determined by the numerical method, as shown in Figure 7.2. For clarity of display, only a small amount of data is shown. The average error of enthalpy effectiveness by Equation (7.3) is 3.6% for dehumidifier and 3.2% for regenerator, which is much smaller than those by Khan's model with 9.5% for dehumidifier and 9.2% for regenerator. The R^2 is also listed in Table 7.1 to show the goodness of fitting. The R-squared value can be interpreted as the proportion of the variance in the data by simplified model attributable to that by numerical model.

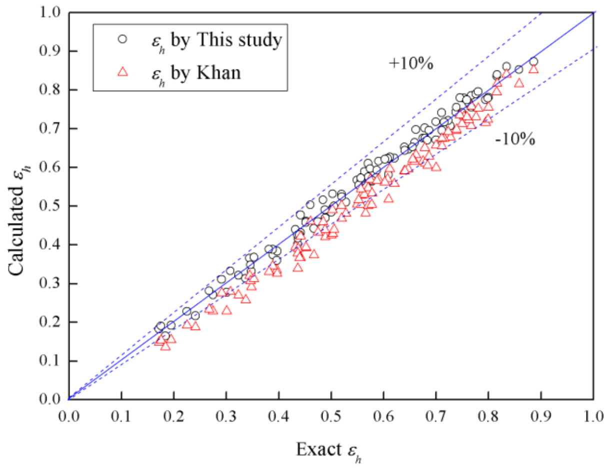

(a) Dehumidifier

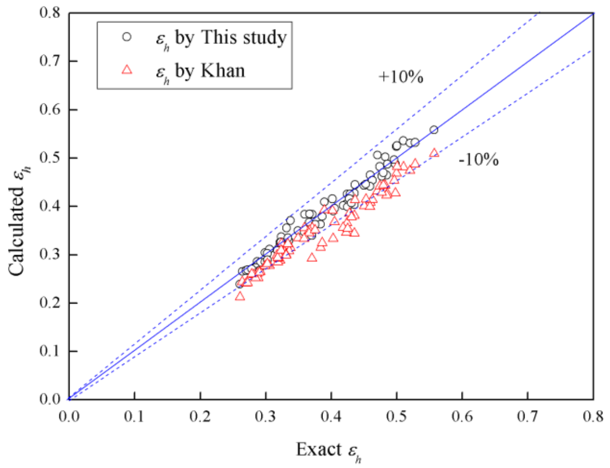

(b) Regenerator

Figure 7.2 Comparison of enthalpy effectiveness calculated by different methods

The mass transfer effectiveness is used for the design of dehumidifier and regenerator with known air inlet and outlet humidity ratio. For the ease of hand calculation, the diagrams of the mass transfer effectiveness at different NTU_m and C_r* are shown in Figure 7.3 for both dehumidifier and regenerator. The diagrams are drawn at constant mass ratio and temperature ratio just to provide preliminary impression about the range of effectiveness. For ratios other than the default ones, the result must be corrected. The ranges of C_r* are different for dehumidification and regeneration, from 0.4 to 1.6 for dehumidification and from 1 to 3 for regeneration. This is because in the regeneration at high temperature, the change rate of saturation enthalpy, which equals to c_{sat} in Equation (7.4), is much larger than that in dehumidification at environmental temperature. Consequently, C_r* is also larger because of the linear relationship with c_{sat}.

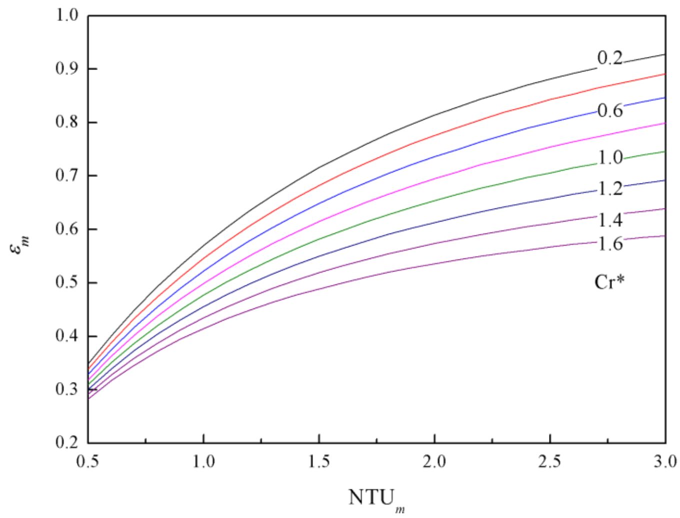

(a) Dehumidifier (with $m_{s,i}/m_a = 0.05$, $t_{a,i}/t_{w,i} = 1.0$)

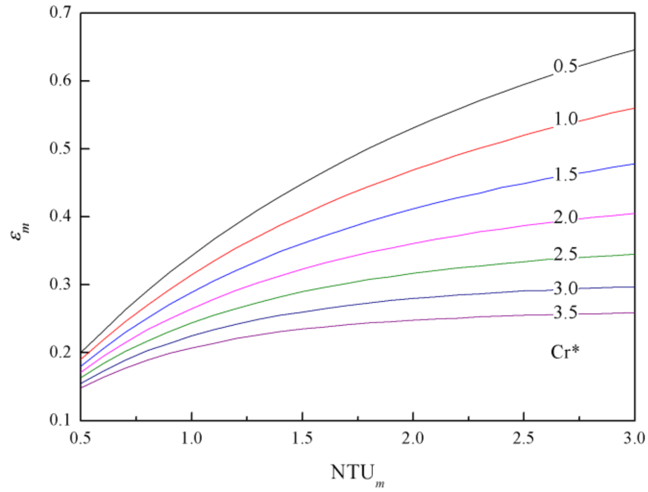

(b) Regenerator (with $m_{s,i}/m_a = 0.05$, $t_{a,i}/t_{w,i} = 0.83$)

Figure 7.3 Effectiveness of mass transfer of internally-cooled dehumidifier and internally-heated regenerator

Because the initially unknown parameter of outlet water temperature is required for the determination of the effectiveness, an iterative procedure is necessary. And because there are four unknown parameters of NTU, the air, water and solution outlet temperatures but only three equations (two correlations of effectiveness and one heat balance), the component still cannot be designed. It seems that another equation for calculating the outlet water or solution temperature is expected. This will be solved in the next section.

7.2.2 Effect of Solution Inlet and Outlet Temperatures

The effect of solution inlet and outlet temperatures on the performance of the dehumidifier/regenerator is investigated for two reasons: (1) the two correlations of effectiveness accompanied by the heat balance equation are inadequate for the determination of the water and solution outlet temperatures, and another heat balance equation is to be provided; (2) in the design process, the solution temperature at dehumidifier inlet is unknown and impacted with the solution temperature at regenerator outlet, which complicates the design of the dehumidifier and regenerator. If the effects of solution inlet and outlet temperatures on the performance of dehumidifier and regenerator can be neglected, the above two problems can be solved.

(1) Solution outlet temperature

The water outlet temperature is required for sizing both cooling tower used for dehumidification and heat pump for regeneration. To determine the temperature by heat balance, the solution outlet temperature should be known. However, as discussed above, no such correlation about the solution outlet temperature exists. The problem can be solved by developing a correlation of the temperature difference between solution and water Δt_{sw} with related variables. Δt_{sw} is a function of the NTU_w and SWMR (ratio of solution-to-water mass flow rates).

$$\Delta t_{sw} = \left(c_0 + c_1 \frac{m_{s,i}}{m_w} \right) \left(c_2 + c_3 \ln(-\mathrm{NTU}_w) \right) \tag{7.9}$$

where c_0, c_1, c_2, c_3 are regression coefficients with the values of 0.457, 6.759, 2.986, -1.141 for dehumidifier. The water outlet temperature can therefore be determined by the heat balance equation as

$$t_{w,o} = \frac{m_w c_{p,w} t_{w,i} + m_a \left(h_{a,i} - h_{a,o} \right) + m_{s,i} c_{p,s,i} t_{s,i} - m_{s,o} c_{p,s,o} \Delta t_{sw} + \Delta \bar{h}_d \left(\omega_{a,i} - \omega_{a,o} \right)}{m_w c_{p,w} + m_{s,o} c_{p,s,o}} \tag{7.10}$$

where $\Delta \bar{h}_d$ is the differential heat of dilution per kilogram water, and can be taken as 200 kJ/kg for dehumidification. The solution outlet temperature is

$$t_{s,o} = t_{w,o} + \Delta t_{sw} \tag{7.11}$$

The temperature difference of inlet and outlet water determined by the above method is shown in Figure 7.4. The results by Equation (7.10) agree well with the numerical results, with a maximum error of 3.2%.

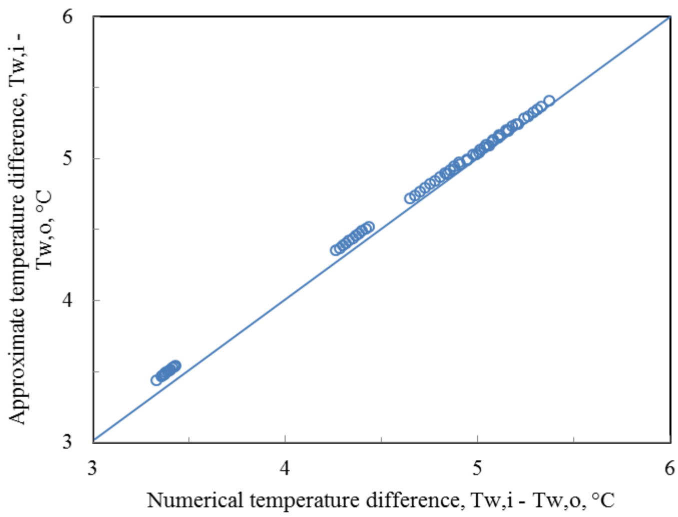

(a) Dehumidifier

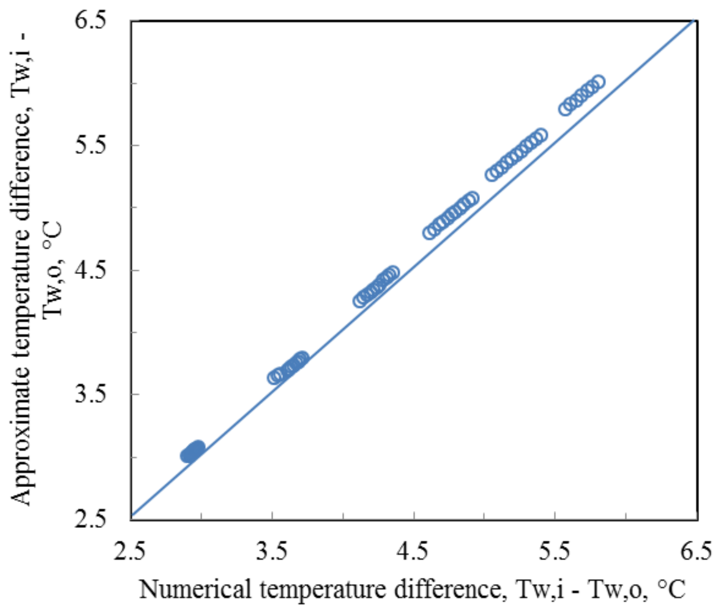

(b) Regenerator

Figure 7.4 Comparison of water temperature difference of by different methods

(2) Solution inlet temperature

The effect of solution inlet temperature $t_{s,i}$ on the performance of the dehumidifier/regenerator is analyzed here because $t_{s,i}$ for dehumidifier is affected by performance of regenerator and solution heat exchanger and vice versa. Iterative calculations may be required to determine $t_{s,i}$ when the heat balance between dehumidifier and regenerator is coupled together. If the effect of $t_{s,i}$ on performance of the dehumidifier and regenerator can be neglected, the interrelated heat balance between dehumidifier and regenerator can be decoupled. This will be discussed as follows. The values of $t_{s,i}$ = 36℃ (dehumidifier) or $t_{s,i}$ = 54℃ (regenerator) are taken as the reference temperatures. The effect of non-dimensional parameter SWMR is also investigated because it is included in the expressions of the two performance indices.

The effects of $t_{s,i}$ on the air outlet humidity ratio $\omega_{a,o}$ for dehumidifier and $X_{s,o}$ for regenerator are shown in Figure 7.5. It is noticed that the effects of $t_{s,i}$ on

$\omega_{a,o}$ and $X_{s,o}$ are relatively small in wide ranges of SWMR and $t_{s,i}$. With the decrease of SWMR, the effect will also decrease due to the lower heat capacity rate of the solution. The maximum difference of $\omega_{a,o}$ at varied $t_{s,i}$ of dehumidifier in the ranges shown is 3.2%. And for regenerator, the maximum difference of $X_{s,o}$ at varied $t_{s,i}$ is only 0.6%. This small errors justify the neglecting of the effects of $t_{s,i}$ on dehumidification or regeneration performance.

The effects of $t_{s,i}$ on the cooling load Q_c for dehumidifier and heating load Q_h for regenerator are shown in Figure 7.6. For the ranges shown, the maximum differences of the cooling load and heating load are 5.8% and 4.8%, respectively. With the increase of effectiveness of the solution-to-solution heat exchanger, the $t_{s,i}$ for dehumidifier decreases and $t_{s,i}$ for regenerator increases, causing smaller difference of cooling load and heating load. Thus, solution-to-solution heat exchanger with high effectiveness is appreciated to reduce the cooling and heating loads.

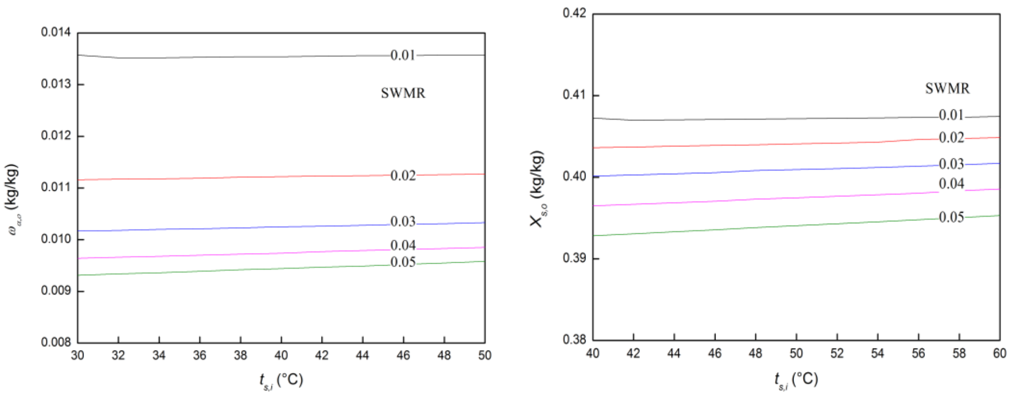

(a) Dehumidifier (AWMR = 1.5) (b) Regenerator (AWMR = 0.8)

Figure 7.5 Effects of solution inlet temperature on air outlet humidity ratio for dehumidifier and solution outlet concentration for regenerator

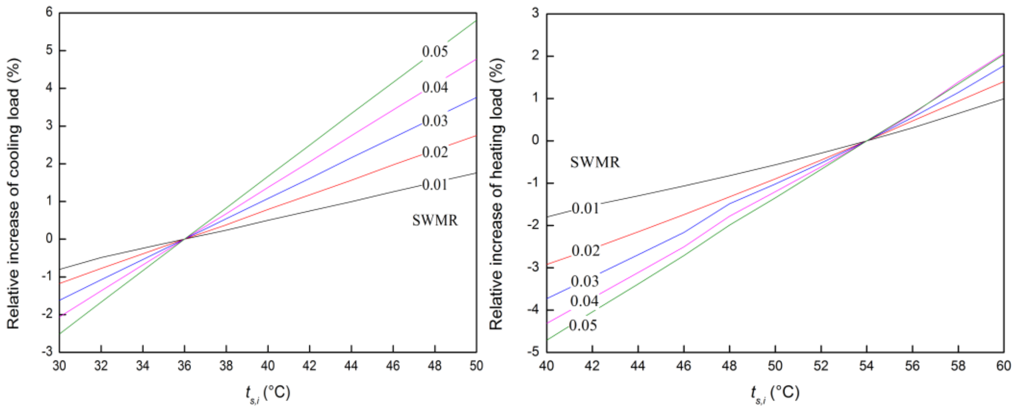

(a) Dehumidifier (AWMR = 1.5) (b) Regenerator (AWMR = 0.8)

Figure 7.6 Effects of solution inlet temperature on the cooling load for dehumidifier and heating load for regenerator

Due to the heat recovery by solution-to-solution heat exchanger, the operation range of $t_{s,i}$ is generally limited to 30-40℃ for dehumidifier and 50-60℃ for regenerator. And the value of SWMR is usually smaller than 0.05. At such conditions, the maximum differences of cooling load and heating load become 2.5% and 2.0%, respectively, and can therefore be neglected.

Thus, with the presence of solution-to-solution heat exchanger, the effects of $t_{s,i}$ on the performance of the dehumidifier and regenerator can be neglected for typical operating range concerned. The design of dehumidifier and regenerator can be decoupled with appropriate selected values of solution inlet temperature, for instance, 36℃ for dehumidifier and 54℃ for regenerator.

7.3 Design Procedure for the Proposed System

The procedure for the design of the proposed system is presented in this section. Due to the coupled performance of dehumidifier and regenerator with other components of the system, iterative approach is necessary for the design of dehumidifier and regenerator. Since the coupled performance of the dehumidifier and regenerator can be decoupled by assuming of constant solution inlet temperature, the interaction between the dehumidification and regeneration subsystems becomes unidirectional. Thus the three subsystems can be designed with the sequence of dehumidification subsystem, cooling subsystem and finally, regeneration subsystem.

7.3.1 Parameters Needed for the Design

Before the design, the indoor design condition and outdoor design weather data for local city should be selected from ASHRAE Handbook of Fundamentals (ASHRAE, 2005) or other sources. For design of dehumidification equipment, the design weather data for dehumidification (dew-point temperature with coincident dry-bulb temperature) should be selected. For given space, its sensible cooling load $Q_{s,z}$, latent cooling load $Q_{l,z}$, and ventilation rate m_{as} are then calculated using cooling load calculation method introduced in previous chapter according to the design criteria and regulations. The exhaust air flow rate m_{ae} should also be determined. The chilled water supply temperature can be ranged from 13-20℃ . The minimum value of chilled water supply temperature should be larger than the dew-point temperature of the indoor air to prevent condensation.

Table 7.2 Parameters required for design of the proposed system

Parameter	Note
t_r	Indoor air temperature
ω_r	Indoor air humidity
$t'_{db,oa}$	Design outdoor air temperature
$t'_{wb,oa}$	The coincident wet-bulb temperature
$t_{db,oa}$	Coincident dry-bulb temperature for design dew-point temperature
$t_{dp,oa}$	Design dew-point temperature
$Q_{s,z}$	Sensible load of the zone
$Q_{l,z}$	Latent load of the zone
m_{as}	Fresh air flow rate
m_{ae}	Exhaust air flow rate
t_{chws}	Chilled water supply temperature

For the heat and mass transfer equipment, the values of effectiveness of heat and/or mass transfer should be pre-determined for their sizing as listed in Table 7.3. With the given effectiveness and fluids flow rates, the dimensions of such components can be directly determined.

Table 7.3 Effectiveness of components

Effectiveness	Value	Note
$\varepsilon_{THE,s}$	0.75	Sensible effectiveness for total heat exchanger, 0.5-0.85
ε_{HE1}	0.75	Effectiveness for air-to-air heat exchanger, 0.5-0.85
ε_{HE2}	0.75	Effectiveness for air-to-air heat exchanger, 0.5-0.85
ε_{SHE}	0.9	Effectiveness for solution heat exchanger, 0.8-0.95
ε_{CC}	0.8	Effectiveness for air-to-water heat exchanger, 0.7-0.9
ε_{FC}	0.8	Effectiveness for air-to-water heat exchanger, 0.7-0.9

7.3.2 Design of the Dehumidification and Cooling Subsystems

The design of dehumidification and cooling subsystems includes the design of three key components of total heat exchanger, dehumidifier and chiller. Other heat exchangers can be easily sized with their effectiveness and fluids flow rates as described by in the textbook related to heat exchanger (Incropera, 2002).

The membrane total heat exchanger composed has two types of dependent effectiveness: sensible effectiveness and latent effectiveness. When either of the two types of effectiveness is determined, the other is determined accordingly. The detailed design process of membrane enthalpy exchanger is introduced by Zhang (2002) and will not go into the details here. With given sensible effectiveness $\varepsilon_{THE,s}$, the dimensions and latent effectiveness of the total heat exchanger can be determined.

The detailed iterative procedure of design for dehumidifier is described below.

(1) Determine the known humidity ratios at different points. The air humidity ratio at different points can be determined as:

$$\omega_{a,3} = \omega_{a,4} = \omega_{a,5} = \omega_{a,7} = \omega_{a,6} - \frac{Q_{l,z}}{m_a h_{fg,0}} \tag{7.12}$$

(2) Assuming the exhaust air temperature $t_{a,7}$. Because $t_{a,7}$ is necessary for the performance of the calculation of the total heat exchange, it should be assumed first. Here, it is assumed to be $t_{a,7}= t_{a,1}$;

(3) Determine the temperatures and humidity ratios of the fresh air and exhaust air leaving the total heat exchanger with the following equations:

$$\begin{aligned} \omega_{a,2} &= \omega_{a,1} - \varepsilon_{\mathrm{THE},l} \frac{m_{ae}}{m_{as}} (\omega_{a,1} - \omega_{a,7}) \\ \omega_{a,8} &= \omega_{a,7} + \varepsilon_{\mathrm{THE},l} \left(\omega_{a,1} - \omega_{a,7}\right) \end{aligned} \tag{7.13}$$

$$\begin{aligned} t_{a,2} &= t_{a,1} - \varepsilon_{\mathrm{THE},s} \frac{m_{ae}}{m_{as}} (t_{a,1} - t_{a,7}) \\ t_{a,8} &= t_{a,7} + \varepsilon_{\mathrm{THE},s} (t_{a,1} - t_{a,7}) \end{aligned} \tag{7.14}$$

(4) Determine the properties of solution at inlet of dehumidifier. The solution flow rate m_{s1} is generally 1/10-1/30 of that of the processing air. A smaller solution flow rate is selected for lower dehumidification rate. For initial design, m_{s1} can be taken as $0.05m_{as}$. The solution inlet concentration X_{s1} is in the range of 0.3-0.42. A larger value is selected for lowest supply air humidity ratio. The solution inlet temperature t_{s1} is set to be 36℃ ;

(5) Determine the solution outlet flow rate m_{s2} and concentration X_{s2} of the dehumidifier according to mass balance:

$$m_{s2} = m_{s1} + m_{as}(\omega_{a,2} - \omega_{a,3}) \tag{7.15}$$

$$X_{s2} = m_{s1} X_{s1} / m_{s2} \tag{7.16}$$

(6) Determine the mass flow rate of cooling water. Assume the cooling water outlet temperature $t_{clwr} = t_{clws} + 5$, and the temperature difference between the leaving air and entering water Δt_{aw} = 1℃. Therefore, the cooling water flow rate can be preliminarily determined by the heat balance equation as:

$$m_{clw} = \frac{m_{as} c_{p,m} [t_{a,2} - (t_{clws} + \Delta t_{aw})] + m_{as} (\omega_{a,2} - \omega_{a,3}) h_{fg,0}}{c_{p,w} (t_{clwr} - t_{clws})} \tag{7.17}$$

(7) Calculate the equilibrium humidity ratio ω_e by the properties of the solution at temperature t_{clws} and concentration X_{s1}, and the corresponding saturated air enthalpy h_e by

$$h_e = (c_{p,a} + c_{p,v} \omega_e) t_{clws} + \omega_e h_{fg,0} \tag{7.18}$$

(8) Calculate the C_r* and ε_m by Equation (7.4) and (7.8) with known data;

(9) Calculate NTU_m of dehumidifier by the rearranged form of Equation (7.8):

$$\mathrm{NTU}_m = \begin{cases} \dfrac{1}{C_r^* - 1} \dfrac{1}{b_0 + b_1 \dfrac{m_{s,i}}{m_a}} \ln\left(\dfrac{\dfrac{\varepsilon_m}{b_2 t_{a,i} / t_{w,i}} - 1}{\dfrac{\varepsilon_m}{b_2 t_{a,i} / t_{w,i}} C_r^* - 1} \right) & (C_r^* \neq 1) \\ \dfrac{1}{b_0 + b_1 \dfrac{m_{s,i}}{m_a}} \dfrac{\dfrac{\varepsilon_m}{b_2 t_{a,i} / t_{w,i}}}{1 - \dfrac{\varepsilon_m}{b_2 t_{a,i} / t_{w,i}}} & (C_r^* = 1) \end{cases} \tag{7.19}$$

(10) Determine the dimensions of the dehumidifier. For typical design, the air channel depth is 0.0035 m; the width of the channel is 1 m; the air flow velocity in the channel is 2 m/s. The number of channel n is

$$n = \frac{m_a}{\rho_a v_a d_{ch} W} \tag{7.20}$$

where ρ, v is the density and velocity of the air, respectively; d_{ch} and W is the depth and width of the channel, respectively.

The area for mass transfer is

$$A = 2nWH \tag{7.21}$$

The mass transfer coefficient is determined by:

$$h_D = 1.86\,\mathrm{Re}_a^{1/3}\,\mathrm{Pr}_a^{1/3}\left(\frac{d_{eq}}{H}\right)^{1/3}\frac{\lambda_a}{d_{eq}c_{p,a}} \tag{7.22}$$

where Re, Pr, λ are the Reynolds number, Prandtl number and thermal conductivity of the air, respectively; d_{eq} is the equivalent diameter of the channel and equals to $2d_{ch}$.

Because both the mass transfer coefficient and area are related with the height of the dehumidifier H, the H can be calculated by rearranging Equations (7.20), (7.21) and (7.22) as

$$H = \left(\frac{NTU_m \rho_a v_a c_{p,a} d_{ch}}{2\times 1.86\,\mathrm{Re}_a^{1/3}\,\mathrm{Pr}_a^{1/3}(2d_{ch})^{-0.667}\lambda_a}\right)^{1.5} \tag{7.23}$$

(11) Calculate the enthalpy effectiveness ε_h by Equation (7.3) with known air enthalpies. The overall heat transfer coefficient between water and solution can be taken as 270 W/(m^2·K). And determine the air outlet enthalpy by

$$h_{a,3} = h_{a,2} - \varepsilon_h (h_{a,2} - h_e) \tag{7.24}$$

(12) Determine the cooling water outlet temperature t_{clwr} by Equation (7.10). This calculated temperature is compared with the assumed one.

If the difference exceeds the tolerance, go to step (8) to recalculate the dehumidifier size until converged.

(13) Calculate the air outlet temperature $t_{a,3}$ with known humidity ratio and enthalpy by

$$t_{a,3} = \frac{h_{a,3} - \omega_{a,3} h_{fg,0}}{c_{p,a} + c_{p,v}\omega_{a,3}} \quad (7.25)$$

(14) For the sensible heat exchanger after the dehumidifier (HE1), there is,

$$\begin{aligned} t_{a,4} &= t_{a,3} - \varepsilon_{\mathrm{HE1}} \frac{m_{ae} c_{p,a}}{m_{as} c_{p,a}} (t_{a,3} - t_{a,6}) \\ t_{a,7} &= t_{a,6} + \varepsilon_{\mathrm{HE1}} (t_{a,3} - t_{a,6}) \end{aligned} \quad (7.26)$$

(15) The obtained $t_{a,7}$ by the last step is compared to the assumed value. If the difference is large than the tolerance, go to step (3) until the convergence is achieved.

The additional sensible cooling load for the fresh air is

$$Q_{s,oa} = m_{as} c_{p,m} (t_{a,4} - t_{a,r}) \quad (7.27)$$

Thus, the total sensible cooling load of the chiller is

$$Q_c = Q_{s,z} + Q_{s,oa} \quad (7.28)$$

With the determined value of total sensible cooling load, chilled water supply temperature and outdoor air temperature, the capacity of the chiller can therefore be determined.

7.3.3 Design of the Regeneration Subsystem

The regeneration subsystem includes four components: the regenerator, heat pump, sensible heat exchanger after the regenerator (HE2) and the solution heat exchange (SHE). With given effectiveness and fluid flow rates, the dimensions of HE2 and SHE can be determined using the correlations of Effectiveness and NTU (Incropera, 2002). For typical design conditions, 54℃ is an appropriate value for the solution inlet temperature t_{s3}. Iteration approach is adopted for the design of regenerator due to the correlated performance of the regenerator and HE2. The procedure for the regenerator design is described below.

(1) Assume the air outlet temperature of the regenerator $t_{a,10} = t_{hws}$ - 5℃ ;

(2) Determine the air inlet temperature $t_{a,9}$ and humidity ratio $\omega_{a,9}$ of the regenerator, by the following equation,

$$\begin{aligned} t_{a,9} &= t_{a,8} + \varepsilon_{\mathrm{HE1}}(t_{a,10} - t_{a,8}) \\ \omega_{a,9} &= \omega_{a,8} \end{aligned} \tag{7.29}$$

(3) Determine solution inlet mass flow rate m_{s3} and outlet humidity ratio $\omega_{a,10}$ by mass balance:

$$\begin{aligned} m_{s3} &= m_{s2} \\ \omega_{a,10} &= \omega_{a,9} + \frac{m_{s3} - m_{s1}}{m_{ae}} \end{aligned} \tag{7.30}$$

(4) Select the hot water supply temperature t_{hws}. The hot water supply temperature is generally in the range of 55-65℃ . Higher temperature is required for larger X_{s1}. An initial value of 60℃ is selected. If the required X_{s1} cannot be met or the size of the regenerator is too large, a larger value can be selected;

(5) Determine the mass flow rate of hot water. Assume the hot water outlet temperature $t_{hwr} = t_{hws}$ - 5℃ , the temperature difference between the outlet air and inlet water Δt_{aw} = -2℃ . The hot water flow rate can be determined by;

$$m_{hw} = \frac{m_{ae} c_{p,m} \left[(t_{hws} + \Delta t_{aw}) - t_{a,9} \right] + m_{ae} (\omega_{a,10} - \omega_{a,9}) h_{fg,0}}{c_{p,w} (t_{hws} - t_{hwr})} \tag{7.31}$$

(6) Calculate the equilibrium humidity ratio ω_e by the properties of the solution at temperature t_{hws} and concentration X_{s3}, and the corresponding saturated air enthalpy h_e by

$$h_e = (c_{p,a} + c_{p,v} \omega_e) t_{hws} + \omega_e h_{fg,0} \tag{7.32}$$

(7) Calculate the C_r*, ε_m for the regenerator by Equation (7.4) and (7.8);

(8) Calculate NTU_m of the regenerator by the Equation (7.19);

(9) Determine the dimensions of the regenerator. The air channel depth d_{ch}, the width of the channel W, the air flow velocity in the channel are the same with those of the dehumidifier. The number of channel n is determined by Equation (7.20). The height of the regenerator H can be determined by Equation (7.23). The area for heat and mass transfer is determined by Equation (7.21);

(10) Calculate the enthalpy effectiveness ε_h of the regenerator by Equation (7.3). And then determine the air outlet enthalpy $h_{a,10}$ by:

$$h_{a,10} = h_{a,9} - \varepsilon_h (h_{a,9} - h_{a,e}) \tag{7.33}$$

(11) Determine air temperature at the regenerator outlet $t_{a,10}$ with the known enthalpy $h_{a,10}$ and humidity ratio $\omega_{a,10}$;

(12) Determine the water outlet temperature t_{hwr} by Equation (7.10).This calculated temperature is compared with the assumed one. If the difference exceeds the tolerance, go to step (7) to recalculate the dehumidifier size until converged;

(13) The obtained $t_{a,10}$ by the last step is compared to the assumed value. If the difference exceeds the tolerance, go to step (2) and repeat the

above steps until the convergence is achieved. The dimensions of the regenerator are then determined.

The capacity of the heat pump is determined by the heat required for regeneration:

$$Q_h = m_w c_{p,w}(t_{hws} - t_{hwr}) \quad (7.34)$$

With the heat capacity, hot water supply temperature, and the predefined source water temperature of 35-45℃, the size of the heat pump can be selected.

7.3.4 Design Tool for the Proposed System

An Excel tool for the design of the proposed system is developed using the procedure described above. The dimensions of the dehumidifier and regenerator can be easily determined. And the chiller and heat pump can then be properly sized. The interface for the design tool is shown in Figure 7.7. The summary of design results of an example system applied for an office building in Hong Kong is shown in Figure 7.8 with input parameters shown in Figure 7.7.

Predesign Tool for Novel Air-conditioning System with Liquid Desiccant
9/25/2011

Input Parameter	Value	Unit	Note
Indoor air temperature	24	℃	Defualt value is 24
Indoor air humidity ratio	0.0092	kg/kg	for RH=50%
Design outdoor air temperature	29.3	℃	Mean coincident dry-bulb temperature for dehumidification
Outdoor air humidity ratio	0.0222	kg/kg	Humidity ratio corresponding to the dew point for dehumidification
Design outdoor air temperature	32.2	℃	Design dry-bulb temperature for cooling
Wet-bulb temperature	26.5	℃	Mean coincident wet-bulb temperature for cooling
Sensible load of the zone	10	kW	Sensible cooling load of the zone
Latent load of the zone	1	kW	
Fresh air flow rate	0.5	kg/s	
Exhaust air flow rate	0.5	kg/s	
Effectiveness of Component	**Value**	**Unit**	**Note**
$\varepsilon_{THE,s}$	0.75		Sensible effectiveness of the total heat exchanger, from 0.6-0.8
ε_{HE1}	0.7		Effectiveness of the air-to-air heat exchanger after the dehumidifier, fro
ε_{HE2}	0.7		Effectiveness of the air-to-air heat exchanger after the regenerator, from
ε_{SHE}	0.9		Effectiveness of the solution heat exchanger, default is 0.9
ε_{CC}	0.8		Effectiveness of the dry cooling coil, default is 0.8
ε_{FC}	0.8		Effectiveness of the fan coil, default 0.8
User Selected Parameters	**Value**	**Unit**	**Note**
Chilled water supply temperture, Tchws	17	℃	
Cooling water from cooling tower, Tclws	29.2	℃	usually about 2°C above the wet bulb temperature of the outdoor air
Hot water from heat pump, Thws	56	℃	range from 50-70°C, depending on the solution concentraion
Solution inlet temperture for absorber, Ts1	36	℃	default value if 36°C
Solution inlet concentration, Xs1	0.4	kg/kg	default is 0.4. Higher concentration for lower supply air dew-point
Solution inlet temperature for regenerator, Ts3	54	℃	default value is 54°C
Solution flow rate	0.025	kg/s	larger flow rate for higher dehumidification rate, default is 0.05ma

States of the fluid	1	2	3	4	5	6	7	8
temperature, ℃	29.3	26.9	27.1	24.9		24.0	26.1	28.5
humidity ratio, kg/kg	0.0222	0.0136	0.0084	0.0084	0.0084	0.0092	0.0092	0.0178
mass flow rate, kg/s	0.5	0.5	0.5	0.5	0.5	0.5	0.5	0.5
States of the fluid	**12**	**13**	**14**	**15**	**16**	**17**	**18**	**19**
	Tchws	**Tchwr1**	**Tchws**	**Tchwr2**	**Tclws**	**Tclwr**	**Thws**	**Thwr**
water temperature, ℃	17.00	22.00	17.00	23.34	29.20	34.41	56.00	51.70
water mass flow rate, kg/s	0.4761905		0.02		0.30		0.60	
LOAD (kW)	10		0.5941776		6.586336		10.9029383	
States of the fluid	**S1**	**S2**	**S3**	**S4**				
Temperature, ℃	36.00		54.00					
Solution mass flow rate, kg/s	0.03	0.03	0.03	0.03				
concentration	0.40	0.36	0.36	0.40				

Figure 7.7 Interface of the predesign tool for the novel air-conditioning system

Summary of Design	Value	Unit
Chiller capacity	10.59	kW
Cooling tower capacity	6.59	kW
Heat pump capacity	10.90	kW
Dehumidifier Area	100.83	m2
Dehumidifier Height	0.85	m
Regenerator Area	55.12	m2
Regenerator Height	0.47	m

Figure 7.8 Summary of the results for an example design

7.4 Summary

For the design of liquid desiccant dehumidifier, an effectiveness-NTU model is developed. The model is presented by two correlations of performance indices: enthalpy effectiveness and mass transfer effectiveness that are related with typical non-dimension parameters. The model assumes that the heat capacity of the solution is kept unchanged in the process. The model is validated with the results by numerical model.

A procedure and design tool for design of the proposed system is presented in this chapter. Due to the coupled performance of the dehumidifier and regenerator with other units, iterative approach is adopted for the design of the system. The procedures for the design of the key components of dehumidifier, regenerator, chiller and heat pump are introduced in details.

An Excel design tool is developed to ease design of the proposed system by HVAC engineers. With this design tool, the proposed new system can be easily and properly designed by engineer without many calculations. An application of the proposed system for hot and humid climate will be exemplified and studied in next chapter.

CHAPTER 8 APPLICATION EXAMPLE OF THE PROPOSED SYSTEM IN HOT AND HUMID CLIMATE

The superiority of the proposed system over the standard one has been proved by the exergy analysis. In this chapter, the annual energy performance of the proposed system is investigated for a typical office building in hot and humid climate of Hong Kong and is compared with that of the standard liquid desiccant system. The thermal performance of proposed system and its subsystems at different weather condition parameters of outdoor air temperature, humidity ratio and SHR are investigated to provide insight information about the operation of the system.

8.1 Building and System Description

8.1.1 Details of Building

A single zone of the 16 identical zones of a 16-story office building in Hong Kong (22°N, 114°E) is simulated in this study. The zone is 50 m long in the south and north direction, 10 m wide and 3 m high. The air-conditioned floor area is 450 m^2. It has four heavyweight external walls with 50% of glazing area. The construction of the envelope is the same as the RTS representative zone heavy construction (ASHRAE, 2005). The *U* factor of the external wall is 0.389 W/m^2-K. The insulated 4 mm double-pane window (WinID 2002 in TRNSYS 15 Window Lib) with 45% inside louver shading is adopted. Its center-of-glass *U*-value is 1.3 W/m^2-K, solar transmittance 0.426, and normal SHGC 0.591 (TRNSYS, 2006). The overall thermal capacitance of the zone is 1800 kJ/K.

The lighting and equipment loads are 19.0 W/m^2 and 12.4 W/m^2, respectively, with 40% convective portion, scheduled from 9 to 19 hour on workday and from 9 to 13 hour on Saturday. An occupancy pattern of 56 persons (8 m^2/person) is scheduled from 9 to 19 h on workday and from 9 to 13 on Saturday. The sensible and latent heat generated per occupant is 75 W and 75 W per person. Fresh air rate is 7.4 L/s/person. Total fresh air flow rate is 0.5 kg/s.

The indoor condition is maintained as 24°C with 50% RH from 9 to 19 h on workdays and from 9 to 13 on Saturday, and off on Sunday. The hourly energy simulations of the two systems had been conducted using the TMY weather data of 1995 in Hong Kong for the total 8760 hours. All the energy consumptions by the components are converted to primary energy. The energy conversion efficiency is 0.42 for electricity and 1.0 for natural gas used by boiler.

8.1.2 Details of the Air-conditioning System

The design sensible cooling load is 33 kW and the design heating load is 12.2 kW for each zone. It should be noticed that each zone had its own air-handling unit while the chilled water, hot water and cooling water required by the zone are treated centrally for the whole building. Therefore, the above mentioned design loads should be multiplied by the number of identical zones for the sizing of chiller, heat pump and cooling tower.

Two air-cooled screw-type chillers manufactured by Trane with the rated capacity of 228 kW are used (Trane, 2002). The parameters used for compressor simulation are listed in Table 8.1. One water-source scroll-type heat pump manufactured by McQuay with a rated capacity of 195 kW is selected (McQuay, 2009). The coefficients in the correlations for heat pump simulation are listed in Table

8.2.

The selected cooling tower has a cooling capacity of 105 kW for each cell with water flow rate of 4.8 kg/s at the leaving water temperature of 30°C and the wet-bulb temperature of 28°C. The rated fan power for each cell is 0.66 kW for air flow rate of 3.6 m^3/s. The coefficients *c* and *n* in the NTU correlation of the cooling tower (Braun et al., 1989) are 2.3 and -0.72, respectively (Lu and Cai, 2002). The cooling tower has 1 cell in the new system and 2 cells in the standard system.

Table 8.1 Identified parameters for the compressor of Trane RTAD-100STD

W_{loss} (kW)	α	V_s (m3/s)	$A_{leakage}$ (cm^2)	Δp_{pump} (kPa)
18.69	0.0045	0.1826	0.89	5.134

where

W_{loss} = Electro-mechanical loss (kW)
α = Electro-mechanic loss factor proportional to the internal power
V_s = full-load refrigerant volume flow rate at the compressor inlet (m^3/s)
$A_{leakage}$ = Leakage area (cm^2)
Δp_{pump} = the pressure jump of the by-passed refrigerant at part-load (kPa)

Table 8.2 Coefficient for the performance fitting equations of the heat pump

Coefficient	CAPFT	EIRFT	EIPFPLR
a	0.37642	0.84399	0.04411957
b	-0.00107	0.00598	0.64036703
c	2.01E-05	0.000356306	0.31955532
d	0.01794	-0.0187	
e	0.000286	0.000396203	
f	-0.00018	-0.000625703	

8.1.3 Operation Controls

In this study, the flow rates of cooling water for dehumidifier, hot water for regenerator and desiccant solution are kept constant as listed in Table 8.3. The chilled water supply temperature is maintained at 16°C and the chilled water flow rate changes to satisfy the sensible cooling load. The condensing temperature of the chiller is maintained at 48°C. The cooling water temperature is determined by the cooling tower with the fans running at full speed.

In the novel system, the source water flow rate of the heat pump is constant. If the quantity and quality of heat recovered from the recovery condenser of chiller is adequate enough for regeneration, the heat pump is turned off and bypassed.

The humidity ratio of the supply air is maintained to its set-point by adjusting of the inlet solution concentration of the dehumidifier X_{s1}. This inlet solution concentration of dehumidifier, which equals to the leaving solution concentration of the regenerator, is controlled by the hot water supply temperature. That is, humidity ratio of the supply air is indirectly controlled the hot water supply temperature t_{hws}.

The total heat exchanger is controlled by enthalpy. When the outdoor air enthalpy is larger than that of the exhaust air, the total heat exchanger runs at its full effectiveness. If the enthalpy level of the outdoor air is lower than that of the exhaust air, the total heat exchanger is bypassed.

The upper limit of temperature of supply air is 20°C. When the air temperature entering the cooling coil is larger than 20°C it is cooled. When the air temperature entering the cooling coil is lower than its upper limit, no cooling or heating is provided to take full advantage of the sensible cooling capacity of the fresh air.

Table 8.3 Operation parameters

Parameter	Novel	Standard
m_{clw}	0.3 kg/s	0.5 kg/s
m_{hw}	0.5 kg/s	1 kg/s
m_{s1}	0.0167 kg/s	0.0167 kg/s
t_{chws}	16°C	16°C
t_{cd}	48°C	48°C

8.2 Annual Energy Performance

The operating hours of the components are different for the two systems. The simulation results show that, out of 2871 occupied hours of the year, the operating hours of the chiller are similar. However, the operating hour of the heating components differ greatly. The number of operation hours of the boiler is 2567 while that of heat pump is only 1736. It is because the heat recovered from the recovery condenser is sufficient for the regeneration without using heat pump in many hours.

The annual energy performances of the two systems are listed in Table 8.4. The amounts of annual primary energy consumption per unit floor area by chillers are 53.6 kWh/m^2 by the novel system and 50.4 kWh/m^2 by the standard system. The chiller power of the standard system is smaller than that of the novel system. However, the difference is small, only about 6%. This difference is mainly caused by the reduced cooling load of the chiller due to the sensible heat recovery by evaporative cooling in the standard system. The resulting small difference indicates the ineffectiveness of such recovery by evaporative cooling, as described in the exergy analysis. Furthermore, although the energy used by the chiller in the novel system is larger, its averaged COP is slightly larger than the one of the standard system. This is favorable from the energy point of view. It is caused by the reduced fan power of the novel system due to the removal of partial condensing heat in the recovery condenser.

Table 8.4 Annual energy performances of the two systems

	Chiller		HP/Boiler		Total	
	PE (kWh/m^2)	Avg. COP	PE (kWh/m^2)	Avg. COP	PE (kWh/m^2)	Avg. COP
Standard	50.4	3.43	110.8	0.85	161.2	1.66
Novel	53.6	3.55	10.2	7.67	63.7	4.21
Difference					-60.5%	

The annual primary energy used for regeneration is 10.2 kWh/m^2 by heat pump in the novel system and 110.8 kWh/m^2 by boiler in the standard system. The primary energy usage of the boiler is about 10 times larger than that of the heat pump due to the low COP of the boiler and the large regeneration heat requirement. The averaged COP of the heat pump is 7.67, which is about 9 times of that of the boiler. Here, the COP of the heat pump is defined based on electric power, and the COP of the boiler is set to be equal to its efficiency.

The total annual primary energy consumption is 63.7 kWh/m^2 by the novel system and 161.2 kWh/m^2 by the standard system. This implies that as compared to the standard liquid desiccant cooling system, the primary energy efficiency can be improved by 60.5% with the innovative liquid desiccant dehumidification system. The average COP of the novel system can be as high as 4.21, which is not only much higher than that of the standard system, but also higher than that of conventional air-conditioning system.

Furthermore, from Table 8.4, the primary energy consumption of the proposed system is decreased by 60.5%. This sharp reduction is the results of four improvements: (1) total heat exchanger and sensible heat exchanger (THE&HE1) that recover both the latent and sensible heat of exhaust air, resulting in reduced dehumidification and regeneration load; (2) sensible heat exchanger (HER) that recovers the waste heat of scavenging air; (3) condensing heat of chiller used directly for desiccant regeneration; and (4) heat pump that recovers condensing heat of chiller for regeneration.

The annual primary energy saving per floor area by HER, $\overline{W}_{\mathrm{HER}}$ is the sum of corresponding primary energy that should otherwise be used by boiler to produce the heat recovered by HER throughout the year $\overline{Q}_{\mathrm{HER}}$. It can be calculated by

$$\overline{W}_{\mathrm{HER}} = \overline{Q}_{\mathrm{HER}} / \eta = \sum \overline{m}_{a,10} c_{p,a} (t_{a,10} - t_{a,9}) / \eta_b \tag{8.1}$$

where $\overline{m}_{a,10}$ is the air flow rate per floor area and the boiler efficiency $\eta_b = 0.85$.

The annual primary energy saving per floor area by THE&HE, $\overline{W}_{\mathrm{THE\&HE}}$, is the sum of energy savings for regeneration and cooling. It can be determined by

$$\overline{W}_{\mathrm{THE\&HE}} = \left(\overline{Q}_{\mathrm{STD,reg}} - \overline{Q}_{\mathrm{NEW,reg}} - \overline{Q}_{\mathrm{HER}}\right) / \eta_b + \left(\overline{W}_{\mathrm{STD,chiller}} - \overline{W}_{\mathrm{NEW,chiller}}\right) \tag{8.2}$$

where, $\overline{Q}_{\mathrm{STD,reg}}$ and $\overline{Q}_{\mathrm{NEW,reg}}$ are the regeneration heat required per unit floor area by the standard system and the new system, respectively; $\overline{W}_{\text{STD,chiller}}$ and $\overline{W}_{\text{NEW,chiller}}$ are the primary energy consumption per unit floor area for cooling by the standard system and the new system, respectively.

The third annual primary energy saving, $\overline{W}_{\text{NO-HP}}$, per floor area is the direct use of condensing heat in chiller for regeneration without operating a heat pump.

$$\overline{W}_{\text{NO-HP}} = \overline{Q}_{\text{NO-HP}} / \eta_b \tag{8.3}$$

The last annual primary energy saving per floor area is the heat generation by an efficient heat pump rather than a boiler, which can be calculated by:

$$\overline{W}_{\text{HP}} = \left(\overline{Q}_{\text{NEW,reg}} - \overline{Q}_{\text{NO-HP}}\right)\left[1/\eta_b - 1/\left(COP_{\text{HP}}\eta_w\right)\right] \tag{8.4}$$

where $\eta_w = 0.42$ is the conversion factor from fuel energy to electricity.

The amount of annual primary energy saving per floor area & average percentage of contribution due to these four improvements are listed in Table 8.5. It is noticed that the contribution of total heat exchanger and sensible heat exchanger accounts for 30.9%, while that of heat pump accounts for 31.9%. The role of recovery heat exchanger cannot be neglected because it also accounts for about one third of energy saving. Furthermore, in the proposed system, the heat pump utilizing condensing heat with an average temperature of 33.45°C, when other heat sources are to be utilized, the COP of heat pump would be decreased. For example, when the absorption heat released in the dehumidifier with an average temperature of 27.78°C is used, the average COP of heat pump would decrease from 7.67 to 6.1, a 25.8% reduction.

Table 8.5 Energy saving contribution by each improvement

	THE&HE	HER	NO-HP	Heat pump	Total
PE saving (kWh/m^2)	30.13	33.18	3.01	31.10	97.5
Average percentage	30.9%	34.1%	3.1%	31.9%	100%

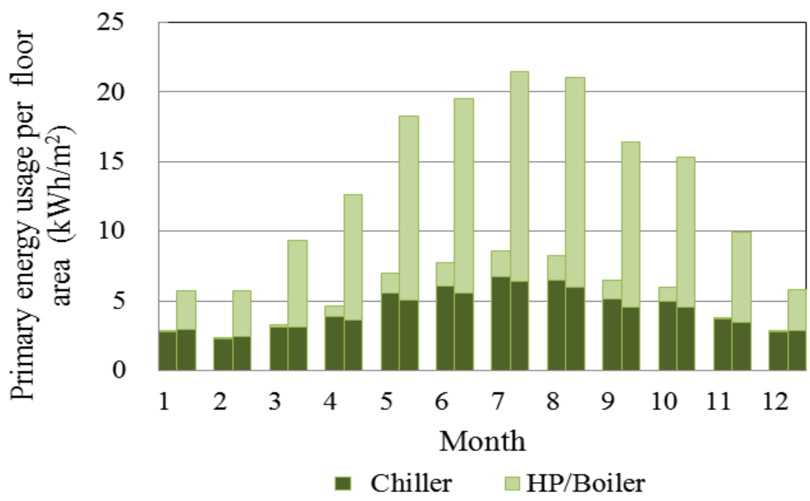

Figure 8.1 Monthly primary energy consumption (Left for novel system, right for standard system)

Detailed energy performance of the two systems can be studied from the monthly primary energy usage, as shown in Figure 8.1. For both systems, the maximum energy uses of chiller, HP/boiler and thus the system appear in July, while the minimum energy uses appear in February. The chiller primary energy uses of the two systems for all the months are close, and the chiller energy uses of the novel system in most of the months are slightly larger, as mentioned in the yearly analysis.

The primary energy uses for desiccant regeneration differ greatly for the two systems. In the standard system, the monthly energy use for desiccant regeneration predominates in all of the months. Yet the energy uses for regeneration only accounts for only a small part of the total energy consumption in the novel system. Furthermore, for many operating hours in the winter season of the new system, i.e., from November to March, there is no or only a small amount of energy used for regeneration. This is because the heat recovered from the chiller condensing heat is sufficient enough to satisfy the heat required and thus no heat pump is needed. This saves a large amount of energy.

8.3 Thermal Performance Variation with weather conditions

Besides the energy analysis, the variations of thermal performance of the system with weather conditions are studied to provide detailed operation information of the two systems. The weather condition parameters include the outdoor air temperature, humidity ratio and SHR (sensible heat ratio of the total cooling load of the space). While outdoor air temperature and humidity ratio determines the amount of cooling load, the SHR allocates the portions of load that are to be handled by the cooling equipment and dehumidification equipment in the proposed system.

8.3.1 Desiccant dehumidification and regeneration sub-systems

The outdoor air humidity ratio is the key parameter that will influence the performance of the liquid desiccant dehumidification and regeneration sub-systems, while the effect of outdoor air temperature is relatively small because the sensible load is handled separately by the fan coils installed in the zone.

The variation of thermal performance of desiccant subsystem with the outdoor air humidity ratio is to be investigated, which is reflected by the variation of key parameters of solution concentration required at the dehumidifier inlet, hot water supply temperature and regeneration heat required. The hot water supply temperature is also called regeneration temperature and the regeneration heat required is called heating load. The distributions of the three parameters with the outdoor air humidity ratio throughout the year are shown in Figure 8.2 and 8.3. For clarity, the points in the figures are averaged one.

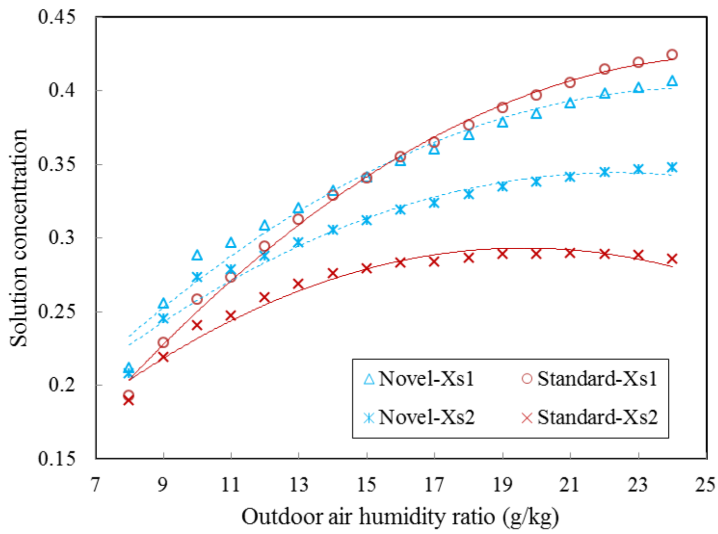

Figure 8.2 Solution concentrations at dehumidifier inlet and outlet vs. outdoor air humidity ratio

As shown in Figure 8.2, the inlet solution concentration required at dehumidifier to maintain the set-point of humidity ratio of supply air increases quadratic-polynomially with outdoor air humidity ratio for both systems. The inlet solution concentration X_{s1} varies from 0.2 to 0.42. The outlet solution concentration X_{s2} is also shown in Figure 8.2. Since the solution flow rate is the same for the two systems, the change of solution concentration in the dehumidifier of the standard system is much larger than that of the proposed system due to its higher dehumidification load on dehumidifier. Due to the designs and operation parameters of the two systems, the inlet solution concentration of the standard system at high outdoor air humidity ratio is larger than that of the proposed system. However, when outdoor air humidity ratio is lower than a critical value (15 g/kg for this case), the inlet solution concentration required by the standard system becomes smaller than that of the proposed system. The reasons for this intersection are discussed below. Due to the decreased mass transfer performance of total heat exchanger at lower outdoor air humidity ratio, the dehumidification loads of dehumidifiers of the two systems becomes closer. Because both the size of dehumidifier and cooling water flow rate of the standard system are larger than those of the proposed system, the dehumidifier of the standard system can handles larger load at lower inlet solution concentration. Thus the solution concentration required is lower at low outdoor air humidity ratio for the standard system.

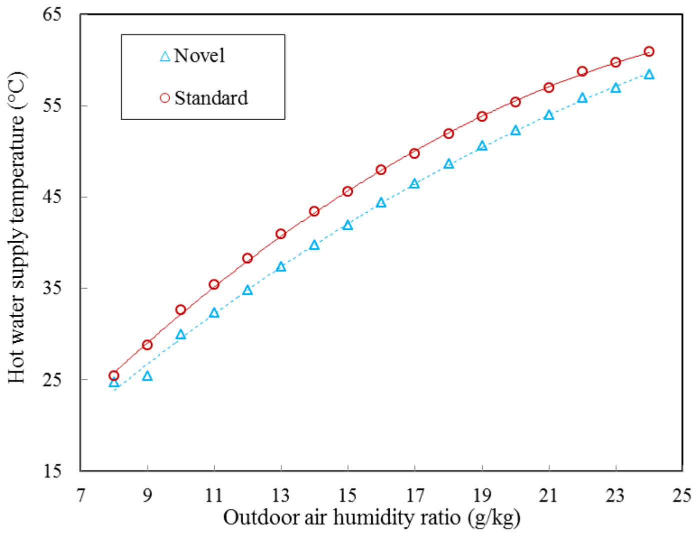

Figure 8.3 Hot water supply temperature vs. outdoor air humidity ratio

The hot water supply temperature required for desiccant regeneration at different outdoor air humidity ratio is shown in Figure 8.3. The hot water supply temperature required to concentrate the weak solution is determined by the solution concentration at dehumidifier inlet. Consequently, the hot water supply temperature will decrease proportionally with outdoor air humidity ratio because the inlet solution concentration of dehumidifier decreases with outdoor air humidity ratio. Furthermore, it is noticed that the required hot water supply temperature of the standard system is always larger than that of the novel system, even when the required solution concentration X_{s1} is lower than that of the novel one. The reason is that there is no heat recovery from the scavenging air in the standard system, which wastes a large amount of heat and results in higher regeneration temperature.

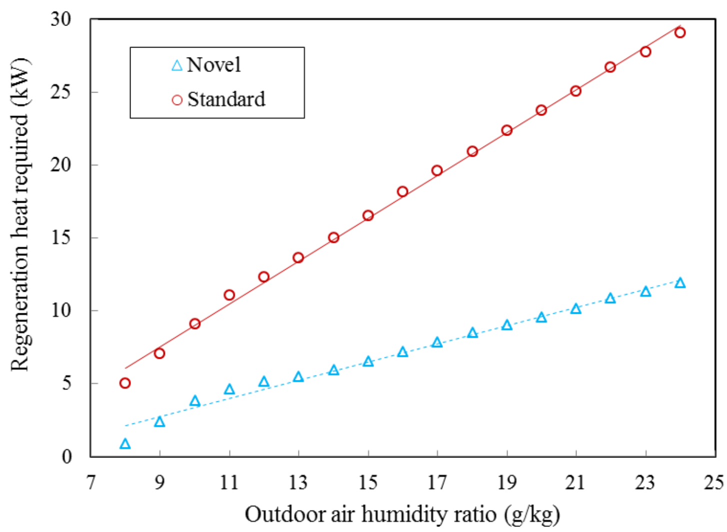

Figure 8.4 Regeneration heat required vs. outdoor air humidity ratio

The heat required for desiccant regeneration, also called heating load, presents linear relationship to outdoor air humidity ratio for both systems, as shown in Figure 8.4. The heating load of the standard system is about 2.4 times of that of the proposed system at the highest outdoor air humidity ratio. And the difference of heating load between the two systems decreases proportionally with outdoor air humidity ratio. The small heating load of the proposed system is primarily due to the installation of the total heat exchanger and heat exchanger of scavenging air. The decreasing of heating load difference between the two systems with outdoor air humidity ratio is caused by the decreased performance of total heat exchanger at lower outdoor air humidity ratio. With the decrease of outdoor air humidity ratio, the driving force for vapour transfer in the total heat exchanger is decreased, which means that the latent loads on dehumidifiers of the two system becomes close and consequently the closer heating loads.

Thus, for the proposed system, the regeneration heat required and regeneration temperature is lower than those of the standard one throughout the year. The control scheme of constant solution flow rate with variable concentration can effectively reduce the regeneration temperature required at part-load condition. The decreased regeneration temperature will help to increase the COP of heat pump.

8.3.2 Heat recovery subsystem

The total heat exchanger plays an important role in the proposed system for heat recovery. It can effectively reduce the cooling and dehumidification load by recovering sensible and latent cooling energy from the exhaust air. Thus the regeneration load and temperature as well as the cooling load of the dehumidifier are reduced consequently, resulting in less power consumption, as discussed above.

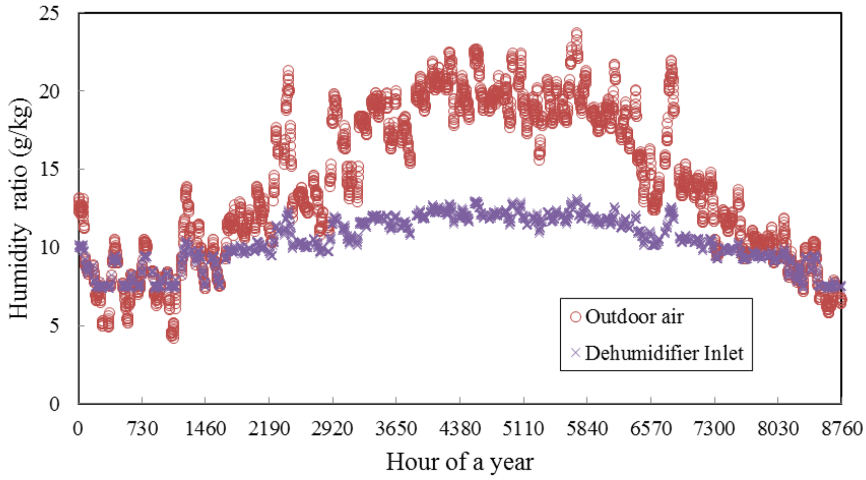

Figure 8.5 Annual distribution of air humidity ratio at outdoor and dehumidifier inlet

Furthermore, another important role of the total heat exchanger is the latent load balancing to remove those peak dehumidification loads on dehumidifier and the corresponding regeneration load. As shown in Figure 8.5, although the outdoor air humidity ratio ranges from 5 to 24 g/kg throughout the year, the air humidity ratio leaving the total heat exchanger is balanced to a narrow range of 8-13 g/kg. This means that the maximum dehumidification load on the dehumidifier is greatly reduced. Therefore, the sizes of the dehumidifier, regenerator and capacity of heat pump and water pumps can all be reduced.

Thus, due to the total heat exchanger, not only the operation cost is significantly reduced, but also the initial cost. The amount of heat recovered by the total heat exchanger at different conditions is discussed in next section.

The heat recovered by the total heat exchanger from the exhaust air is affected by the outdoor air temperature, humidity ratio and SHR. Two heat recovery ratios are defined to represent the relative amount of heat recovered to total cooling load. They are total heat recovery ratio and latent heat recovery ratio defined as the total or latent heat recovered by the total heat exchanger to the total cooling load, respectively.

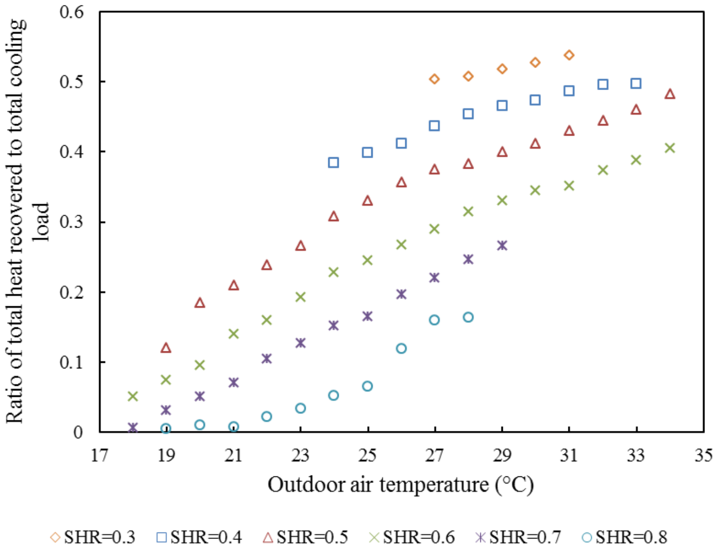

Figure 8.6 Total heat recovery ratio vs. SHR and outdoor air temperature

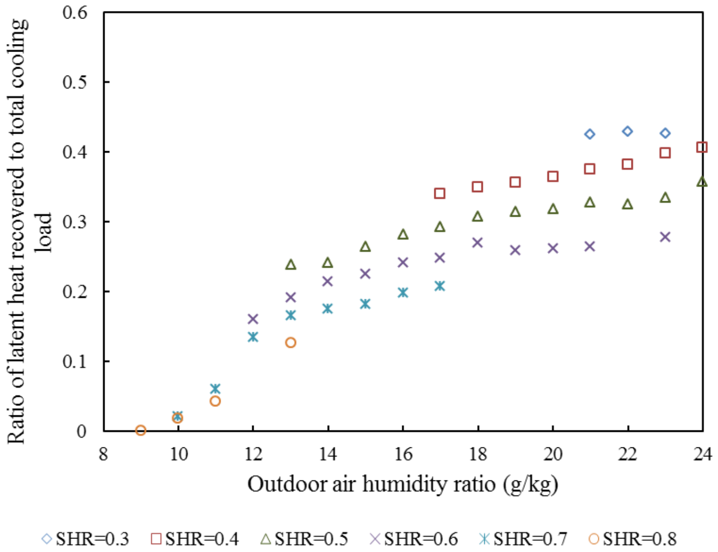

Figure 8.7 Latent heat recovery ratio vs. SHR and outdoor air humidity ratio

For a given SHR, the total heat recovery ratio increases almost linearly with the outdoor air temperature, as shown in Figure 8.6. Although the total cooling load increases with outdoor air temperature, the increase rate of total heat recovered exceeds that of the cooling load, resulting in the increased total heat recovery ratio. The latent heat recovery ratio also presents linear relationship with outlet humidity ratio, as shown in Figure 8.7.

The total heat recovery ratio is in inverse proportion to SHR. The reason is that for lower SHR, more moisture can be removed by the total heat exchanger due to larger vapor pressure difference of the two air streams. Because the latent load increase per unit moisture is much larger than the sensible load increase per unit temperature, the total heat recovery ratio would be higher at lower SHR, and vice versa.

Thus, it can be concluded that total heat exchanger is more efficient for hot and humid climates with higher outdoor air temperature, humidity ratio, and lower SHR.

It is noticed that for SHR < 0.3 and SHR > 0.8, the total heat recovery ratio is zero, which implies that there is no heat recovery. For cases with SHR > 0.8, the enthalpy of the exhaust air is less than that of the fresh air and the total heat exchanger is bypassed. From the SHR distribution, the corresponding outdoor air temperatures of such cases are located near or below the indoor air temperature, and the enthalpy of the process air is normally less than that of the exhaust air.

8.3.3 Heat pump

The realtionship between COP of heat pump with SHR and outdoor air humidity ratio is shown in Figure 8.8. The range of SHR with operation of heat pump is 0.3-0.7. For hours with SHR ≥ 0.8, because of the low or no regeneration load and temperature, no heat pump is required. When $0.8 \leq$ SHR < 1.0, the regeneration load is small enough to be satisfied simply by the heat recovered from condensing heat of chiller due to small dehumidification load. When SHR = 1.0 there is no dehumidification and regeneration load and thus no heat pump is required.

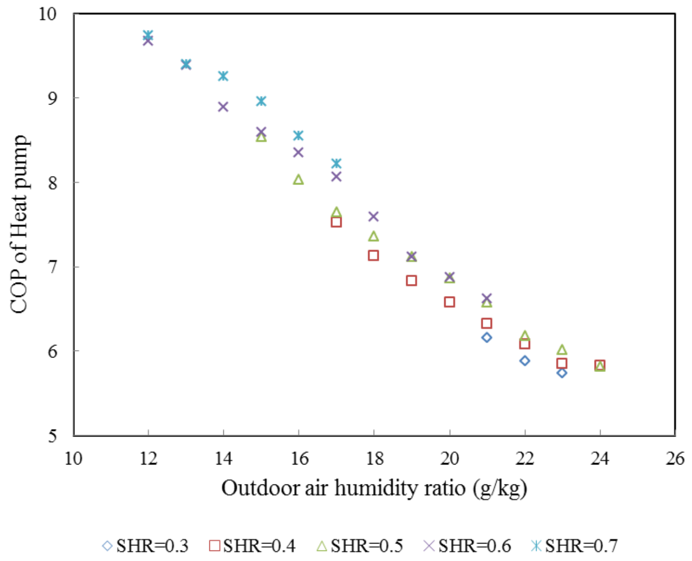

Figure 8.8 COP of the heat pump vs. outdoor air humidity ratio

The COP of heat pump increases proportionally with SHR and inverse proportionally with outdoor air humidity ratio. Compared to chiller, the COP of heat pump presents tight relationship with SHR because the heating load for regeneration is the function of SHR.

The COP of heat pump is much larger than that of chiller, even at its hardest operation conditions. The high COP is caused by three reasons. Firstly, the temperature lift of the heat pump for this study is smaller that that of chiller. The source heat of the heat pump comes from the waste heat of condenser and thus the source water temperature can be as high as 43°C. The regeneration hot water supply temperature is decreased to as low as 60°C due to the adoption of low-flow internally-heated regenerator. And this temperature can be further reduced at higher SHR and lower outdoor air humidity ratio, as shown in Figure 8.8. The maximum temperature lift for the heat pump is less than 25℃ . Secondly, the compressor of the heat pump is digital scroll type whose performance is almost not influenced with part-load operation. The highest COP of 9.8 occurs at SHR = 0.8 and outdoor air humidity ratio lower than 12 g/kg. The temperature lift of the heat pump can be less than 15°C at such cases.

8.3.4 Chiller

The chiller should be run for a wide range of SHR as long as there is cooling requirement in the zone, even for cases with SHR = 1.0. The performance of the chiller is mainly influence by the outdoor air temperature and part-load ratio (PLR) of chiller. In contrast to conventional air-conditioning system, the effect of SHR on the performance of chiller is small because the chiller handles the sensible load only and has little relationship with SHR when it runs at constant condensing temperature.

The effect of outdoor air temperature and PLR of chiller on the COP of chiller is demonstrated in Figure 8.9. It is noticed that the maximum COP of chiller occurs at a moderate outdoor air temperature of 25°C. The reason is that although the chiller is supposed to attain higher COP at lower outdoor air temperature, its PLR is noticeable decreased, resulting in lower COP. The COP of the air-cooled chiller can be as high as 3.9 because its evaporating temperature is elevated due to the high chilled water supply temperature and also because the installation of the recovery condenser which effectively reduces the fan power consumption.

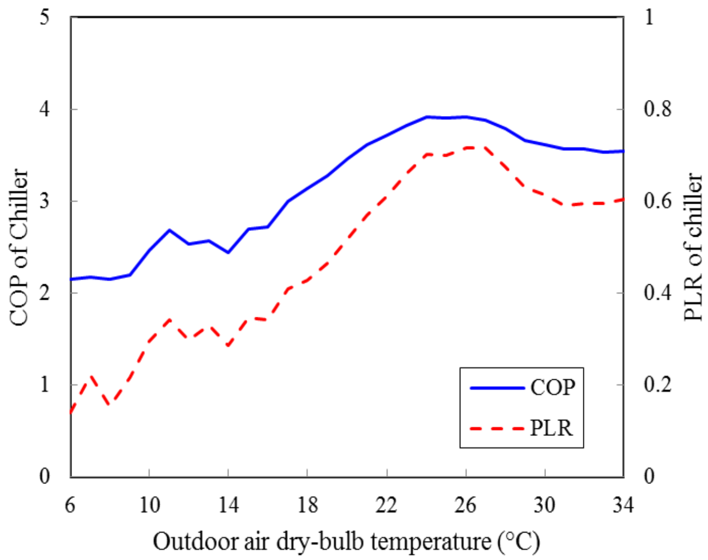

Figure 8.9 Effect of outdoor air temperature and PLR on the COP of chiller

8.4 Summary

The annual energy performance and the variation of operation parameters of the proposed system are investigated for a typical office building in Hong Kong and are compared with the standard liquid desiccant system. The effects of condition parameters of dry-bulb temperature, humidity ratio and SHR on the performance of the system are investigated. The following conclusions are derived:

1. The proposed system is more energy efficient than the standard system. The average COP of the proposed system is 4.22 while that of the standard system is only 1.66.
2. The energy saving comes from the reduced regeneration load and high COP heating equipment of heat pump that recovers condensing temperature of chiller. The reduced regeneration load is reduced by the installation of total heat exchanger and the heat exchanger after regenerator to recover the sensible heat of scavenging air.

3. The total heat exchanger can reduce not only the operation cost, but also the initial cost of the system. Because the maximum dehumidification load is balanced to a low level, the size of liquid desiccant system can be greatly reduced.
4. The total heat recovered ratio increases outdoor air temperature and humidity ratio and decreases with SHR. This shows that the total heat exchanger is more efficient for hot and humid climates.
5. The COP of heat pump is influenced by SHR and outdoor air humidity ratio, which increases with SHR and decreases with outdoor air humidity ratio. The high COP at low outdoor air humidity ratio and high SHR are the results of the reduced regeneration load and temperature at such cases.
6. The COP of chiller is mainly influenced by outdoor air temperature and its part-load ratio, rather than by outdoor air humidity and SHR.

CHAPTER 9 SENSITIVITY ANALYSIS OF DESIGN PARAMETERS

Chapter 6 and 7 provide the design methods for properly and simply design of the proposed system, and the thermal performance of such designed system is investigated in Chapter 8. In this chapter, the optimal design and sensitivity analyses of key independent operation parameters of the proposed system, as well as chiller size, are conducted. The influences of these parameters on energy consumption of the proposed system at different weather conditions are investigated to provide guidelines for design of the proposed system.

9.1 Introduction

The proposed system for thermal study of last chapter is designed by the simplified design method for liquid desiccant subsystem in Chapter 7 with the cooling load determined by rational cooling load calculation method developed in Chapter 6. Little optimization was conducted to harvest the best from the system. The optimization of the proposed system includes two parts, the optimal sizing of components and optimization of operation parameters.

As mentioned in Chapter 4, the key components of the proposed system are dehumidifier, regenerator, total heat exchanger, chiller with heat recovery and heat pump. The dehumidifier, regenerator and total heat exchanger are intrinsically heat and mass exchanger, and larger component size can enhance the perfection of heat and mass transfer process. The energy performance of the system can be improved accordingly at increased initial cost. This becomes an economical problem and is not to be considered here. The chiller sized by design cooling load calculation in Chapter 6 guarantees that the chiller can properly satisfy the cooling load required by the building, neither under-sizing nor oversizing. Yet in the proposed system, although the oversizing of chiller would generally reduce its performance, the performance of heat pump will be improved. Thus, in contrast to conventional air-conditioning system, over-sizing of chiller may no longer be a problem. The effect of oversizing of chiller on the proposed system should be investigated to validate whether over-sizing is beneficial.

In the proposed hybrid system with the control strategy as defined in last chapter, four independent operation parameters, including the desiccant flow rate, m_s, cooling water flow rate, m_{clw}, hot water flow rate, m_{hw}, and more importantly, the condensing temperature of chiller, t_{cd}, are key parameters that influencing the design and operation of the proposed system. The optimization of such parameters can effectively reduce the energy consumption of the system with rationally selected component size.

Thus, he sensitivity analyses of these parameters are carried out to investigate the influence of these parameters and to determine their relationship with weather conditions. Guidelines for optimal design of the proposed system are then provided.

9.2 Optimization of Chiller Size

An oversizing ratio defined as the ratio of selected chiller size to the design cooling load is used to 1) study the effect of over-sizing on the performance of the proposed system; and 2) determine the optimal size of chiller. Its effects on the COP and power consumption of chiller and heat pump are shown in Figure 9.1 and Figure 9.2.

From Figure 9.1, it is noticed that in the proposed system, the COP of heat pump increases linearly with the oversizing ratio because over-sized chiller enhances the perfection of condensing heat recovery process and thus results in elevated water temperature entering the heat pump. However, because the oversized chiller will operate in part-load condition, its COP decreases quickly with oversizing ratio. As the cooling load and heating load are constant, the power consumption increase by chiller will exceed the power consumption decrease of heat pump. The total power consumption therefore increases with oversizing ratio, as shown in Figure 9.2. This indicates that the oversizing of chiller is unfavorable for the proposed system, which further verifies the necessity of a rational design cooling load calculation method as developed in Chapter 6 for proper sizing of chiller.

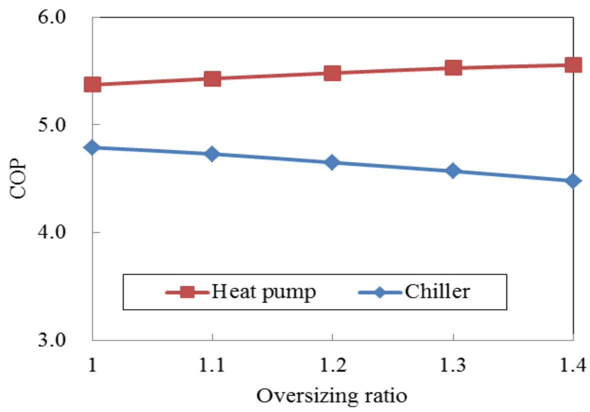

Figure 9.1 Effect of ratio of over-sizing on COP of chiller and heat pump

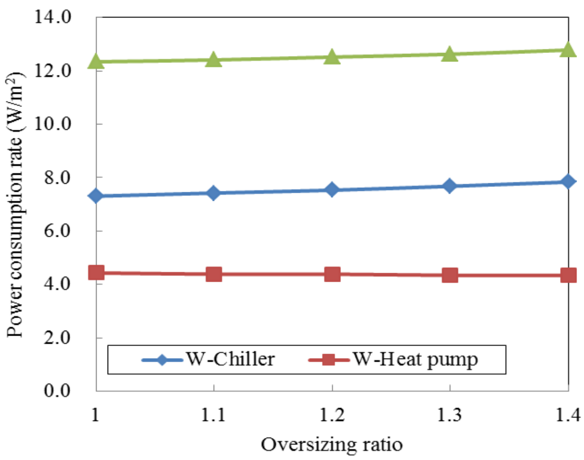

Figure 9.2 Effect of ratio of over-sizing on power consumptions

9.3 Optimization of Design Operation Parameters

In order to harvest the most from the proposed system, the operation parameters should be optimized to reduce the energy consumption for at least the design condition. This can be achieved by any of the optimization method, while the golden section search method is adopted here.

For the design condition, with t_{oa} = 29.0°C, ω_{oa} = 24.0 g/kg and SHR = 0.44, the optimized design parameters are listed in Table 9.1. The corresponding mimimum power consumption rate is 12.3 W/m^2 for the system.

The sensitivity analysis of four independent parameters are conducted below to investigate their effect on the performance of system at different weather conditions. This weather condition is represted by humidity ratio only because the effect of outdoor air temperature has little effect with the parameters concerned. For the analysis of certain paramter, all the other parameters are kept constant at their optimal value.

Table 9.1 Optimal design operation parameters

m_a (kg/s)	m_s (kg/s)	m_{clw} (kg/s)	m_{hw} (kg/s)	t_{cd} (°C)
0.5	0.03	0.4	0.55	40.1

9.4 Sensitivity Analyses of Design Operation Parameters

9.4.1 Condensing temperature of chiller

In the proposed system, the chiller and heat pump are operated in a hybrid mode. The condensing temperature of chiller affects not only the performance of the chiller itself, but also that of heat pump. Higher chiller condensing temperature produces hotter source water and thus improves the COP of heat pump, by scarificing the performance of chiller. The optimal condensing temperature of chiller, which balances the performances of chiller and heat pump, is depended on the ratio of cooling load and regeneration heating load, as well as COPs of both chiller and heat pump.

Figure 9.3 shows the effect of chiller condensing temperature on the energy performance of the proposed system. It is noticed that the optimal condensing temperature equals to the lowest possible condensing temperature for given air-cooled chiller. This implies that the performance of chiller dominates the performance of the proposed system and the selection of condensing temperature should maximize the COP of chiller only. The reasons are explained below. Although the SHR is low at design condition, due to the introduction of heat recovery measures of the proposed system, the regeneration heat required is reduced noticably to be much less than cooling load. The energy demand from heat pump would decrease accordingly.

Also from Figure 9.3, the effect of condensing temperature is small when it is near the lowest chiller condensing temperature; when the condensing temperature further increases, the effect of condensing temperature increases significantly. This reason is that the decreased power consumption by heat pump at elevated condensing temperature cannot conponsate the increase of power consumption by chiller, which would increase sharply with condensing temperature.

Therefore, for general applications, the condensing temperature should be designed close to the lowest chiller condensing temperature to minimize enegy consumption of the proposed system with total heat exchanger.

However, it should be noticed that this conculsion may not applicable to two cases. The first case is systems without total heat exchanger or with total heat exchanger at poor effectiveness. For such systems, the regeneration load would become high enough that the condensing temperature would have to be increased intentionally to balance the performance of chiller and heat pump. Therefore, such design should be prevented. The second case occurs at part-load conditions where chiller condensing temperature is also elevated intentionally to satisfy the regeration heat just by condensing heat of chiller, with heat pump turned off.

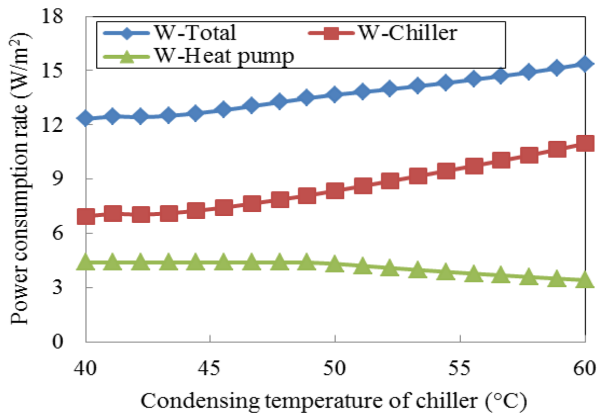

Figure 9.3 Effect of condensing temperature on energy consumption

9.4.2 Hot-water flow rate

The effect of hot water flow rate on energy performance of the proposed system is shown in Figure 9.4. The variation of hot water flow rate is represented by the ratio of mass flow rates of hot water to air because the ratio of flow rates is more meaningful than the abolute value. The air flow rate is kept consontant.

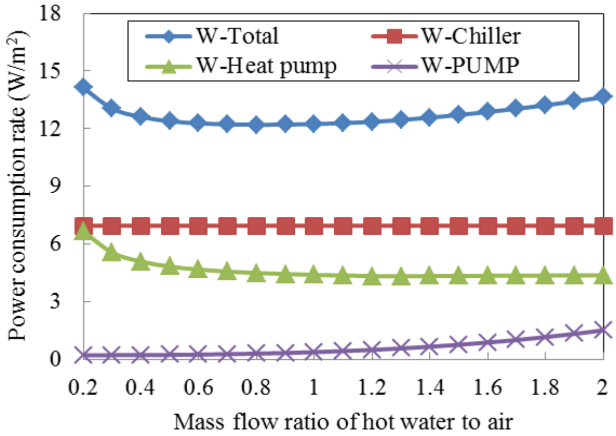

Figure 9.4 Effect of hot water flow rate on energy consumption

As shown in Figure 9.4, the optimal hot water flow rate corresponding to the lowest energy consumption of the proposed system occures when its about 0.9 times of air flow rate. The reason is explained below. When hot water flow rate increases, hot water supply temperature and return temperature will have to be reduced to satisfy the regeneration requirement. The decreased hot water supply temperature increases the COP of heat pump. Although the pump consumption for hot water will increase, its increase is relatively small when the flow rate is low. While the energy consumption of chiller is almost kept constant, the overall energy conumption of system decreases when hot water flow rate increases from a small value. When the hot water flow rate further increase, exceeding an optimal value, the benificial effect of increased hot water flow rate on the COP of heat pump cannot compensate for its side effect on the energy consumption of water pump, the total energy consumption of system would increase.

The optimal value of hot water flow rate would decrease with dehumidification load on dehumidifier, as shown in Figure 9.5. The reason is that decreased dehumidification load would result in decreased regeneration heat required to be supplied by hot water, and thus decreased flow rate. From the results, the optimal range of hot water flow rate for typical applications should be 0.5~1.0 times of fresh air flow rate, with higher value for heavier dehumidification load.

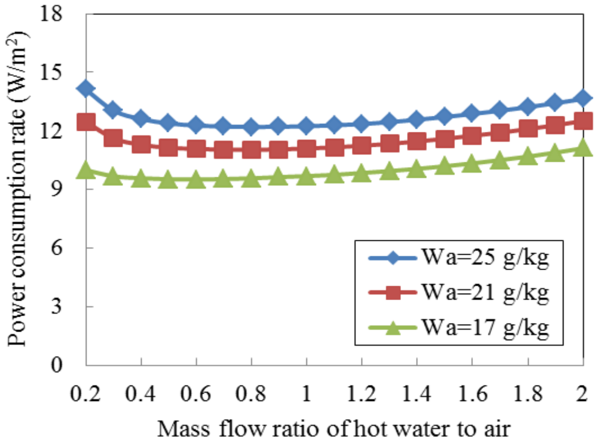

Figure 9.5 Effect of dehumidification load and hot water flow rate on total energy consumption

9.4.3 Cooling water flow rate

The effect of cooling water flow rate on energy consumption of the proposed system is similar to that of hot water flow rate, as shown in Figure 9.6. With the increase of cooling water flow rate, both the dehumidification and cooling performances of the dehumidifier will be enhanced, resulting in decreased desiccant solution concentration for dehumidification and regeneration. The regeneration temperature and load, and thus the power consumption by heat pump will be reduced accordingly. Because the fresh air temperature leaving the dehumidifier decreases, the cooling load of fresh air handled by chiller also decreases. The power consumption by chiller decreases slightly accordingly. Yet since the power use by water pump will increase polynomially with the cooling water flow rate, an optimal value of the cooling water flow rate as shown in Figure 9.6 will occur.

The optimal value of cooling water flow rate would also decrease linearly with dehumidification load, as shown in Figure 9.7. The reason is that decreased dehumidification load would result in decreased heat to be removed by cooling water at decreased flow rate. From the results, the optimal range of cooling water flow rate should be 0.6~1.0 times of fresh air flow rate, with higher value for heavier dehumidification load.

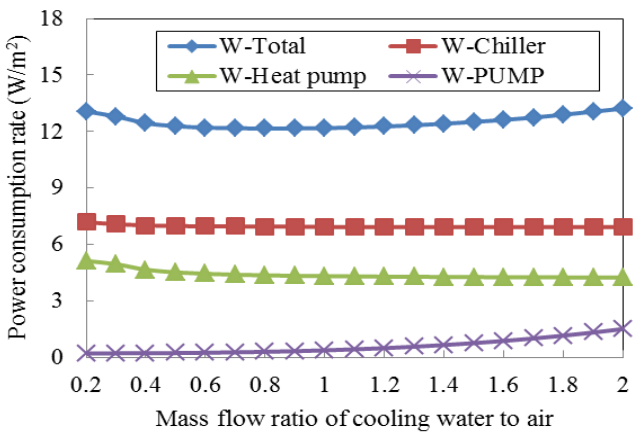

Figure 9.6 Effect of cooling water flow rate on energy consumption

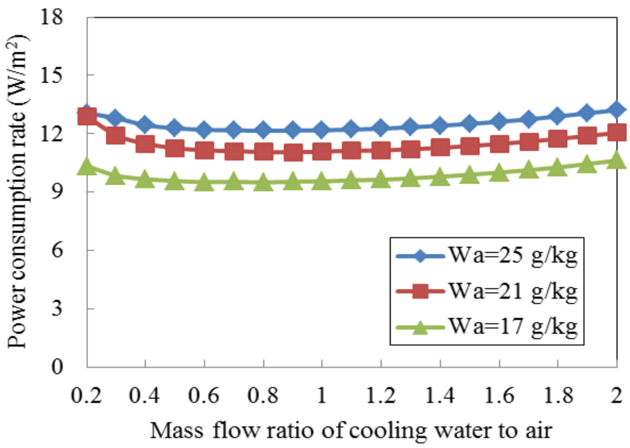

Figure 9.7 Effect of dehumidification load and cooling water flow rate on total energy consumption

9.4.4 Solution flow rate

The effect of solution flow rate on the energy performance of the proposed system is shown in Figure 9.8. It can be noticed that the effect of solution flow rate on the energy performance of the proposed system is relatively small in the given range and that the optimal value of solution flow rate occurs at its possible maximum. According to the experimental results by Lowenstein et al. (2006), the maximum desiccant solution flow rate is limited to about 0.13 times of flow rate of fresh air at face velocity of 2 m/s to prevent the problem of desiccant carry-over. Therefore, in this study, to guarantee operation safety, the minimal value of solution flow rate is set to 0.1 times of fresh air flow rate.

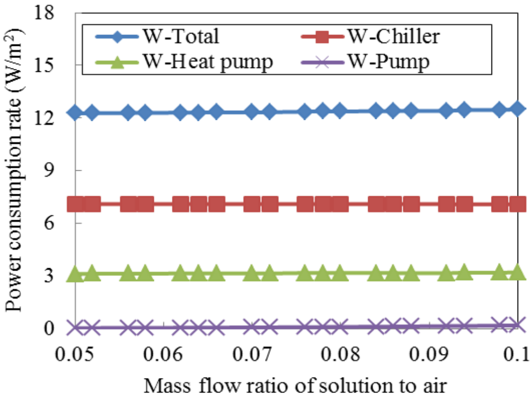

Figure 9.8 Effect of solution flow rate on energy consumption

Also from Figure 9.8, the power consumption by heat pump and by solution pump decreases slightly with solution flow rate. While the power use by chiller is almost kept constant, the total power consumption by the proposed system decreases slightly. The decrease of power use by heat pump is the result of decreased regeneration load and temperature required at larger solution flow rate.

Furthermore, from Figure 9.9, the optimal solution flow rate is not affected by the variation of dehumidification load, still occurring at its possible maximum. Yet this conclusion is just derived from theoretical calculations. In practice, carry-over, rather than energy consumption, is the main concern. Since the effect of solution flow rate on energy consumption is small, it is practical to adopt smaller solution flow rate, say, 0.5-0.1 times of fresh air flow rate.

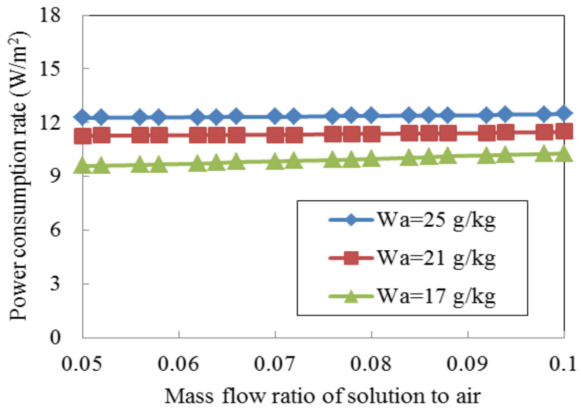

Figure 9.9 Effect of dehumidification load and solution flow rate on total energy consumption

9.5 Summary

In this chapter, the chiller size and independent operation parameters are optimized for design condition and the sensitivity analysis of these parameters at different weather conditions are investigated to find the effect of their variation on the energy consumption of the proposed system. The optimal operation range of these parameters can therefore be identified to guide the optimal design of the proposed system. From the results, the following conclusions can be drawn:

1) Oversized chiller is also unfavorable for the proposed system, although it can reduce the energy consumption of heat pump. Accurate prediction of design cooling load is the prerequisite of proper component sizing;
2) The selection of condensing temperature of chiller affects the performance of system the most among the four parameters. For the proposed system with properly designed total heat exchanger, the optimal condensing temperature would equal to the obtainable minimum of a given air-cooled chiller;
3) The effects of hot water flow rate and cooling water flow rate on the performance of the proposed system are similar. With increase of either

hot or cooling water flow rate, the energy consumption by heat pump decreases, but energy use by water pump increases. Depending on the components design and weather conditions, the optimal value of hot or cooling water flow rate would be about 0.5~1.0 times of fresh air, with higher value for heavier dehumidification load on dehumidifier;

4) The selection of desiccant solution affects the performance of the proposed system the least in the range studied. Its optimal value will equal to the maximum allowable solution flow rate without carry-over. In practical application, it is set to be 0.05~0.1 times of the flow rate of fresh air.

The optimizations of the proposed system in this chapter are only carried out for the design conditions. The optimal operation parameters may vary for different weather conditions. Therefore, hourly optimization should be carried out to obtain their optimal value at different conditions.

CHAPTER 10 CONCLUSIONS AND RECOMMENDATIONS

10.1 Conclusions

A novel hybrid energy-efficient air-conditioning system with DOAS using liquid desiccant is proposed in this thesis through exergy analysis with new method. The detailed simulation method, simplified design method of the proposed system, and RTS-based method for intermittent cooling load calculation design are also developed.

Liquid desiccant dehumidification is a promising alternative to the cooling-based dehumidification, which has the main advantages of decoupled handling of sensible and latent load and of extremely low dew-point temperature of process air. When integrated with dedicated outdoor air system, the air-conditioning system can yield the best possible performance of indoor air quality and thermal comfort. The biggest weakness of conventional liquid desiccant system is low COP due to the regeneration equipment. One of the main contributions of this thesis is to develop an energy-efficient liquid desiccant air-conditioning system by effectively utilizing total cooling potentials of exhaust air and condensing heat of chiller.

The proposed system consists primarily of internally-cooled liquid desiccant dehumidifier, internally-heated regenerator, total heat exchanger, chiller with heat recovery, heat pump and essential heat exchangers. With the DOAS and liquid desiccant dehumidification, the indoor air temperature and humidity ratio can be independently controlled thereby. The cooling load to be handled by chiller is effectively reduced by the total heat exchanger and sensible heat exchanger that recover both sensible and latent cooling energies of exhaust air. In order to reduce the energy consumption for desiccant regeneration, a heat pump utilizing the condensing heat of chiller as source heat is adopted.

Mathematical modeling of various components of the proposed system is conducted and a simulation platform is developed by TRNSYS for energy performance study. A uniform numerical model is presented for internally-cooled liquid desiccant dehumidifier with four flow configurations. And a robust numerical solution is developed to solve the divergence problem, which is characterized by the application of mass transfer term linearization and multi-grid method. A detailed semi-theoretical model of chiller with heat recovery is also developed. The solution algorithms for chiller with two control schemes are described. Simplified models for total heat exchanger and heat pump are introduced as well.

A new method of exergy analysis is proposed to (1) rationally quantify the real exergy gain for the desired function of equipment or system, and each exergy destruction/loss caused by each factor, and (2) guide the development of HVAC system with thermodynamic perfection. The new exergy analysis method is characterized by classifying the exergies of the fluids into dry-exergy, wet-exergy, cold-exergy and heat exergy, depending on the state of the fluid corresponding to the reference state. These exergies can then be determined as beneficial exergy gains or exergy destructions/losses, depending on the desired function of equipment or system. The new exergy analysis method is illustrated and exemplified by two typical components of liquid desiccant system, sensible heat exchanger and liquid desiccant dehumidifier. The new exergy analysis method is applied to the standard air-conditioning system with DOAS using liquid desiccant to identify its weakness. A novel integrated air-conditioning system with DOAS using liquid desiccant is then developed based on the analytical results. The proposed new system is definitely superior over the standard one in the exergy point of view, whose rational exergy efficiency is 8.0% as compared to 3.1% of the standard system.

For the proper design of the proposed system, a new method for intermittent peak cooling load calculations has been developed based on both the current RTS method and the principles of heat transfer. The new method utilizes the technical data available in the current RTS method to compute zone responses to a change in space air temperature without the need for regenerating new data set. It simplifies the RTS calculation by the derived equations in a close form, and only needs one more step after the conventional RTS calculations. Both the overall RTS coefficients and the hourly cooling loads computed in the RTS procedure are utilized to estimate the additional cooling loads due to a change from continuous to intermittent operation. A large number of simulations with different building constructions, WWR and zone orientations are conducted. The results show that the hourly peak cooling load in intermittent operation may be 2.5–30% larger than that in continuous operation. The additional peak cooling load increases proportionally with building weight and turn-off hours and inverse-proportionally with WWR. It also varies with different orientations, and may reach its highest in east-facing zones.

An effectiveness-NTU model of dehumidifier and regenerator is proposed for easy design by engineer. The model is characterized by two correlations of performance indices: enthalpy effectiveness and mass transfer effectiveness. The model also assumes that the heat capacity of solution is kept constant. With this model, a design procedure for sizing of the components at design condition is presented. Due to the coupled performance of dehumidifier and regenerator with other units, iterative approach is adopted. An Excel design tool using the introduced design method and procedure is developed to ease the design of the proposed system by engineers.

The annual energy performance of the proposed system is exemplified for a typical office building in hot and humid climate of Hong Kong, and is compared with that of standard liquid desiccant system to find the energy saving potentials. The weather parameters of temperature, humidity ratio, and sensible heat ratio on the performance of components and system are investigated as well. The results indicate that: 1) the proposed system is more suitable for hot humid climate with small SHR than cooling-based dehumidification. The averaged COP of the proposed system is 4.21 while that of the conventional liquid desiccant system is only 1.66. This high COP of the prosed system results from the decreased heat required for desiccant regeneration and high performance water-source heat pump. In the winter season, although there is heating load requirement, no heat pump is needed because the heat recovered from the condensing heat of chiller is sufficient to satisfy the requirement; 2) the total heat exchanger plays an important role in the proposed system. It can effectively decrease and balance the dehumidification load for the dehumidifier. Therefore, not only the operation cost is reduced, but also the initial cost because of smaller capacities for the dehumidifier, regenerator, cooling tower and heat pump. The total heat recovered ratio increases with outdoor air temperature and humidity ratio and decreases with SHR. This explains why the total heat exchanger is more efficient for hot and humid climates; 3) the COP of heat pump increases with SHR and decreases with outdoor air humidity ratio. The high COP at low outdoor air humidity ratio and high SHR are the results of the reduced regeneration load and temperature at such cases; 4) the COP of chiller decreases with outdoor air temperature and its part-load ratio, but has little relationship with outdoor air humidity and SHR.

The optimizations of chiller size and independent operation parameters, including solution flow rate, hot water flow rate, cooling water flow rate and condensing temperature of chiller, are conducted to harvest the best from the proposed system. Sensitivity analyses of the four parameters are carried out to find their effect on the power consumption of the proposed system and to find their optimal operation range at different weather conditions to guide optimal design at the initial stage. The results indicated that: 1) Oversized chiller is also unfavorable for the proposed hybrid system, although it can reduce the energy consumption of heat pump. Accurate prediction of design cooling load is the prerequisite of proper component sizing; 2) the selection of condensing temperature of chiller affects the performance of system the most among the four parameters. For the proposed system with properly designed total heat exchanger, the optimal condensing temperature would equal to the obtainable minimum of a given air-cooled chiller; 3) the effects of hot water flow rate and cooling water flow rate on the performance of the proposed system are similar. With increase of either hot or cooling water flow rate, the energy consumption by heat pump decreases, but energy use by water pump increases. Depending on the components design and weather conditions, the optimal value of hot or cooling water flow rate would be about 0.5~1.0 times of fresh air flow rate, with higher value for heavier dehumidification load on dehumidifier; 4) the selection of desiccant solution affects the performance of the proposed system the least in the range studied. Its optimal value will equal to the maximum allowable solution flow rate without carry-over. In practical application, it is set to be 0.05~0.1 times of fresh air flow rate.

10.2 Recommendations for Future Work

This study has provided the necessary computational-efficient methods and tools for the effective and efficient optimal design of the proposed system in terms of life-cycle cost, including capital and operation costs. Hence, the further extension of this study could be to develop a methodology for the above-mentioned purpose.

Designing a building services system with the aim to optimize the system life-cycle cost will involve detailed evaluation of the impacts of a large variety of design variations and optional features. The effect of each option and, where they may be simultaneously used, each combination of the options, needs to be evaluated, so as to inform selection of the most effective combination for adoption. This involves huge amount of computational work that can only be practically handled with the use of an accurate and efficient energy simulation model.

The new methodology to be developed is intended to avoid the tedious hourly simulations. First, conduct the statistical analysis of daily outdoor air dry-bulb and wet-bulb temperature averages and their variation ranges, and the daily total solar radiation and hourly solar radiation averages. Note that these statistical data should be also associated with the average dry-bulb temperature and the total solar radiation in the previous one day, three days and seven days. This associated information is used to take into account the effect of weather previously occurring before the day under consideration. Second, apply RTS-based method with near-extreme daily weather conditions to generate the peak cooling load for selecting the size of components in the proposed system. Third, divide the statistical weather into the number of bins. How many bins needed depends on a trade-off between computational efficiency and required accuracy. A mathematical model for computing the hourly cooling loads caused by a heat source in the periodic time duration of seven days needs to be developed, using the similar principle for deriving the RTS-based method. This model will be eventually simplified as a function of hourly heat values on the current day and the average heat values on the previous days. Using this simplified model and the statistical weather data, the hourly cooling loads in each bin can be calculated in the condition of given outdoor air dry-bulb and wet-bulb temperatures. Fourth, compute hourly energy consumption by the proposed system using the hourly cooling loads obtained in the last step and the simplified tool developed in this study. Fifth, the system life-cycle cost can be determined, which consists of the capital and operation costs. The capital cost depends on the size of each component in the system. The operation energy cost is a function of the summation of the products of the energy consumption and the frequency percentage of outdoor weather in each bin, and the price of energy. The minimum life-time cost can be found by any suitable optimization method with varying the design parameters in the system.

REFERENCES

Alalawi, M. A. M. (1999). Experimental and theoretical evaluation of the effect of CO2-based demand-controlled ventilation strategies on energy consumption. Ann Arbor, Mich., University of Colorado.

Ali, A. and K. Vafai (2004). "An investigation of heat and mass transfer between air and desiccant film in an inclined parallel and counter flow channels." *International Journal of Heat and Mass Transfer* 47 (8-9): 1745-1760.

Ali, A. and K. Vafai, et al. (2004). "Analysis of heat and mass transfer between air and falling film in a cross flow configuration." *International Journal Of Heat And Mass Transfer* 47 (4): 743-755.

Ali, A. A. (2003). Analysis of heat and mass transfer between air and falling film desiccant for different flow configurations in the presense of ultrafine particles. Columbus, Ohio, Ohio State University. Ph. D.

Alizadeh, S. and W. Y. Saman (2002). "An experimental study of a forced flow solar collector/regenerator using liquid desiccant." *Solar Energy* 73 (5): 345-362.

Alizadeh, S. (2008). "A Feasibility Study of Using Solar Liquid-Desiccant Air Conditioner in Queensland, Australia." *Journal of Solar Energy Engineering* 130 (2): 021005-9.

Alpuche, M. G. and C. Heard, et al. (2005). "Exergy analysis of air cooling systems in buildings in hot humid climates." *Applied Thermal Engineering* 25 (4): 507-517.

Ameel, T. A. and K. G. Gee, et al. (1995). "Performance predictions of alternative, low cost absorbents for open-cycle absorption solar cooling." *Solar*

Energy 54 (2): 65-73.

Arif-uz-Zaman, M. and M. R. Khan (1993). "Atmospheric moisture: a potential source of energy." *Renewable Energy* 8 (3): 941-945.

ASHRAE (2007a). ANSI/ASHRAE Standard 62.1: Ventilation for acceptable indoor air quality. Altanta, ASHRAE.

ASHRAE (2005). ASHRAE Handbook - Fundamentals. Atlanta, ASHRAE.

ASHRAE (2007b). ASHRAE Standard 90.1 - 2007: Energy Standard for Buildings Except Low-Rise Residential Buildings. Atlanta, GA, ASHRAE.

ASHRAE (2008). ASHRAE Handbook - HVAC Systems and Equipment. Atlanta, ASHRAE.

ASHRAE (1993). ASHRAE Handbook - Fundamentals. Atlanta, ASHRAE.

Babakhani, D. and M. Soleymani (2010). "Simplified analysis of heat and mass transfer model in liquid desiccant regeneration process." *Journal of the Taiwan Institute of Chemical Engineers* 41 (3): 259-267.

Bejan, A. (2006). Advanced engineering thermodynamics. Hoboken, NJ, John Wiley & Sons.

Bourdouxhe, J. and J. LeBrun, et al. (1999). HVAC1 Toolkit: a toolkit for primary HVAC system energy calculation. Atlanta, Ga., ASHRAE.

Braun, J. E. and S. A. Klein, et al. (1989). "Effectiveness models for cooling towers and cooling coils." *ASHRAE Transactions* 95 (2): 164-174.

Chao, C.Y.H. and J.S. Hu (2004). "Development of a Dual-Mode Demand Control Ventilation Strategy for Indoor Air Quality Control and Energy Saving", *Building and Environment*, 39(4): 385-397.

Chao, C.Y.H. and C.W. Kwong (2007). Energy in Buildings in Hong Kong - A Lesson for the Mainland?, Invited Talk in the Special Session on Building

Energy in China – the Present and the Future, Special Session, the 6th International Conference on Indoor Air Quality, Ventilation and Energy Conservation in Buildings, Sendai, Japan, Oct 28 – 31.

Chen, T. Y. (2003). "A method for the direct generation of comprehensive numerical solar building transfer functions." *Solar Energy* 74 (2): 123-132.

Chen, T. Y. and A. K. Athienitis (1993). "Computer generation of semi-symbolic thermal network functions of buildings." *Building and Environment* 28 (3): 301-309.

Chen, T. Y. and Y. C. Lee (2006). Study on air handling systems for displacement ventilation combined with cooled ceiling in the tropic region. Proceedings of the 5th International Conference on Sustainable Energy Technologies. Vicenza, Italy.

Chen, T. and Z. Yu (2009). "A statistical method for selection of sequences of coincident weather parameters for design cooling load calculations." *Energy Conversion and Management* 50 (3): 813-821.

Chua, K. J. and S. K. Chou, et al. (2007). "A comparative study of different control strategies for indoor air humidity." *Building and Energy*(39): 537-545.

Conde, M. R. (2004). "Properties of aqueous solutions of lithium and calcium chlorides: Formulations for use in air conditioning equipment design." *International Journal of Thermal Sciences* 43 (4): 367-382.

Conde-Petit, M. (2007). Liquid desiccant-based air-conditioning systems — LDACS. 1st European Conference on Polygeneration, Tarragona, Spain.

Conde-Petit, M. and R. Weber (2006). OPEN ABSORPTION SYSTEM FOR COOLING AND AIR CONDITIONING USING MEMBRANE CONTACTORS.

Daou, K. and R. Z. Wang, et al. (2006). "Desiccant cooling air conditioning: a review." *Renewable and Sustainable Energy Reviews* 10 (2): 55-77.

Dengta, C. (2004). Studies on the Character of Corona Discharge and Performance of Fog-removal about Wire-mesh Electrode. Xi'an, Xi'an University of Architecture and Technology. Master of Science.

Doetsch, G. (1974). Introduction to the theory and application of the Laplace trans- formation : A table of Laplace transformations. New York, Springer-Verlag.

EERE (2008). "EnergyPlus." *http://apps1.eere.energy.gov/buildings/energyplus/*.

Evenko, V. (1996). "Exergetic efficiency of heat exchangers." *Chemical and Petroleum Engineering* 32 (1): 37-42-42.

Factor, H. M. and G. Grossman (1980). "A packed bed dehumidifier/regenerator for solar air conditioning with liquid desiccants." *Solar Energy* 24 (6): 541-550.

Fumo, N. and D. Y. Goswami (2002). "Study of an aqueous lithium chloride desiccant system: air dehumidification and desiccant regeneration." *Solar Energy* 72 (4): 351-361.

Gandhidasan, P. and M. R. Ullah, et al. (1987). "Analysis of heat and mass transfer between a desiccant-air system in a packed tower." *Journal of Solar Energy Engineering* 109 (2): 89-93.

Gommed, K. and G. Grossman (2007). "Experimental investigation of a liquid desiccant system for solar cooling and dehumidification." *Solar Energy* 81 (1): 131-138.

Harriman III, L. G. and M. J. Witte, et al. (1999). "Evaluating Active

Desiccant Systems fro Ventilating Commercial Buildings." *ASHRAE Journal* 10 (41): 28-34.

Harriman, L. G. (1994). "The basics of commercial desiccant systems." *Heating, Piping and Air Conditioning* 66 (7): 77-85.

Harriman, L. G. I. and D. Plager, et al. (1998). "Dehumidification and cooling loads from ventilation air." *ASHRAE Journal* 40 (11): 37-45.

Harriman, L. G. and J. Judge (2002). "Dehumidification equipment advances." *ASHRAE Journal* 8 (44): 22-29.

Harriman, L. G. (2008). The ASHRAE Guide for Buildings in Hot and Humid Climates. Atlanta, ASHRAE.

Harris, S. M. and F. C. McQuiston (1988). "A study to categorize walls and roofs on the basis of thermal response." *ASHRAE Transactions* 2 (94): 688-715.

Hassan, M. S. and A. A. M. Hassan (2009). "Performance of a proposed complete wetting surface counter flow channel type liquid desiccant air dehumidifier." *Renewable Energy* 34 (10): 2107-2116.

Heinzen, R. and M. Krause, et al. (2007). Theoretical Performance Analysis of a Liquid Desiccant Air-Conditioning System for Heating and Cooling. Proc. 2nd International Conference Solar Air-Conditioning, Tarragona.

Hepbasli, A. (2008). "A key review on exergetic analysis and assessment of renewable energy resources for a sustainable future." *Renewable and Sustainable Energy Reviews* 12 (3): 593-661.

Hoenig, S. A. (1987). Method and Apparatus for Electrostatic extraction of droplets from gaseous medium, U.S. Patent #4670026.

Hoenig, S. A. (2001). Apparatus Using High Electric Fields to Extract Water Vapor from an Air Flow, U.S. Patent #US 2001/0029842 A1.

Hoenig, S. A. (2001). Apparatus for Extracting Water Vapor from Air, U.S. Patent #6302944 B1.

Hoenig, S. A. and E. P (2002). An Electrostatic System for Removing Water Vapor from Air. Proceedings of the ESA-IEJ Joint Symposium on Electrostatics, Northwestern University, Chicago, Laplacian Press.

Hydeman, M. and K. L. Gillespie (2002). "Tools and techniques to calibrate electric chiller component models." *ASHRAE Transactions* 1 (108): 733-741.

Incropera, F. P. (2002). Fundamentals of heat and mass transfer. Hoboken, NJ, John Wiley.

Iu, I. (2006). "PRF/RTF Generator." *http://www.hvac.okstate.edu/*.

Jae-Weon, J. and S. A. Mumma (2007). "Binary Enthalpy Wheel Humidification Control in Dedicated Outdoor Air Systems." *ASHRAE Transactions* 113 (2): 220-226.

Jain, S. and P. K. Bansal (2007). "Performance analysis of liquid desiccant dehumidification systems." *International Journal of Refrigeration* 30 (5): 861-872.

Jaradat, M. and R. Heinzen, et al. (2008). A Novel Generator Design for a Liquid Desiccant Air Conditioning System. EuroSun 2008, Lisbon, Portugal.

Jin, H. and J.D. Spitler. (2002). "A Parameter Estimation Based Model of Water-To-Water Heat Pumps for use in Energy Calculation Programs". *ASHRAE Transactions*. 108(1): 3-17.

Jin, X. M. (1986). Air-conditioning load calculation and computer programs. Tianjin, Tianjin University Press.

Katejanekarn, T. and S. Chirarattananon, et al. (2009). "An experimental study of a solar-regenerated liquid desiccant ventilation pre-conditioning system." *Solar Energy* 83 (6): 920-933.

Kessling, W. and E. Laevemann, et al. (1998). "Energy storage for desiccant cooling systems component development." *Solar Energy* 64 (4-6): 209-221.

Kettler, J. P. (1998). "Controlling minimum ventilation volume in VAV systems." *ASHRAE Journal* 5 (40): 45-50.

Khan, A. Y. (1998). "Cooling and dehumidification performance analysis of internally-cooled liquid desiccant absorbers." *Applied Thermal Engineering* 18 (5): 265-281.

Khan, A. Y. and F. J. Sulsona (1998). "Modeling and parametric analysis of heat and mass transfer performance of refrigerant cooled liquid desiccant absorbers." *International Journal of Energy Research* 22 (9): 813-832.

Kim, D. S. and I. C. A. Ferreira (2006). "A Gibbs energy equation for LiBr aqueous solutions." *International Journal of Refrigeration* 29 (1): 36-46.

Kinsara, A. A. and O. M. Al-Rabghi, et al. (1998). "Parametric study of an energy efficient air conditioning system using liquid desiccant." *Applied Thermal Engineering* 18 (5): 327-335.

Kinsara, A. A. and M. M. Elsayed, et al. (1996). "Proposed energy-efficient air-conditioning system using liquid desiccant." *Applied Thermal Engineering* 16 (10): 791-806.

Krause, M. and W. Saman, et al. (2005). Regenerator Design for Open Cycle Liquid Desiccant Systems –Theoretical and Experimental Investigations. International Conference Solar Air-Conditioning, Staffelstein, DE.

Li, Z. and X. Liu, et al. (2005). "New type of fresh air processor with liquid desiccant total heat recovery." *Energy and Buildings* 37 (6): 587-593.

Lin, K. and H. Xu (2008). "Simplified calculation of intermittent coefficient of cooling load for office buildings." *Heating Ventilating & Air Conditioning* 38 (9): 20-25.

Liu, W. and Z. Lian, et al. (2007). "Energy consumption analysis on a dedicated outdoor air system with rotary desiccant wheel." *Energy* 32 (9): 1749-1760.

Liu, X. H. (2011). "Personal Communication.".

Liu, X. H. and X. M. Chang, et al. (2009). "Performance analysis on the internally cooled dehumidifier using liquid desiccant." *Building and Environment* 44 (2): 299-308.

Liu, X. H. and Y. Jiang, et al. (2007). "Heat and mass transfer model of cross flow liquid desiccant air dehumidifier/regenerator." *Energy Conversion and Management* 48 (2): 546-554.

Liu, X. and Y. Jiang, et al. (2008). "Analytical solution of combined heat and mass transfer performance in a cross-flow packed bed liquid desiccant air dehumidifier." *International Journal of Heat and Mass Transfer* 51 (17-18): 4563-4572.

Liu, X. and Z. Li, et al. (2006). "Annual performance of liquid desiccant based independent humidity control HVAC system." *Applied Thermal Engineering* 26 (11-12): 1198-1207.

Longo, G. A. and A. Gasparella (2005). "Experimental and theoretical analysis of heat and mass transfer in a packed column dehumidifier/regenerator with liquid desiccant." *International Journal of Heat and Mass Transfer* 48 (25-26): 5240-5254.

Lowenstein, A. and S. Slayzak, et al. (2006). A zero carryover liquid-desiccant air conditioner for solar applications. ASME International Solar Energy Conference, Denver, Colorado.

Lowenstein, A. (2008). "Review of Liquid Desiccant Technology for HVAC Applications." *HVAC&R Research* 14 (6): 818-839.

Lowenstein, A. (2005). High Efficiency Liquid-Desiccant Regenerator for Air Conditioning and Industrial Drying, Final Report for Department of Energy Contract No. DE-FG36-03GO13170. Princeton, NJ, AIL Research, Inc.

Lowenstein, A. and S. Slayzak, et al. (1998). Advanced Commercial Liquid-Desiccant Technology Development Study, National Renewable Energy Laboratory.

Lu, L. and W. Cai (2002). A universal engineering model for cooling towers. The Ninth International Refrigeration and Air Conditioning Conference at Purdue, West Lafayette.

Lu, L. (2005). "Study on the Application of Electrostatic Precipitator to the Recovery of Water in Vapor." *Energy Conservation Technology (In Chinese)* 134 (23): 502-504.

Marletta, L. (2010). Exergy analysis of solar cooling systems: a technical report of subtask C3 of IEA SHC Task 38. Italy, University of Catania.

Mathews, J. H. (1992). Numerical methods for mathematics, science, and engineering. Englewood Cliffs, N.J., Prentice Hall.

McQuay (2009). Templifier heat recovery water heaters catalog.

McQuay (2009). "Heat Recovery Chiller Systems." *A/SP TSC(05/09).*

McQuay (2008). Large Air-cooled Screw Chiller: ALS163.2-344.3ST/LN, McQuay.

McQuay (2002). Chiller Plant Design - Application Guide, McQuay Air conditioning.

McQuiston, F. C. and J. D. Spitler (1992). Cooling and Heating Load Calculation Manual, 2nd Edition. Atlanta, ASHRAE Inc.

McQuiston, F. C. and J. D. Parker (1994). Heating, ventilating, and air conditioning : analysis and design. Hoboken, NJ, John Wiley & Sons.

McQuiston, F. C. and J. D. Parker, et al. (2005). Heating, ventilating, and air conditioning : analysis and design. Hoboken, NJ, John Wiley & Sons.

Meckler, G. (1986). "Innovative ways to save energy in new buildings." *Heating/Piping/Air Conditioning* 58 (5): 87-92.

Mesquita, L. C. S. and S. J. Harrison, et al. (2006). "Modeling of heat and mass transfer in parallel plate liquid-desiccant dehumidifiers." *Solar Energy* 80 (11): 1475-1482.

Morris, W. (2003). "The ABCs of DOAS - Dedicated outdoor air systems." *ASHRAE JOURNAL* 45 (5): 24-29.

Mumma, S. A. (2001). "Overview of Integrating Dedicated Outdoor Air Systems with Parallel Terminal Systems." *ASHRAE Transactions* 107 (1): 545-552.

Mumma, S. A. (2007). "DOAS & desiccants." *Engineered Systems* 24 (8): 37-49.

Mumma, S. A. and B. W. Lee (1998). "Extension of the multiple spaces concept of ASHRAE Standard 62 to include infiltration, exhaust/exfiltration, interzonal transfer, and additional short circuit paths." *ASHRAE Transactions* 2 (103): 894-905.

Mumma, S. A. (2001). "Dedicated Outdoor Air-Dual Wheel System Control Requirements." *ASHRAE Transactions* 107 (1): 147-155.

Niu, J. L. and L. Z. Zhang, et al. (2002). "Energy savings potential of chilled-ceiling combined with desiccant cooling in hot and humid climates." *Energy and Buildings* 34 (5): 487-495.

Novoselac, A. and J. Srebric (2002). "A critical review on the performance and design of combined cooled ceiling and displacement ventilation systems." *Energy and Building* 5 (34): 497-509.

Ober, V. and D. Y. Goswami (1998). A Review of Liquid Desiccant Cooling. Advance in Solar Energy. K. W. Boer. Boulder, Colorado, American Solar Energy Society, Inc. 12: 431-470.

Oberg, V. and D. Y. Goswami (1998). "Experimental Study of the Heat and Mass Transfer in a Packed Bed Liquid Desiccant Air Dehumidifier." *Journal of Solar Energy Engineering* 120 (4): 289-297.

Oliveira, A. C. and C. F. Afonso, et al. (2000). "Thermal performance of a novel air conditioning system using a liquid desiccant." *Applied Thermal Engineering* 20 (13): 1213-1223.

Ozgener, O. and A. Hepbasli (2007). "Modeling and performance evaluation of ground source (geothermal) heat pump systems." *Energy and Buildings* 39 (1): 66-75.

Palacios-Bereche, R. and R. Gonzales, et al. (2010). "Exergy calculation of lithium bromide–water solution and its application in the exergetic evaluation of absorption refrigeration systems LiBr-H2O." *International Journal of Energy Research*: n/a-n/a.

Pesaran, A. A. and T. R. Penney, et al. (1992). Desiccant Cooling: State-of-the-Art Assessment. Golden, National Renewable Energy Laboratory.

Press, W. H. (1992). Numerical recipes in FORTRAN: the art of scientific computing. Cambridge, Cambridge University Press.

Rahamah, A. and M. M. Elsayed, et al. (1998). "A numerical solution for cooling and dehumidification of air by a falling desiccant film in parallel flow." *Renewable Energy* 13 (3): 305-322.

Ren, C. Q. and M. Tu, et al. (2007). "An analytical model for heat and mass transfer processes in internally cooled or heated liquid desiccant-air contact units." *International Journal of Heat and Mass Transfer* 50 (17-18): 3545-3555.

Rudoy, W. and J. F. Cuba (1979). Cooling and heating load calculation manual. Atlanta, ASHRAE.

Rudoy, W. and F. Duran (1975). "Development of an Improved Cooling Load Calculation Method." *ASHRAE Transactions* 81 (2): 19-69.

Saman, W. Y. and S. Alizadeh (2002). "An experimental study of a cross-flow type plate heat exchanger for dehumidification/cooling." *Solar Energy* 73 (1): 59-71.

Shirey III, D. and H. Henderson Jr. (2004). "Dehumidification at part load." *ASHRAE Journal* 4 (46): 42-48.

Shrivastava, D. and T. A. Ameel (2004). "Three-fluid heat exchangers with three thermal communications. Part A: general mathematical model." *International Journal of Heat and Mass Transfer* 47 (17-18): 3855-3865.

Shukuya, M. and A. Hammache (2002). Introduction to the concept of exergy—for a better understanding of low-temperature-heating and high-temperature-cooling systems. Otamedia Oy, Espoo, VTT.

Smith, J. M. and H. C. Van Ness, et al. (2005). Introduction to chemical engineering thermodynamics. New York, McGraw-Hill.

Sowell, E. F. (1988). "Classification of 200,640 parametric zones for cooling load calculations." *ASHRAE Transactions* 94 (2): 754–777.

Sowell, E. F. (1988). "Cross-check and modification of the DOE-2 program for calculation of zone weighting factors." *ASHRAE Transactions* 94 (2): 737–753.

Sowell, E. F. (1988). "Load calculations for 200,640 zones." *ASHRAE Transactions* 94 (2): 716–736.

Spitler, J. D. and D. E. Fisher (1999). "Development of Periodic Response Factors for Use with the Radiant Time Series Method." *ASHRAE Transactions* 105 (2): 491-509.

Spitler, J. D. and D. E. Fisher (1999). "On the Relationship between the Radiant Time Series and Transfer Function Methods for Design Cooling Load Calculations." *International Journal of Heating, Ventilating, and Air-Conditioning and Refrigerating Research* 5 (2): 125-138.

Spitler, J. D. and D. E. Fisher, et al. (1997). "The Radiant Time Series Cooling Load Calculation Procedure." *ASHRAE Transactions* 103 (2): 503-515.

Stanke, D. A. (1998). "Ventilation where it's needed." *ASHRAE Journal* 10 (40): 39-47.

Stevens, D. I. and J. E. Braun, et al. (1989). "An effectiveness model of liquid-desiccant system heat/mass exchangers." *Solar Energy* 42 (6): 449-455.

Stevens, D. I. (1988). Analysis of Liquid-desiccant Systems and Component Modeling. Madison, University of Wisconsin-Madison.

Szargut, J. (2005). Exergy analysis: technical and ecological applications. Southampton, Wit Press.

Szargut, J. and D. R. Morris, et al. (1988). Exergy analysis of thermal, chemical, and metallurgical processes. New York, Hemisphere.

Tao, WQ (2001). Numerical Heat Transfer. Xi'an, China, Xi'an Jiaotong University Press.

Thompson, D. A. (2004). "Enthalpy pump." *US 6684649*.

TIAX (2004). Review of Thermally Activated Technologies, Final Report to the U.S. Department of Energy, the Distributed Energy Program, U.S. Department of Energy.

Torio, H. and A. Angelotti, et al. (2009). "Exergy analysis of renewable energy-based climatisation systems for buildings: A critical view." *Energy and Buildings* 41 (3): 248-271.

Trane (2002). "Air-cooled series R rotary liquid chiller." *RLC-PRC006-EN*.

TRNSYS (2006). TRNSYS16 - A Transient System Simulation Program. Madison, WI, University of Wisconsin-Madison.

Tsatsaronis, G. (2007). "Definitions and nomenclature in exergy analysis and exergoeconomics." *Energy* 32 (4): 249-253.

Tu, M. and C. Ren, et al. (2009). "Simulation and analysis of a novel liquid desiccant air-conditioning system." *Applied Thermal Engineering* 29 (11-12): 2417-2425.

Turner, S. C. (2011). "What's New in ASHRAE's Standard on Comfort." *ASHRAE Journal* 53 (6): 42-48.

Uchiyama, H. and M. Jyumonji (1995). "Field Experiments of an Electrostatic Fog-liquefier." *Journal of Electrostatics* 1 (35): 133-143.

Uchiyama, H. and M. Yjumonji (1989). "Development of an Electrostatic Fog-Liquefier and its Field Experiments." *Japanese Journal of Applied Physics* 11 (28): 2319-2320.

Wang, T. and P. Wang (1995). "Discuss of the Application of High-voltage electrostatic Water Recovery Technology in Wet Cooling Tower." *Shanxi Electric Power (In Chinese)* 16-20 (2).

Waugaman, D. G. and A. Kini, et al. (1993). "A Review of Desiccant Cooling Systems." *Journal of Energy Resources Technology* 115 (1): 1-8.

Wyssen, I. and L. Gasser, et al. (2010). Chiller with small temperature lift for efficient building cooling. Proceedings of the REHVA Clima 2010. Antalya, Turkey.

Xu, X. H. (2011). Personal Communication.

Yin, Y. and X. Zhang (2008). "A new method for determining coupled heat and mass transfer coefficients between air and liquid desiccant." *International Journal of Heat and Mass Transfer* 51 (13-14): 3287-3297.

Yin, Y. and X. Zhang (2010). "Comparative study on internally heated and adiabatic regenerators in liquid desiccant air conditioning system." *Building and Environment* 45 (8): 1799-1807.

Yin, Y. and X. Zhang, et al. (2009). "Model validation and case study on internally cooled/heated dehumidifier/regenerator of liquid desiccant systems." *International Journal of Thermal Sciences* 48 (8): 1664-1671.

Yu, B. F. and Z. B. Hu, et al. (2009). "Review of research on air-conditioning systems and indoor air quality control for human health." *International Journal of Refrigeration* 1 (32): 3-20.

Yu, F. W. and K. T. Chan (2008). "Improved energy performance of air cooled centrifugal chillers with variable chilled water flow." *Energy Conversion and Management* 49 (6): 1595-1611.

Zhang, L. Z. and J. L. Niu (2002). "Effectiveness Correlations for Heat and Moisture Transfer Processes in an Enthalpy Exchanger With Membrane Cores."

Journal of Heat Transfer 124 (5): 922-929.

Zhang, L. Z. and D. S. Zhu, et al. (2005). "Thermodynamic modeling of a novel air dehumidification system." *Energy and Buildings* 37 (3): 279-286.

Zhang, L. Z. and J. L. Niu (2003). "Indoor humidity behaviors associated with decoupled cooling in hot and humid climates." *Building and Environment* 38 (1): 99-107.

Zhu, W. and Z. Li, et al. (2010). "In situ performance of independent humidity control air-conditioning system driven by heat pumps." *Energy and Buildings* 42 (10): 1747-1752.

Zografos, A. I. and C. Petroff (1991). "A liquid desiccant dehumidifier performance model." *ASHRAE Transactions* 1 (97): 650-656.

APPENDIX A PROPERTIES OF AQUEOUS SOLUTION OF LITHUM CHLORIDE

The equilibrium pressure of saturated water vapor above aqueous solution of lithium chloride can be calculated by

$$p(X,t) = p_{\mathrm{H2O}}\pi_{10} f(X,\theta) \tag{A.1}$$

where X is the solution concentration (kg/kg); t is the solution temperature (°C), θ is the reduced temperature with critical temperature of water, θ = (t+273.15)/373.946. f is the regression function which is expressed as

$$f(X,\theta) = A + B\theta$$
$$A = 2 - \left[1 + \left(\frac{X}{\pi_0}\right)^{\pi_1}\right]^{\pi_2} \qquad B = \left[1 + \left(\frac{X}{\pi_3}\right)^{\pi_4}\right]^{\pi_5} - 1 \tag{A.2}$$
$$\pi_{10} = 1 - \left[1 + \left(\frac{X}{\pi_6}\right)^{\pi_7}\right]^{\pi_8} - \pi^9 e^{-\frac{(X-0.1)^2}{0.005}}$$

p_{H2O} is the vapor pressure of water over liquid phase which is calculated by

$$\ln\frac{p_{\mathrm{H2O}}}{p_{c,\mathrm{H2O}}} = \frac{a_0\tau + a_1\tau^{1.5} + a_2\tau^3 + a_4\tau^4 + a_5\tau^{7.5}}{1-\tau} \quad \text{with} \quad \tau = 1\text{-}\frac{t+273.15}{373.945} \tag{A.3}$$

where $p_{c,\mathrm{H2O}}$ is the critical pressure of water (22.064 MPa).

The regression parameters for the vapor pressure equation are listed in Table A.1.

Table A.1 Parameters for the vapor pressure equation

Type	0	1	2	3	4	5	6	7	8	9
π	0.28	4.3	0.6	0.21	5.1	0.49	0.36	-4.75	-0.4	0.03
a	-7.858	1.84	-11.78	22.67	-15.93	1.775				

The equilibrium humidity ratio of saturated water vapor above aqueous solution can be calculated by

$$\omega(X,t) = 0.622\times10^{-3}\frac{p(X,t)}{p_{atm}} \tag{A.4}$$

where p_{atm} is the atmosphere pressure (kPa).

The specific heat capacity of the solution is expressed as

$$c_{p,s}(X,t) = c_{p,\mathrm{H2O}}(\theta) \times \left[1 - f_1(X) f_2(\theta)\right] \tag{A.5}$$

where the specific heat of liquid water is calculated by

$$c_{p,\mathrm{H2O}}(\theta) = a_0 + a_1\theta^{0.02} + a_2\theta^{0.04} + a_3\theta^{0.06} + a_4\theta^{1.8} + a_5\theta^{8} \tag{A.6}$$

The functions f_1 and f_2 are given by

$$\begin{gathered} f_1(X) = \begin{cases} b_0 X + b_1 X^2 + b_2 X^3 & \text{for } X \le 0.31 \\ b_3 + b_4 X & \text{for } X > 0.31 \end{cases} \\ f_2(\theta) = b_5\theta^{0.02} + b_6\theta^{0.04} + b_7\theta^{0.06} \\ \theta = \frac{t + 273.15}{228} - 1 \end{gathered} \tag{A.7}$$

The regression parameters for the vapor pressure equation are listed in Table A.2.

Table A.2 Parameters for the specific heat capacity equation

Type	0	1	2	3	4	5	6	7
a	88.789	-120.196	-15.926	52.465	0.108	0.469		
b	1.440	-1.243	-0.121	0.128	0.629	58.523	-105.634	47.795

The density of the lithium chloride solution is expressed as

$$\rho_s(X,t) = \rho_{\mathrm{H2O}}(\tau) \sum_{i=0}^{3} a_i \left(\frac{X}{1-X}\right)^i \tag{A.8}$$

where ρ_{H2O} is the density of liquid water at temperature t and is calculated from

$$\begin{gathered} \rho_{\mathrm{H2O}}(\tau) = 322 \times (1 + b_0\tau^{1/3} + b_1\tau^{2/3} + b_2\tau^{5/3} + b_3\tau^{16/3} + b_4\tau^{43/3} + b_5\tau^{110/3}) \\ \tau = 1 - \theta = 1 - \frac{t + 273.15}{373.945} \end{gathered} \tag{A.9}$$

The regression parameters for the density equation are listed in Table A.3.

Table A.3 Parameters for the density equation

Type	0	1	2	3	4	5
a	1.0	0.540966	-0.303792	0.100791		
b	1.99377	1.09852	-0.50945	-1.76191	-44.90055	-723692.26186